11:10:28 OCA PAD AMENDMENT - PROJECT HEADER INFORMATION 11/27/91

Active

Project #: B-03-602 Cost share #: Rev #: 3
Center # : 10/24-6-R6642-3A0 Center shr #: OCA file #:
Work type : RES
Contract#: 5 R01 NS24602-03 Mod #: ADMIN 11/22/91 Document : GRANT
Prime #: Contract entity: GTRC

Subprojects ? : N CFDA:
Main project #: PE #: N/A

Project unit: BEC Unit code: 03.010.203
Project director(s):
KENNEDY P R ESML (404)894-4257

Sponsor/division names: DHHS/PHS/NIH / NATL INSTITUTES OF HEALTH
Sponsor/division codes: 108 / 001

Award period: 901201 to 920331 (performance) 920531 (reports)

Sponsor amount	New this change	Total to date
Contract value	0.00	142,662.00
Funded	0.00	142,662.00
Cost sharing amount		0.00

Does subcontracting plan apply ?: N

Title: STRUCTURE & CONNECTIONS OF RED NUCLEUS

PROJECT ADMINISTRATION DATA

OCA contact: Kathleen R. Ehlinger 894-4820

Sponsor technical contact

DR. EUGENE OLIVER
(301)496-1431

NINCDS, NATL INSTITUTES OF HEALTH
FEDERAL BUILDING, RM 1004
7550 WISCONSIN AVENUE
BETHESDA, MD. 20892

Sponsor issuing office

MR. DWIGHT H. MOWERY, JR.
(301)496-9231

NINCDS, NATL INSTITUTES OF HEALTH
FEDERAL BUILDING, RM 1004
7550 WISCONSIN AVENUE
BETHESDA, MD. 20892

Security class (U,C,S,TS) : U ONR resident rep. is ACO (Y/N): N
Defense priority rating : N/A NIH supplemental sheet
Equipment title vests with: Sponsor GIT X

Administrative comments -
ISSUED TO REVISE DELIVERABLE SCHEDULE.

GEORGIA INSTITUTE OF TECHNOLOGY
OFFICE OF CONTRACT ADMINISTRATION

NOTICE OF PROJECT CLOSEOUT

Closeout Notice Date 12/23/92

Project No. B-03-602_____ Center No. 10/24-6-R6642-3A0_

Project Director KENNEDY P R_____ School/Lab BEC_____

Sponsor DHHS/PHS/NIH/NATL INSTITUTES OF HEALTH_____

Contract/Grant No. 5 R01 NS24602-03_____ Contract Entity GTRC

Prime Contract No. _____

Title STRUCTURE & CONNECTIONS OF RED NUCLEUS_____

Effective Completion Date 920331 (Performance) 920531 (Reports)

Closeout Actions Required:	Y/N	Date Submitted
Final Invoice or Copy of Final Invoice	Y	_____
Final Report of Inventions and/or Subcontracts	Y	_____
Government Property Inventory & Related Certificate	N	_____
Classified Material Certificate	N	_____
Release and Assignment	Y	_____
Other _____	N	_____

CommentsEFFECTIVE DATE 12-1-90. CONTRACT VALUE $142,662._____

_____

Subproject Under Main Project No. _____

Continues Project No. B-03-631_____

Distribution Required:

Project Director	Y
Administrative Network Representative	Y
GTRI Accounting/Grants and Contracts	Y
Procurement/Supply Services	Y
Research Property Managment	Y
Research Security Services	N
Reports Coordinator (OCA)	Y
GTRC	Y
Project File	Y
Other HARRY VANN-FMD_____	Y
FRED CAIN-OOD_____	Y

NOTE: Final Patent Questionnaire sent to PDPI.

Reprinted from Trends in Neurosciences

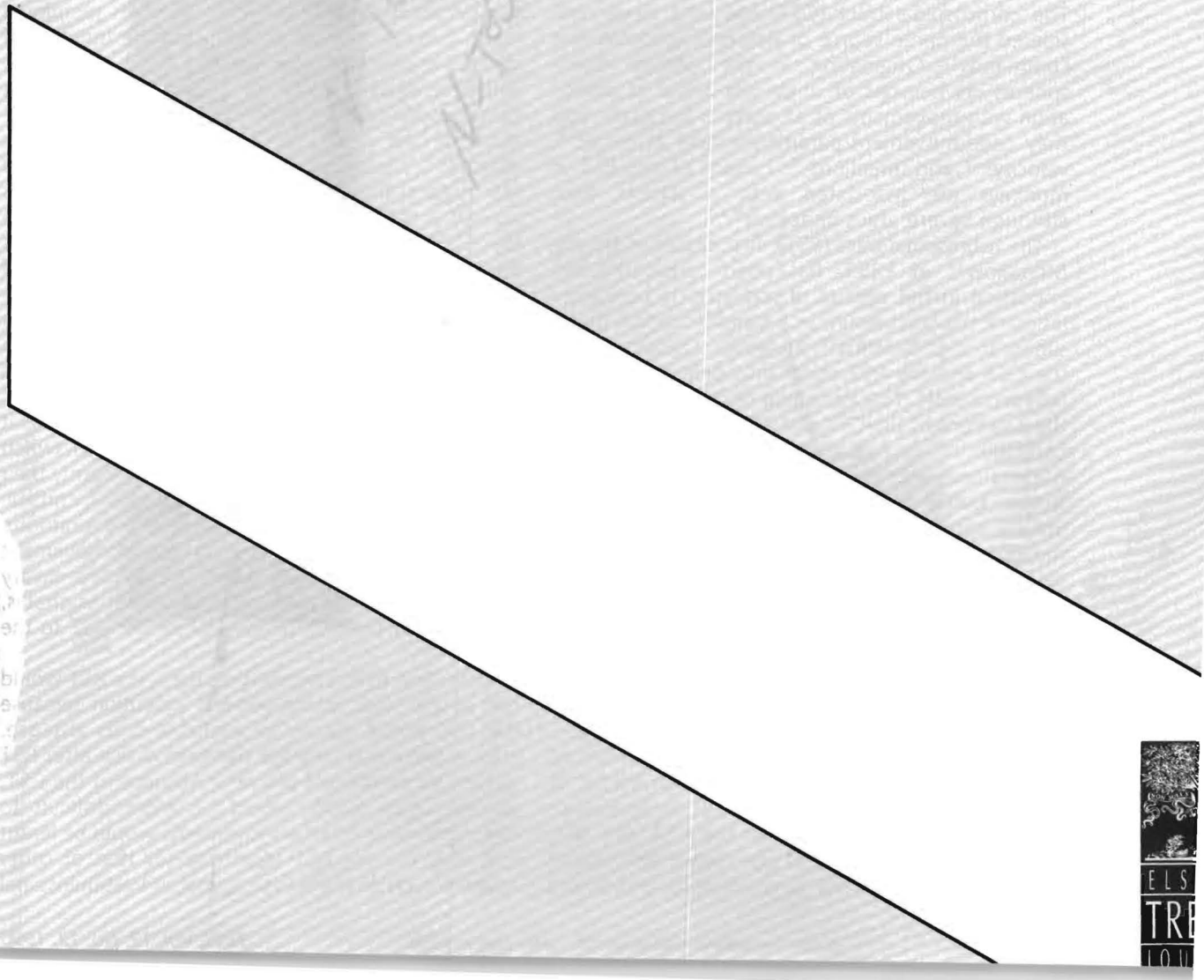

Corticospinal, rubrospinal and rubro-olivary projections: a unifying hypothesis

Philip R. Kennedy

ilip R. Kennedy is at the Neuroscience aboratory, Georgia Institute of Technology, Room 325, Centennial Research Building, 400 10th Street, Atlanta, GA 30332, USA.

There has been a dispute about the corticospinal and rubrospinal tracts for about 100 years. Both are descending motor pathways and have remarkably similar functional properties. It has been proposed previously that each system is primarily active in different movement contexts. The corticospinal tract is most involved when a new movement is being learnt, while the rubrospinal tract is preferentially active when automated movements are being executed. However, what structure decides which system should be in use? In this article Philip Kennedy discusses the evidence that the rubro-olivary tract switches between the two systems depending on the context of the movement.

The corticospinal tract (CST) has long been considered the prime source of descending movement commands[1]. Originating in the cortical hemispheres, its neurons of origin are active in association with movements of all parts of the body, and they code movement parameters such as force[2–4], velocity[5–7] and direction[4–8]. Lesions of the CST in monkeys are associated with a paresis that, although severe, does disappear[9,10].

The rubrospinal tract (RST), first described by von Monakow[11] in 1883, has been considered less important in the control of movements because a lesion of this tract results in a transient deficit that is similar to a CST deficit[12]. However, lesions of both the CST and the RST result in a deficit that never fully recovers[12]. This intriguing finding suggests that the functions of the CST and RST are interrelated. In conscious, moving monkeys recordings from the red nucleus neurons (that give rise to the RST) suggest further similarities with the CST. These recordings initially suggested a role in the terminal phase of movements[13] but later recordings have shown clearly that RST activity precedes movement and that movement parameters such as force[14], velocity[15] and direction[16] are related to this activity. This striking similarity between the RST and CST is highlighted by the further finding that RST activity is related to individual digit movements[16], not just conjoint or grouped movements of the digits[17]. Moreover, proximal–distal limb representations occur in the red nucleus in a proportion similar to that in motor cortex[17]. This has led to an intense search for differences between the CST and RST, but few have been found. Is one system redundant? Perhaps the answer lies in considering movement context. In this scheme, the CST is predominantly active when new movements are being learned, an idea first proposed by Paillard[18]. The RST, on the other hand, is active when learnt, automated movements are executed, an idea recently discussed by Massion[19].

What, then, has the rubro-olivary projection to do with the RST and CST? This projection originates from the red nucleus, as its name suggests, along with the RST. It projects only to the inferior olivary nucleus[20] and thence to the cerebellum[21]. It indirectly projects to motor areas via the cerebellum and, in addition, only indirectly receives peripheral input. It is not surprising, then, that the function of the rubro-olivary projection has been difficult to elucidate. Neuroanatomical tracing studies show a somatotopic representation[22], while an interpretation of the results of single-unit recordings is difficult[23]. Moreover, recent results with lesioned rats suggest that the rubro-olivary projection plays no part in the control of ongoing movements, as do the CST and RST; interestingly however, it was found to play a role in compensating for lesions of the RST. The present proposal is that if the rubro-olivary projection can compensate for RST lesions by reprogramming the cerebellum and downstream motor systems such as the CST, then it can reprogram the RST in unlesioned animals as the CST is executing new movements. In other words, it programs movements under CST control to switch to RST control. As the movements are learnt, their execution becomes automated under RST control. The activity of CST would remain as a monitoring system ready to respond to changes in movement context. This switching function of the rubro-olivary projection is seen as acting in both directions, that is, it can switch the CST to the RST or the RST to the CST.

According to this hypothesis, then, the RST would not be essential for movement execution because the CST would always be available in its absence. Hence, there was only the transient deficit after RST lesions, as mentioned above[12]. Absence of the CST, on the other hand, would be more difficult to overcome since no new movements would be learnt and only the old RST repertoire (or that of other systems such as the reticulospinal or vestibulospinal

 0166 - 2236/90/$02.00

tracts) would be available for movement control. This is one explanation for the slow recovery after CST lesions[9,10]. The combined loss of the CST and RST would be the most devastating of all because in that situation other systems would have to take over movement execution and motor learning, a situation that is never fully achieved as animals with such lesions do not recover completely[12].

Rubro-olivary projection anatomically links the CST to the RST

In monkeys, CST neurons receive input from many areas of the cortical hemispheres including the sensory, premotor and supplementary areas, and subcortical regions such as the thalamus and basal ganglia[7]. As shown in Fig. 1, CST output passes down through the diencephalon to the brainstem where it largely decussates before descending to the contralateral spinal cord. It terminates in gray matter throughout the full length of the cord, with some terminations on the motor neurons of the ventral horn and the intermediate gray but most on the dorsal horn[24]. Of relevance to the present discussion is that it collateralizes extensively in its descent with collaterals to the red nucleus neurons that give rise to the RST, as shown electrophysiologically[25] and anatomically[26]. Note that the red nucleus in monkey has histologically distinct divisions known as the magnocellular (RNm) and parvocellular (RNp) divisions (not shown) that give rise to the RST and the rubro-olivary projection (Fig. 1). In rat, however, double-labelling experiments show that the same neurons give rise to the RST and to the rubro-olivary projection so that the divisions are not histologically distinct[27,28]. However, because they are functionally distinct (see below), they will be treated here as distinct entities.

In monkey, RST axons leave RNm and decussate immediately before descending to the contralateral spinal cord, terminating mainly in the intermediate gray, with a small proportion on the motor neurons of the ventral horn[24]. RNm neurons receive input from the cortical hemispheres, mainly area 4, with a convergence ratio of 10:1 (Ref. 26). In addition, they receive input from about 40% of CST axons. These inputs terminate on distal parts of the dendrites. Input from the interposed nucleus of the cerebellum terminates on more proximal parts of the dendrites and soma, and is therefore more efficacious in driving RST neurons. This is shown in Fig. 2. The situation is essentially similar in rat and monkey, except that in rat, the RST collateralizes extensively to the cerebellum[29], lateral reticular nucleus[30,31] and inferior olivary nucleus[27,28]. In addition, both dentate and interposed nuclei project to the red nucleus as described below. For the sake of clarity, the connections pertaining primarily to the monkey are shown in Fig. 2.

In both monkey and rat, the neurons in the red nucleus that give rise to the rubro-olivary projection are 'great communicators' receiving massive input from the cortical hemispheres and relaying this via the cerebellum to the RST neurons. In monkey, these cortical areas include motor areas 4 and 6

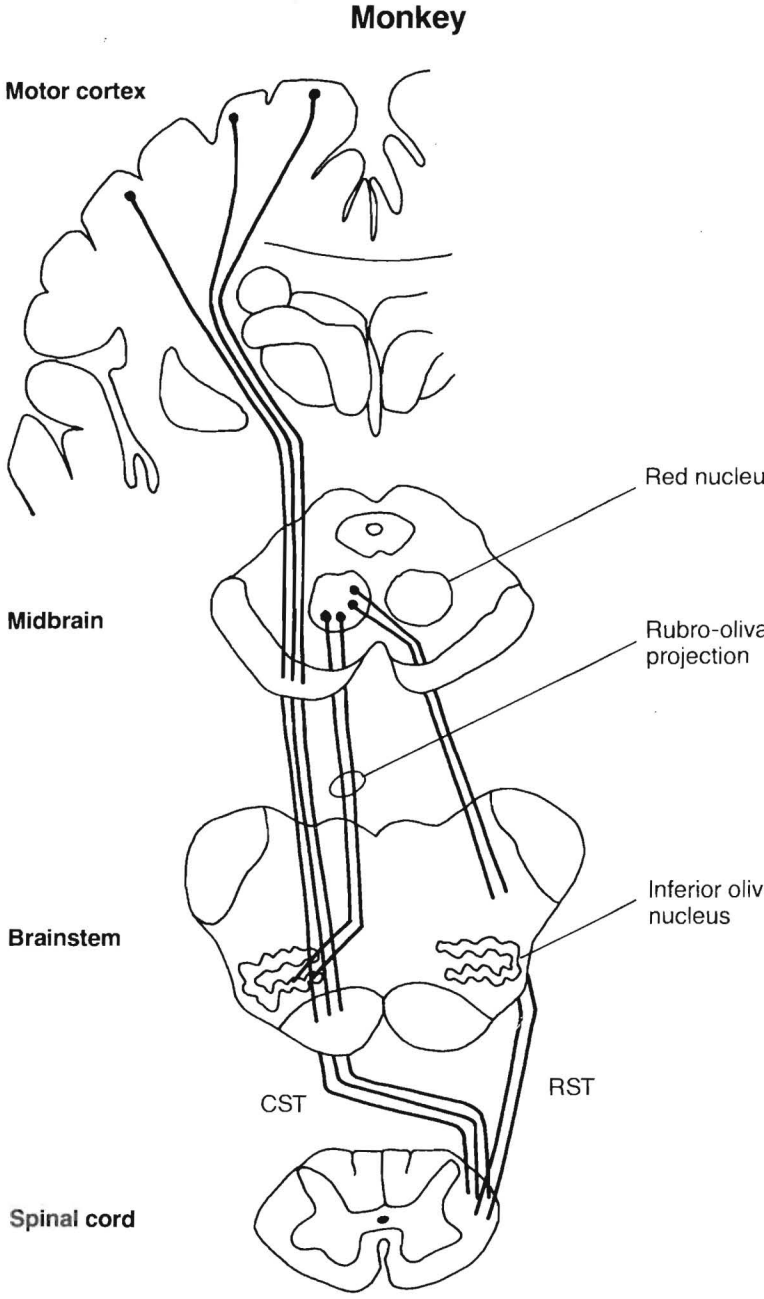

Fig. 1. *Sections of monkey brain at the level of the motor cortex, midbr brainstem and spinal cord showing the origin of the corticospinal tract (C its passage through the midbrain where collaterals travel to the red nucl and on to the pyramids where it decussates before descending in dorsolateral funiculus of the spinal cord. The rubrospinal tract (RST) origin from the red nucleus in the midbrain, crosses immediately to descend thro the lateral brainstem to the dorsolateral funiculus of the spinal cord whe intermingles with the CST. In rat, the CST and RST remain separate in spinal cord, with the CST descending in the ventral part of the dorsal colu (not shown). In both species, the rubro-olivary projection descends from red nucleus in the midbrain to the inferior olivary nucleus in the ipsilat brainstem. In rat, however, the rubro-olivary projection is a collateral of RST.*

(premotor and supplementary), area 8, parietal area 5 and cingulate areas 24 and 31 (Ref. 26). These areas are more extensive than those from which the CST originates, and there is a massive 100:1 convergence onto the neurons of origin of the rubro-olivary projection[26]. Moreover, these cortical

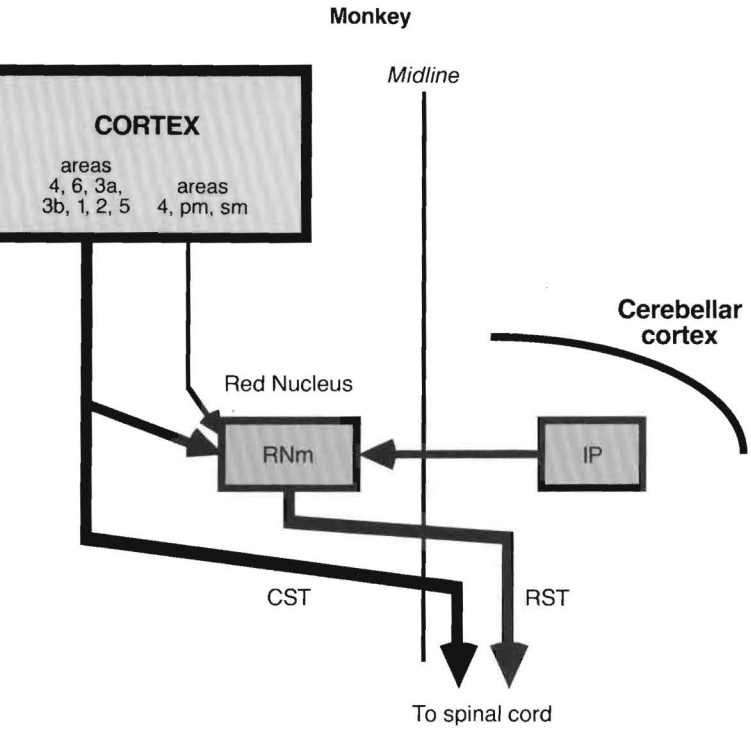

g. 2. *Crossed corticospinal tract (CST) of the monkey sends collaterals to eurons of origin of the rubrospinal tract (RST) in the magnocellular division of e red nucleus (RNm). This division also receives some direct input from areas and 6 of the motor cortex, and a more dominant input from the interposed ucleus (IP) of the cerebellum.*

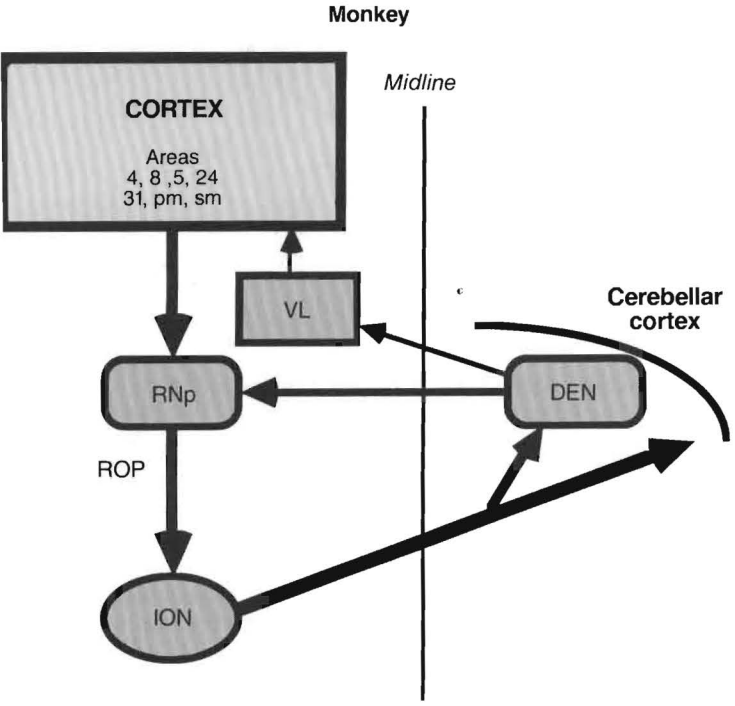

. 3. *Distinct system in the monkey originates from widespread areas of the tex which send a massive input to neurons of origin of the rubro-olivary jection located in the parvocellular division of the red nucleus (RNp). There ot a relay to the spinal cord, but instead to the inferior olivary nucleus (ION) ich projects to the cerebellum. The cerebellum, including its dentate nucleus N), projects back onto neurons of RNp, and also to the ventrolateral leus of the thalamus (VL) for relay back to the cortex. Abbreviations: pm, motor area; sm, supplementary motor area.*

neurons originate mainly from lamina Va, dorsal to lamina Vb in which corticospinal and corticorubrospinal neurons reside[26]. Unexpectedly, this enormous input to rubro-olivary projection neurons of origin does not descend as a major alternative motor output to the spinal cord but instead projects to the ipsilateral inferior olivary nucleus, specifically the principal and medial accessory divisions. These divisions project via the climbing fibers to the cerebellar nuclei and overlying cortices[21]. The interposed nucleus projects to the red nucleus neurons that give rise to the RST. The dentate nucleus projects to the motor cortex via the ventrolateral nucleus of the thalamus as well as feeding back onto red nucleus neurons that give rise to the rubro-olivary projection. Clearly, as summarized in Fig. 3, rubro-olivary projection neurons are the 'great communicators' between extensive cortical areas and the RST via the inferior olive and cerebellum.

The anatomical links described above pertain mainly to the monkey and are more complex in the rat. Figure 4 is an attempt to simplify this complexity. There are two major differences germane to the discussion. The first is that the rubro-olivary projection in rat is wholly or partly a collateral pathway of the RST[16,28]. The second is that the full rostrocaudal extent of the red nucleus receives input from the cerebellar dentate nucleus[32]. Other recent studies show that neurons from the full rostrocaudal extent of the red nucleus project to the spinal cord as the RST[27,28]. A rostrocaudal overlap of the projections of cerebellar dentate and interposed nuclei has been described[33]. Thus, dentate and interposed nuclei project to the red nucleus and terminate on neurons that give rise to both the RST and the rubro-olivary projection (Fig. 4). These connections in rat are emphasized since some of the findings described below were made in this species.

Similarities between CST and RST functions

In monkey, movement parameters are common to both the CST and RST. These parameters are velocity (CST[5–7]; RST[14–17]), force (CST[2,3,7]; RST[14,34]) and timing (CST[2,7]; RST[14–17,34]). Most reports show that neural activity is related to particular directions of movements (CST[4,8]; RST[15–17]) but not all agree[4]. The parts of the body represented in each area are similar, with a greater representation of distal than proximal limbs (CST[35,36]; RST[15,17,23,37]). Lesions of the CST[9,10,38] disrupt movements as do RST lesions[12,39] but recovery rates are markedly different, as described above.

Differences between CST and RST functions

There is a big difference in the recovery time from lesions of the CST[9,10,38] and the RST[12,39]. Both systems are reported to differ in their responses to sensory stimuli (CST[40]; RST[14,23,41,42]), although there is not full agreement[43]. An analysis of the neurophysiological properties of both systems[14] shows at least five distinct differences, these differences indicating that the CST is a more 'sensitive' system than the RST.

(1) The ratio of peak activity to baseline activity in

the spike-triggered averages of muscle activity is greater for the CST (14.6 : 1) than for the RST (6.8 : 1). This is interpreted as implying that the CST has a greater effect on specific muscles than the RST, or that the muscles are more sensitive to the CST than to the RST.

(2) Measurements of static torque exerted during performance of the same task show that each CST neuron on average fired 480 times per second for each Newton meter of torque exerted, compared with 128 times per second for RST. This is interpreted as indicating that the CST can 'fine-tune' torque control better than the RST.

(3) Flexion/extension bias is different. The CST neurons are almost equally related to flexor and extensor muscles, whereas the RST neurons are more often related to extensors. This relative lack of flexor control for the RST implies that this system has a smaller repertoire of control properties and is a less sensitive control system.

(4) Phasic/tonic properties differ. The paramount control signal of RST neurons is phasic, whereas CST neurons are almost as often tonic as phasic and fire during constant velocity or ramp movements as well. Only the occasional RST neuron has ramp properties[15,43].

(5) The average lead time for CST neurons[14] is 71 ms, which is shorter than the average lead time for RST neurons (96 ms[14], 92 ms[16] and 80 ms[15]).

Further differences are shown in Table 1 of Cheney *et al.*[14] Overall, these differences in the properties of the CST and RST indicate that the CST has more sensitive control over movements than the RST. This would be expected of an adaptive system, such as that proposed for the CST, whereas an automated system, such as that proposed for the RST, will be less sensitive and still maintain robust operation in its role as an automaton.

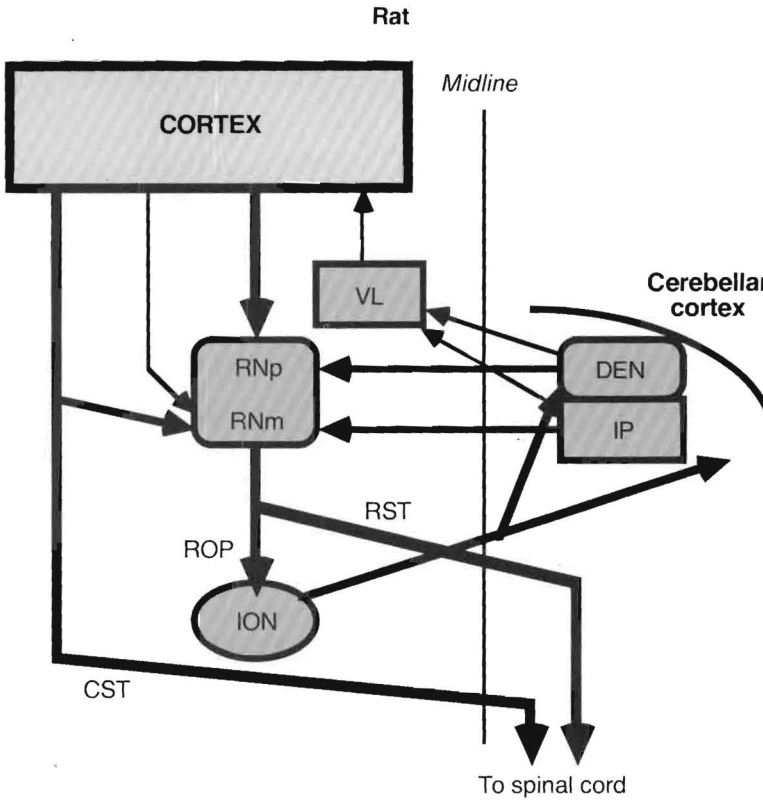

Fig. 4. *Connections in rat are more complex than in the monkey because divisions of red nucleus (RN) are functionally distinct but histologically sim Thus, no boundary is shown between RNp and RNm in this diagram. Beca neurons in RN can be double-labelled from ION and the spinal cord, output path from inferior olivary nucleus (ION) is shown singly and t bifurcates, projecting to the ION as the rubro-olivary projection (ROP) an the spinal cord as the rubrospinal tract (RST). The ION then projects to cerebellar nuclei which relay to the red nucleus (RNm and RNp) and also to cortex via the ventrolateral nucleus of the thalamus (VL).*

Functions of the enigmatic rubro-olivary projection

The inferior olivary nucleus and the cerebellum are involved in error detection[44,45], event detection[46] and classical conditioning[47]. Axonal connections from cortical hemispheres to this complex of adaptive motor control systems come partly from the rubro-olivary projection, as previously discussed (Figs 3 and 4). Theories have included the rubro-olivary projection in motor learning[45,48] and even in the mental practice of movements[21]. Experimental evidence is only now accumulating that shows the rubro-olivary projection is involved in these functions.

This evidence[39] was obtained from experiments in rats; a rubro-olivary projection has recently been described[49]. Rats were trained to walk on a slowly rotating horizontal bar suspended 0.7 m above a cushion. This sensitive test of motor control was scored for an 80% success rate that counted footslips as failures. Normal rats learned to walk on the bar in four days and then received RST transections or fiber-sparing lesions of the red nucleus. Rodents, unlike monkeys and cats, have separate RSTs and CSTs, so that RST lesions not involving the CST could be made[39]. The results are shown in Fig. 5. Lesions of the RST at cervical segment 3–4 produced an ipsilateral hemiparesis that recovered in a few days. A subsequent lesion of the opposite red nucleus also showed a rapid recovery. However, a lesion of red nucleus that was not preceded by an RST lesion showed no recovery or a very slow recovery over months. Control lesions of structures surrounding the red nucleus, or partial lesions of the red nucleus, showed rapid recovery.

These results are interpreted as follows. (1) Since RST lesions in rats leave the CST and the rubro-olivary projection intact, the rapid recovery may be the result of CST activity, as expected from Lawrence and Kuypers' results in monkeys[9]. Assuming the rats before lesioning were operating under automated RST control, it is proposed that the rubro-olivary projection assisted the system in switching to CST control. (2) Lesioning the red nucleus after the RST lesions destroyed the neurons of origin of the rubro-olivary projection but because recovery from the RST lesions had already occurred, i.e. the system was now under CST control, no undue delay in recovery was seen. (3) Red nucleus lesions performed in the presence of an intact RST would have simultaneously destroyed both the

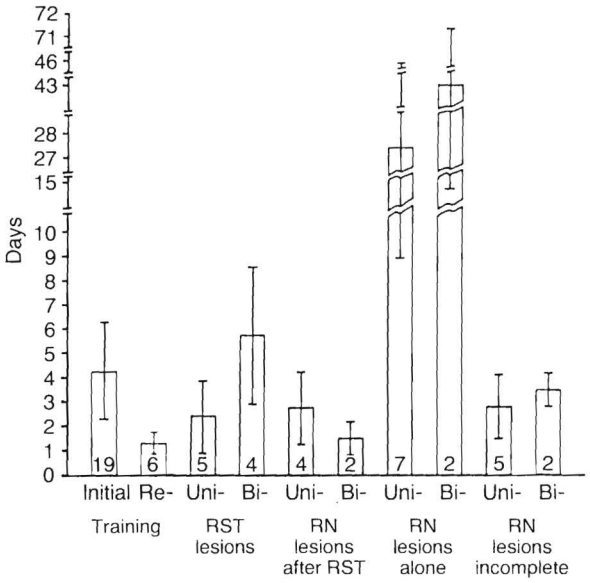

Fig. 5. *Rats took four days on average to learn to walk on a rotating bar with 80% success. After uni- or bilateral rubrospinal tract (RST) lesions they walked on the bar within a few days. Lesions of the red nucleus (RN) in rats that had compensated for RST lesions, produced no loss of ability to walk on the rotating bar. However, red nucleus lesions alone produced a prolonged deficit in rotating bar walking. Incomplete lesions of the red nucleus, or lesions surrounding the red nucleus, produced no such deficit. When only the RST was lesioned compensation could occur, but since compensation did not occur with red nucleus lesions that involve neurons that give rise to the RST and the rubro-olivary projection, the implication is that the rubro-olivary projection is important for the compensation. Further interpretations are in the text. Numbers of animals used in each test are at the base of each bar.* (Taken, with permission, from Kennedy and Humphrey[39].)

neurons of origin of the rubro-olivary projection and those of the RST, so that despite an intact CST, switching from the RST to the CST could not occur. This strongly indicates that the rubro-olivary projection was the key to the recovery.

These interpretations suggest that the rubro-olivary projection is involved in switching, or reprogramming, from automated RST control to CST control. Figure 4 (pertaining to the rat) shows the available pathways. As the RST-lesioned rat attempts to walk on the rotating bar, error signals ascend to the cortex (and other areas, including the cerebellum). It is proposed that descending motor commands also descend to the rubro-olivary projection as corollary discharges. These then project via the rubro-olivary projection to the inferior olivary nucleus and cerebellum, and then loop back via the ventro-lateral nucleus of the thalamus to the cortical neurons of origin of the CST.

There is also a loop by which the rubro-olivary projection could be involved in switching from the CST to the RST. This is also shown in Fig. 4. After a lesion to the CST, error signals would ascend to the cortex (and other areas, including the cerebellum), and corrective signals would descend both to the disrupted CST and to the rubro-olivary projection as corollary discharges. The corollary discharges going to the rubro-olivary projection would then project to the inferior olivary nucleus and cerebellum, and thence to RST neurons. RST neurons would then send descending commands to the spinal cord and muscles.

Selective CST lesions have not been made in the rat. Pyramidotomies involve important nearby structures such as the inferior olivary nucleus (for an example see Fig. 1 in Ref. 50) so that a lack of compensation is to be expected. Lesions of the CST in the spinal cord have not been reported in the literature. Cortical lesions do produce a long-lasting deficit[51] but since such lesions destroy projections to the rubro-olivary projection, compensation or reprogramming by way of the rubro-olivary projection, inferior olivary nucleus and cerebellum, could not have been possible. Clearly, a selective lesion of the CST is necessary to test fully the hypothesis in the rat.

In the monkey, pyramidal lesions can be more selective because of the ease of ablation. Schwartzman[10] found that after unilateral pyramidal lesions recovery of arm and individual finger function occurred when the monkeys were trained on a keyboard over a number of years. The slow recovery is not surprising since the rubro-olivary projection is attempting to reprogram the unsophisticated RST automaton (or other systems such as reticulospinal or vestibulospinal systems). Lawrence and Kuypers also found recovery after pyramidotomy[9] but without recovery of fine finger movements. This may be because observations were only continued over two months, and the animals were not retrained. It could also be the result of damage to the nearby inferior olivary nucleus. Primate cortical lesions, as in the rat, would also damage inputs to the rubro-olivary projection, and so would not be expected to show full recovery.

Implications

The preceding evidence has important implications for the recovery of function in humans and animal models of stroke. Humans do not have a distinct RST descending from the midbrain[52]. This reduction or absence of the RST may explain why human recovery from stroke is slower or less complete than in other mammals.

The hypothesis also has important implications for motor learning and adaptation. It provides a hypothetical framework for experiments aimed at understanding the functions of the CST, RST and rubro-olivary projection in the context of motor performance, specifically during motor learning and adaptation. Simultaneous long-term recordings from related neurons in each system during these motor behaviors may answer some of these questions. Note that the hypothesis suggests that the rubro-olivary projection is only an instructor that can switch between either system depending on the context of the movement. The results of the rat lesion experiments described above suggest that the rubro-olivary projection has no role in memory. If it

SOCIETY FOR NEUROSCIENCE
1992 ABSTRACT FORM

Read all instructions before typing abstract.
See *Call for Abstracts* and reverse of this sheet.
Complete abstract and **all boxes at left and below** before making copy
(please type or print in black ink).

____ Check here if this is a REPLACEMENT of abstract submitted earlier. REMIT a nonrefundable $30 for each replacement abstract.
Replacement abstracts must be RECEIVED by MAY 12, 1992.

First (Presenting) Author

Provide full name (no initials), address, and phone numbers *of first author on abstract. You may present only one abstract.*

Dr. Dianyi Yu
Neuroscience Lab
400 10th St., CRB Room 325
Georgia Tech
Atlanta, GA 30332 Fax: (404) 894-7339
Office: (404) 727-0354 Home: (404) 955-4094

SMALLEST RECOMMENDED TYPE SIZE: 10 POINT

SAMPLE:
1992 Annual Meeting
Anaheim, California
October 25–30, 1992

DEADLINE FOR POSTMARKING:

MAY 1, 1992

An asterisk must be placed after the sponsor's (signing member) name on the abstract.

Presentation Preference

Check one: ☐ poster ☒ slide

Themes and Topics

See list of themes and topics. Indicate below a first and second choice appropriate for programming and publishing your paper.

1st theme title: Motor Systems theme letter: G
1st topic title Spinal Cord and Brain Stem topic number: 101

2nd theme title: Motor Systems theme letter: G
2nd topic title Cerebellum topic number: 97

Special Requests (e.g., projection requirements)

Include nonrefundable ABSTRACT HANDLING FEE of $30 payable to the Society for Neuroscience. DRAWN ON A U.S. BANK IN U.S. DOLLARS ONLY. Submission of abstract handling fee does not include registration for the Annual Meeting.

REDEFINING RED NUCLEUS: ANTEROGRADE PROJECTIONS FROM RED NUCLEUS TO THE INFERIOR OLIVARY NUCLEUS IN RAT. **D.Yu* and P.R.Kennedy. Neuroscience Lab, Georgia Tech, Atlanta, GA 30332.**

To confirm the retrograde labelling of red nucleus neurons from targets such as the inferior olivary nucleus (Yu et al., Soc. Neurosci. Abstr.,17(1)469, 1991), anterograde studies were undertaken.

Both WGA-HRP and PHA-L were injected stereotaxically into the red nucleus of adult female Long Evans rats. 5 to 15 nl of WGA-HRP were pressure injected while meniscus movement was observed. WGA-HRP or PHA-L were also iontophoretically injected using 2.5 uA monophasic cathodal pulses 100 ms in duration at 5 Hz for 10, 5 or 2.5 mins. Standard perfusion and tissue processing techniques were used.

Both tracers revealed terminal stippling contained within the boundaries of the inferior olivary nucleus (ION). Evidence of fibers in the brainstem was also seen. The very small injection sites associated with PHA-L injections within red nucleus resulted in terminal labeling confined to specific sub-divisions of ION.

These anterograde tracing studies corroborate the retrograde studies in providing evidence for the existence of a rubro-olivary projection in the rat.

Supported by NS grant 24602.

KEY WORDS: (see instructions p. 4)

1. Inferior Olivary Nucleus
2. Red Nucleus
3. WGA
4. PHA-L

Signature of Society for Neuroscience member required below. ***No member may sign more than one abstract. The signing member must be an author on the paper and an asterisk must be placed after the sponsor's (signing member) name on the abstract.***

The signing member certifies that any work with human or animal subjects related in this abstract complies with the guiding principles for experimental procedures endorsed by the Society. This signature acknowledges that each author on this abstract has given consent to appear as an author.

Society for Neuroscience member's signature | Dianyi Yu (Printed or typed name) | (404) 727-0354 (Telephone number)

SOCIETY FOR NEUROSCIENCE
1991 ABSTRACT FORM

Read all instructions before typing abstract.
See *Call for Abstracts* and reverse of this sheet.
Complete abstract and all boxes
at left and below before making copy.

____ Check here if this is a REPLACEMENT of abstract submitted earlier. REMIT a nonrefundable $30 for each replacement abstract. Replacement abstracts must be RECEIVED by MAY 10, 1991.

First (Presenting) Author

Provide full name (no initials), address, and phone numbers *of first author on abstract. You may present only one abstract.*

Dianyi Yu

Neurosci. Lab, CRB

Georgia Tech.

Atlanta, GA 30332

Fax: (404) 894-3120

Office: (404) 894-4257 Home: (404) 939-9541

SMALLEST RECOMMENDED TYPE SIZE: 10 POINT

SAMPLE:
1991 Annual Meeting
New Orleans, Louisiana
November 10–15

DEADLINE FOR POSTMARKING:

MAY 1, 1991

Presentation Preference

Check one: X poster ☐ slide

Themes and Topics

See list of themes and topics. Indicate below a first and second choice appropriate for programming and publishing your paper.

1st theme title: Motor Systems

theme letter: G

1st topic title Spinal Cord & Brainstem topic number: 101

2nd theme title: Same

theme letter: ___

2nd topic title Cerebellum

topic number: 97

Special Requests (e.g., projection requirements)

Include nonrefundable ABSTRACT HANDLING FEE of $30 payable to the Society for Neuroscience, DRAWN ON A U.S. BANK IN U.S. DOLLARS ONLY.

REDEFINING RAT RED NUCLEUS: MULTIPLE LABELLING OF INDIVIDUAL NEURONS FROM SPINAL CORD, INFERIOR OLIVARY NUCLEUS AND CEREBELLAR NUCLEI. **D.Y.Yu, S.Na*, J. Wilson* and P.R.Kennedy. Neurosci. Lab, Georgia Tech, Atlanta, GA 30332.**

Previous studies (Tucker and Kennedy, Soc. Neurosci. Abstr. 1990, 16(1):729) showed that Red Nucleus (RN) neurons were doubly labelled from the spinal cord and inferior olivary nucleus (ION). About two thirds of RN neurons that projected to the spinal cord also projected to the ION. Huisman et al. (Brain Res., 1983, 264:181-196) showed that RN neurons also projected to both the spinal cord and the cerebellar nuclei (CbN). The possibility that individual RN neurons might project to all three targets was examined using Fluorogold, Diamidino Yellow and WGA-HRP.

Each neuron was examined under brightfield and fluorescent light. The previous findings of double labelling between spinal cord and ION, and spinal cord and CbN were confirmed. A new finding of neurons doubly labelled from ION and CbN was made. More importantly, some RN neurons were triply labelled. We are analyzing labelled neuron classes, their numbers and distributions. In sum, individual RN neurons project to spinal cord, ION and CbN.

Grant: NS 24602-03.

KEY WORDS: (see instructions pg. 4)

1. Red Nucleus
2. Inferrior Olivary Nucleus
3. Cerebellar Nuclei
4. Rubrospinal Tract

Signature of Society for Neuroscience member required below. *No member may sign more than one abstract. The signing member must be an author on the paper.*

The signing member certifies that any work with human or animal subjects related in this abstract complies with the guiding principles for experimental procedures endorsed by the Society.

Society for Neuroscience member's signature

Dianyi Yu
Printed or typed name

(404) 894-4257
Telephone number

SUBMITTED TO J. COMP. NEUR

Paper 1 (of 2).

Redefining Rat Red Nucleus: I. Cytoarchitecture, and Projections to Inferior Olivary Nucleus, Spinal Cord and Cerebellum.

Philip R. Kennedy, Sara A. Lee and Dianyi Yu.

Neuroscience Laboratory
Bioengineering Center
Room 325, Centennial Research Building
Georgia Institute of Technology
Atlanta, Georgia 30332.

Short Title: Cytoarchitecture and projections of Rat Red Nucleus.

Key Words: Anterograde; retrograde; Fluorogold; WGA-HRP; PHA-L; Diamidino Yellow.

38 text pages, 16 figures, 1 table.

Correspondance: Dr. Kennedy, address as above, phone 404-894-4257, fax 404-894-7025.

Last Update: 9/24/92.
Filename: ANATPA-1.92

ABSTRACT

Five types of neurons were identified in rat red nucleus by thionin staining and their numbers and normal distributions were analyzed. Three types of parvicellular neurons and two types of magnocellular neurons were found. The parvicellular neurons were located throughout the nucleus and overlapped the magnocellular neurons which were confined to the caudal two-thirds approximately. Injections of WGA-HRP and PHA-L largely confined to the red nucleus anterogradely labelled the inferior olivary nucleus (ION), spinal cord (SC) and cerebellum (CB). Retrograde tracers from these targets confirmed the anterograde findings and allowed identification of the labelled neurons. All five types of neurons were labelled from each target.

Distinct divisions could not be clearly defined on the basis of neuronal cytoarchitecture since the distributions of different neurons overlap extensively. Nor could a definition be made on the basis of projections of specific neurons to specific targets since all five types of neurons have multiple projections that do not follow a discernable pattern of organization.

INTRODUCTION

The term red nucleus is often used without distinguishing between its parvicellular and magnocellular divisions. These histological divisions have been recognized in most mammals (Massion, '67). In the monkey, for example, the transition between divisions is abrupt, with parvicellular neurons found in the rostral parvicellular division, and two types of magnocellular neurons found caudally (King et al., '71). There is also a clear functional difference between these divisions in the monkey (Kennedy et al., '86). In the rat also, there is evidence for a functional difference between these divisions as defined by their projections (Kennedy and Humphrey, '87). There is no evidence in rat, however, for histologically distinct divisions on the basis of light microscopic examination because neurons of different morphological shapes and sizes are not neatly separated into rostral and caudal distributions. These neurons have been classified on the basis of four different sizes (Reid et al., '75). The giant and large neurons were found mainly in the caudal region and designated magnocellular, and the medium and small neurons were found mainly in the rostral region and were designated as parvocellular, though large neurons extended rostrally. In the present study, we confirm that neurons are graded from large to small, and in addition, find that neurons of different dimensions are morphologically similar to those seen in monkey, namely, some are parvicellular-like and others are magnocellular-like (as

defined below). The first part of this paper briefly re-examines the classification of red nucleus neurons in rat and their distribution within the nucleus in the expectation that nuclear divisions (if they exist) might be redefined on that basis.

Projections from red nucleus have been described. Neurons of the magnocellular division give origin to the rubro-spinal tract (RST) that projects to the contralateral spinal cord and brainstem in monkey (Miller and Strominger '73) and cat (Edwards '72). The brainstem targets include facial, trigeminal and lateral reticular nuclei. In the rat, the RST is said to arise from both magnocellular and parvocellular divisions, but the definition of divisions is based solely on rostral and caudal distributions, and since retrogradely labelled neurons are found throughout the nucleus they are assumed to arise from both divisions (Shieh et al., '83, Brown '74). We believe that a more precise definition based on other critieria such as neuronal morphology is needed. Projections to the cerebellum (CB) have also been described in the rat (Huisman et al., '83). Projections to ipsilateral ION are described in man (Nathan and Smith, '82), monkey (Bebin '56, Courville and Otabe '74, Strominger et al., '79) and cat (Conde and Conde '82) and arise from neurons of the parvicellular division. In rat, Brown et al. (1977) found some evidence of a projection but considered it insufficient, as did later workers (Carlton et al., 1982; Rutherford et al., 1982). With the use of newer techniques, however, a rubro-olivary projection has been described (Kennedy

'87b). Its neurons of origin, however, are not defined. To further confuse the picture in the rat, some descending projections to ION also branch to the SC and CB (Kennedy '87a, Tucker et al., '89, Yu et al., '91).

An attempt is made in the second part of this paper to clarify this situation by defining the types of neurons that contribute to the output projections. For example, parvicellular neurons might be expected to project exclusively to ION, or magnocellular neurons to SC. Unfortunately, such a clear separation between divisions and projections in the monkey (Massion '67, Courville and Otabe '74, Strominger et al., '79, Kennedy et al., '86), is not found in the rat. We find instead that all five types of neurons project to all three targets. There are, however, some relative differences in the numbers and distributions of projecting neurons. The further finding that each type of neuron can project to two and three targets is presented in a following paper. Preliminary results have been presented (Yu et al., 1991; Tucker and Kennedy, 1990; Tucker et al., 1989).

METHODS

Cytoarchitectural Studies

Five female Long Evans hooded rats between 3 and 6 months of age are used. After an euthanitizing dose of Nembutal (0.3 ml of 65 mg/ml, intraperitoneally) they are perfused through the heart with 250 mls of normal saline followed by 250 mls of 10% formalin. After removal of the brain, further fixation is assured by immersion in 20% sucrose dissolved in 10% formalin. The complete brain is sectioned coronally (3 rats) or parasagittally (2 rats) every 40 µm on a freezing stage, and every section through the red nucleus (RN) is mounted on alternate subbed slides, thereby producing two sets of almost identical sections. After air-drying overnight, the tissue is dehydrated in 100% alcohol and stained with Thionin (pH not above 3.5 for clearest background) followed by washing in distilled water and graded concentrations of alcohol to lighten the stain as desired. Slides are coverslipped using DPX (BDH Chemicals Ltd., Poole, England) as the mounting medium.

The tissue is microscopically examined under direct light with 10x, 20x or 40x objectives. Neuronal outlines are traced with a drawing tube every 160, 240 or 320 µm. A reference point is marked on each tracing for alignment. This point is 750 µm ventral and lateral to the midpoint of the third ventricle. This is checked by measuring also from a histomark made by passing a needle through

the left side of the brain during freezing. This reference point is used to align each section for digitization on a 12 by 18 inch tablet attached to an 8 MHz Hewlett Packard Vectra computer (Intel 286 microprocessor, 640 KHz RAM, 40 MB hard disc, Intel 80287 math co-processor) that uses software commercially available from Jandel Scientific (Corte Madera, CA 94925). Each of the five neuron types is color-coded during tracing under the 20x objective, the 40x objective is used for confirmation of classification, and each neuron is color-coded when digitized. The program allows two or three dimensional display and plotting of any or all neurons. Plotting is performed on an Hewlett Packard 7475A six pen plotter. Neurons of interest are photographed through the microscope with standard high speed color or black and white film.

Cell counts are obtained from the digitized data and also by counting the neurons directly from the tracings as performed by two observers. If counts differ, the neurons are recounted until agreement is reached.

Anterograde Tracing Studies

Under clean conditions, injections are made under Ketamine anesthesia delivered intraperitoneally in a dose of 100 mg/kg of body weight. Wheat germ agglutinated horse radish peroxidase (WGA-HRP) is pressure injected into the vicinity of RN using micropipettes with tip diameters of 30 um, or by iontophoresis with

tip diameters of about 15 um. In 17 250-300 g female rats, the micropipette is positioned at AP +1.9 to +2.5 mm from the intra aural line and 1 mm from the midline, before being lowered to 6.6-7.1 mm below the cortical surface, with the nose bar elevated to 5.3 mm above 0.0 according to the recommendations of Paxinos and Watson (1982). With pressure injections, movements of the meniscus are carefully observed through a microscope so that injections are minimized to 5 to 15 nl. With iontophoresis, current is monitored across an in-line 100 kOhm resistor, and delivered as 2.5 uA monophasic cathodal (+) pulses 100 ms in duration at 5 Hz for 10, 5 or 2.5 minutes depending on the required size of injection site.

After a survival time of 3 to 4 days, the rats are deeply anesthesized with Ketamine 160 mg/kg body weight, and perfused through the heart with 250 ml of normal saline followed by 500 ml of 4% paraformaldehyde in phosphate buffer (PB) at neutral pH at 4'celcius. A final 250 mls of 10% sucrose in PB is used at 4'Celcius. The brain is placed in 30% sucrose in PB for at least 48 hours at 4'Celcius. Tissue is sectioned at 40 um thicknesses on a freezing microtome into 0.01 M acetate buffer at pH 3.3. The sections are soaked for 20 minutes in 0.01 M acetate buffer containing 100 mg Nitroferricyanide and 5 mg tetra methyl benzidene (TMB) dissolved in 2.5 mls of 100% alcohol for a total volume of 100 mls. To slow the reaction, the pH of the acetate buffer is raised from 3.3 to near 4.5 pH. pH readings of 5 or above

completely arrest the reaction. The reaction product is precipitated by adding 0.8 ml of 0.3% hydrogen peroxide to 80 mls of the above solution for an additional 20 minutes. After soaking, the amount of reaction product is assessed by examination under the light microscope. If too light, further time is spent in freshly made solutions. When satisfactory, the sections are stored in acetate buffer while being mounted on alum coated slides. After air drying overnight, they are coverslipped with DPX and examined under direct light.

In addition to WGA-HRP, Phaseolus vulgaris leucoagglutinin (PHA-L), is also used to examine and confirm the projection by visualizing axons and terminal labelling (Gerfen and Sawchenko, 1984). PHA-L is obtained from Vector laboratories (Burlingame, CA) and dissolved in 10mM phosphate buffer to produce a 2.5% solution. Using the same target coordinates as above, iontophoretic injections are made with a micropipette of tip diamter 10-15 um using a 5 uamp positive current, 7s on, 7s off for 15-17 mins. Pulses are 100 ms in duration delivered at a rate of 5 hz with a constant current device. After 5-7 days survival animals are overdosed with Nembutal and perfused through the heart with 250 mls of normal saline followed by 250 mls of 4% paraformaldehdye and 250 mls of 10% sucrose in phosphate buffer at 4'celcius. Brains are post-fixed overnight in 20% sucrose in phosphate buffer at 4'Celcius. Frozen sections are cut at 40 um thicknesses and collected in ice cold 0.02M potassium phosphate buffered saline

(KPBS). Sections are incubated overnight in KPBS/0.3% TritonX100 with 2% normal rabbit serum (NRS, Cat. no. S-5000). For the next 48 hours the sections are incubated with 2ug/ml affinity-purified goat anti-PHA-L (Cat. no. AS-2224) in KPBS/2% NRS at 4'celcius. After this, the sections are processed for immunoperoxidase labelling using the Vectastatin ABC solution prepared with KPBS. First they are rinsed 2x10 min. with KPBS/2%NRS, incubated for 45-60 min. in diluted biotinylated affinity-purified Anti-Goat IgG, re-rinsed as above, incubated for 45 min. in the Vectastatin ABC solution and rinsed again as above. They are reincubated in the Anti-Goat IgG for 30 min. and rinsed as above, before a second incubation in the Vectastatin ABC solution followed by rinsing as above. They are then reacted for about 5 min. with fresh DAB tetrahydrochloride (0.05%) as the cromagen and 0.004% hydrogen peroxidase in KPBS. The sections are then rinsed in 5x5 min KPBS before mounting onto chrom alum coated slides. After air drying they are coverslipped using DPX and examined under direct light.

Retrograde Dye Tracing Studies

Brainstem Dye Placements: Dyes are placed adjacent to the inferior olivary nucleus (ION) and spread into it as verified histologically in 70 rats weighing between 100 and 325 g. The reported data are selected from female rats which are chosen in order to minimize the presence of artifactual lipofuchsin granules usually present in older rats of either sex or in young adult

males. Some young females weighing around 100g are also used; these produced the most intense labelling per neuron and the largest number of labelled neurons. Fluoro-gold (FG) dye is usually used since it produced the greatest amount of labelling per neuron while fast blue or diamidino yellow (DY) produced little labelling in RN, as also reported by Rutherford et al (1984) for fast blue. Before adopting FG as a routine procedure, other dyes are used including WGA-HRP in 7 rats, DY in 4, Fast Blue in 3, Rhodamine B in 3, and FITC latex beads in 1. FG-soaked gelfoam plegets are placed in an opening in the pyramidal tract a few mm above the foramen magnum. This avoided damage to the olivary nucleus which Blatt and Eisenman (1985) claim produce artifactual abscence of labelling. The tracer could not be transported retrogradely via the rubrospinal tract to the ipsilateral RN since that tract lies opposite the ION on the ventro-lateral part of the brainstem where spread of dye is never seen. Under anesthesia as described above, an anterior neck incision exposed the trachea which is retracted to allow access to the clivus. Tracheotomies are not performed, thus avoiding respiratory difficulties during recovery and resulting in a survival rate close to 100%. Retraction on the trachea is relaxed about every 30 to 60 seconds. Under the operating microscope, the clival bone is removed with a rongeur to expose the brainstem beginning at the foraminal opening and continuing about 3 or 4 mm rostral as far as a small blood vessel running medial to lateral. Just caudal to this vessel, the dura and pyramid are opened with an iridectomy knife and 5/0

forceps to a depth of about 1 mm. One or two plegets of dye-soaked gelfoam, hardly larger than the width of the forceps tip, are inserted into this opening, and the opening in the bone is covered with plain gelfoam. A recent modification is to insert a piece of FG-soaked gelfoam and replace it after about 3 minutes with a fresh piece. This minimized wash-out of the FG.

After a survival time of 10 days, the rats are perfused as described above. Tissue is sectioned on a freezing microtome into 0.01M acetate buffer at pH3.3, mounted on slides and after air drying overnight, coverslipped with DPX as the mounting medium. Every fourth section of tissue is examined under flourescent light at an excitation wavelength of 360 nM, and analyzed as described above.

Spinal Cord Dye Placements: Dyes are placed in the transected dorso-lateral funiculus of the spinal cord in 52 rats. WGA-HRP is used alone or in combination with FG and DY. Diamidino Yellow is usually used when only FG is placed in the brainstem. DY is placed in the spinal cord of 21 rats, WGA-HRP is placed in 20 rats, FG in 2, Nuclear Yellow in 2, Fast Blue in 5, FITC beads in 1, and Rhodamine B in 1. After induction of anesthesia as described above, rats are mounted in the stereotaxic frame with neck flexed. Under clean conditions, a laminectomy is performed at the C3 and C4 levels. After opening the dura, the dorso-lateral funiculus is transected with an iridectomy knife. About 4 to 6 small plegets of

dye-soaked gelfoam are inserted, the laminectomy opening is covered with gelfoam and the skin sutured. Data are analyzed as described above. A typical dye placement site is shown in figure 12.

Cerebellar Dye Placements: Plegets of DY-soaked gelfoam are placed near the cerebellar nuclei in 30 rats by direct insertion with a no. 5 forceps. Pieces of gelfoam are placed 4 to 5 mm deep in two rows directed medially, intermedially and laterally (5 mm deep) for a total of six pieces. Prior to using DY as a routine, other tracers are tested, including WGA-HRP in 9 rats, Rhodamine B in 3, Nuclear Yellow in 3 and FG in 1. In a control study, the DY-soaked gelfoam plegets are placed 2 mm or less into the cerebellar cortex to determine if label appeared in RN.

Determination of Neuronal Type: Two methods are used. In the first, sections are examined initially under fluorescent light, and then re-examined under direct light after lightly staining the same section with thionin. The second method involved normal thionin staining that resulted in disappearance of the dye, so that the neurons are located by placing the drawing-tube image of the thionin stained neurons over the first map drawn from the fluorescent image. In heavily labelled neurons, the fluorescent label remained after light Thionin staining as shown in figures 1A and B. The neuron in figure 1A is photographed under fluorescent light only, and the same neuron is photographed with the addition of direct light to demonstrate the Thionin stain shown in figure

1B. Sufficient label filled the soma and proximal dendrites that positive identification could be made with the FG label alone.

Figure 1 near here

Artifact Differentiation: Distinguishing FG labelling from artifact due to lipofuchsin granules is based on the following criteria. (1) The lipofuchsin granules are usually scant as shown in figure 1E when compared with FG label seen in figure 1F. (2) Artifact had a dull brown to yellowish appearance in contrast to the bright sparkle of the FG when processed as described above. (3) The artifact usually is clumped towards one side of the cytoplasm and usually did not extend into the dendrites (Fig. 1E) in contrast to the FG which is more diffuse and spread at least into the proximal parts of dendrites (Fig. 1D). (4) The artifact is usually present in both RNs, in contrast to the FG which is present ipsilateral to the ION placement site.

RESULTS

Cytoarchitecture

Classification of Neurons

The classification of rat RN neurons is modified from the description of parvicellular and magnocellular neurons in the monkey (King et al., 1971). Parvicellular neurons are defined as having rounded outlines, with a large, almost centrally placed round nucleus, and a small cytoplasmic/nuclear ratio. In other words, their nuclei appear to fill the soma, pushing the stained cytoplasm to one side. In the large parvicellular neurons where the cytoplasm is more extensive, the cytoplasmic/nuclear ratio is larger. Magnocellular neurons have an irregular, rectangular or multipolar outline, a relatively small oval eccentrically placed nucleus, with a large cytoplasmic/nuclear ratio. The nucleus of the smaller magnocellular neurons is not always eccentrically placed. Typical examples of these five different types are given in figure 2.

Figure 2 near here

The most striking difference between rat and monkey RN neurons is size. The large and giant neurons in monkey range from 50 up to 90 μm (King et al., 1971). In rat, all neuronal diameters are as

much as 20 μm smaller. Neuronal diameters are measured under the 40x objective with a calibrated graticule in the eyepiece. The results are plotted in figure 3A and B.

Figure 3 near here

Parvicellular neurons show a trimodal distribution of soma diameters, below 20 μm, between 20 and 30 μm, and above 30 μm. The magnocellular neurons show a bimodal distribution of diameters, with 30 μm being the demarcation point. These sizes define parvicellular neurons as small, medium or large, and magnocellular neurons as small or large. Thus in the rat, there are five types of RN neurons.

Numbers

Neurons are counted in coronal sections at intervals of 320 μm. Raw counts are multiplied by Abercrombie's (1946) correction factor derived for each neuron type. This sub-total is multiplied by the number of sections (eight 40-micron sections per 320 micron interval), and a final total obtained. The results are tabulated in Table 1. This analysis in three rats reveals almost 7,588 defined neurons in rat RN, of which only 17% are magnocellular neurons. Of the 6,340 parvicellular neurons, less than 10% are large, 33% are medium and the remaining 58% are small. Of the magnocellular neurons, small are twice as common as large. These

data are given on the left of the final column in the table. Overall percentages of neuronal types indicate that few are large (8 and 5% for parvicellular and magnocellular neurons respectively), 27% are medium, and 48% and 12% are small parvicellular and magnocellular neurons respectively. These latter percentages are given on the right of the final column in table 1.

Table 1
Tabulation of the five different types of neurons in rat RN.

	Raw Count	Correction Factor	Sub-total	No. of Sections	Final Total	Summary Total
PARVICELL-ULAR						6,340 83%
LARGE	108	* 0.68	73	* 8	588	9% 8%
MEDIUM	359	* 0.73	262	* 8	2,096	33% 27%
SMALL	578	* 0.79	457	* 8	3,656	58% 48%
MAGNOCELL-ULAR						1,248 17%
LARGE	62	* 0.74	46	* 8	368	29% 5%
SMALL	143	* 0.77	110	* 8	880	71% 12%
TOTAL						7,588

Distributions

The red nucleus extends from the caudal pole (left of figure 4A) containing a few hundred neurons of all types, to the wide middle region containing one and a half thousand neurons, to its rostral pole containing many hundreds of neurons. Even though all

five types of neurons are found throughout the red nucleus, distinct differences are seen in the distributions of each type. Large parvicellular and magnocellular neurons are more commonly found in the caudal two-thirds, whereas the small neurons of both types are more commonly found in the rostral two-thirds. The medium parvicellular neurons are found throughout but are more frequent caudally. This is even more obvious in the normalized data shown in figure 4B. There is no abrupt histological junction between caudal and rostral divisions. Instead, there is a gradual transition between overlapping zones that are best described in terms of neuronal size. In addition, the total number of labelled neurons discussed below is a small fraction of the total number of neurons in the nucleus.

Figure 4 near here

Lateral Horn of the Red Nucleus

An unusual feature of rat RN noted by previous authors (Reid et al., 1975) is the lateral protrusion of neurons that begins about 400 μm from the caudal pole. The neurons protrude from the ventro-lateral edge as seen in figure 10, sections 3 to 5. This horn is directed laterally and dorsally. Proceeding rostrally, the area between the horn and the body of the nucleus fills in with RN neurons so that by about 800 μm from the caudal pole the horn is no longer distinct. Even caudally, it tends to blend with surrounding

neurons and is most easily distinguished when its neurons are labelled by tracer from the spinal cord. When neurons of the horn are labelled from the lumbo-sacral spinal cord, a sharp transition is seen between labelled and unlabelled neurons close to the dorsal end of the horn. When label is introduced at the cervical level neurons are labelled throughout the horn. In the body of RN, neurons in the caudal pole are labelled from lumbo-sacral injections of tracer. As one proceeds rostrally, these lumbo-sacral projecting neurons are located ventrally.

Anterograde Tracing Studies

To determine the targets of RN output neurons, injections of WGA-HRP and PHA-L are made in RN. When iontophoresis is used, the injections are largely confined to the body of the nucleus, with minimal spillage along the needle track dorsally. An example of an injection site confined to the caudal pole of RN is shown in figure 5A. Terminal labelling is seen under polarized light in 5B (same rat) and under direct light in 5C (another rat). The label is confined to the principal olivary nucleus (5B and 5C) and medial accessory olivary nucleus (5C left). Little or no label was seen in dorsal accessory nucleus in five labelled cases, though this does not exclude the possibility of DAO projecting neurons. Also labelled were other brainstem targets including the lateral reticular, trigeminal and facial nuclei, the rubrospinal tract, and

the cerebellar nuclei.

Figure 5 near here

PHA-L injections are also confined to RN (except for the diffusion area) as shown in figure 6A for an injection into the body of the nucleus. Axons terminals and their probable synaptic boutons are seen in various areas of ION, mainly PO and MAO in the two successful cases. An example is shown in figure 6B.

Figure 6 near here

These data suggest a connection between RN and ION. To further define this connection, retrograde tracing studies are described. These studies also determine the specific neurons of origin of this connection.

Retrograde Tracing Studies

1. Neurons of Origin of the Rubro-olivary Projection

Brainstem Placement Site

Fluorogold (FG) is used to retrogradely label RN neurons from ION. The technique of placing the FG-soaked plegets of gelfoam

(see Methods) adjacent to the ION allowed the dye to spread over part or all of the ION as shown in figure 7A and B. Sometimes it also spreads beyond the lateral boundary of ION, but since anterograde projections from RN to surrounding areas are not found, except rostrally, these data are included in the analysis. The dye often spreads to the medial part of the opposite ION, or retrogradely labels ION neurons due to uptake by the olivo-cerebellar pathway damaged when passing through the directly labelled ION. This results in labelling of both the ipsilateral and contralateral RN. In a few cases, spread of FG is confined to principal, medial accessory and the adjacent parts of the dorsal accessory olivary nuclei.

Figure 7 near here

FG Labelling in Red Nucleus

Bright, white speckles of FG densely label the cytoplasm of RN neurons. When young rats weighing about 100g are used the speckles of FG are brightest and most widespread as shown in figure 8. In older rats, not used in later experiments, care is taken to distinguish labelled neurons from lipofuchsin artifact as explained in the Methods section and figure 1.

Figure 8 near here

Classification

Labelled neurons are identified according to the classification scheme described in the first part of the Results section. Neurons of all five categories are labelled from ION as shown by the filled bars in figure 9. When the percentages of neurons labelled from the ION are compared to thionin stained controls (light cross hatched bars), the numbers are similar except for the small neurons of both types. Numbers of labelled neurons are discussed below. The other data in this figure will be discussed later.

Figure 9 near here

Distributions

The distributions of the neurons retrogradely labelled after placement of dye in ION are plotted in the top row of figure 10 for sections 160 μm apart from the caudal pole to within 1 mm of the rostral pole. Plots rostral to this point are not shown because they contain only a few FG labelled neurons surrounding the fasciculus retroflexus. Data in the other rows concern neurons labelled by SC and cerebellar placements as discussed below. Neurons labelled with FG from ION are widely distributed within each section except in the dorsal region of the rostral two-thirds of the nucleus. The outlines are obtained by staining with thionin

after analysis of all labelled neurons. Stained neurons are then identified, counted and plotted so that a complete picture is obtained. The lack of any labelling in the dorsal region suggests that neurons here project to other targets such as trigeminal, facial or lateral reticular nuclei (Edwards, 1972, Miller and Strominger, 1973) in which tracers are not placed.

Figure 10 near here

The absolute and normalized values for the distribution of the different types of neurons retrogradely labelled from the ION is shown in figures 11A and B. All neurons are present in almost all sections with the exception of the most rostral regions that lack large parvicellular neurons which are most prominent caudally along with the large magnocellular neurons. The smaller neurons of both types are less frequently labelled when compared to the normal distribution shown for thionin stained neurons in figure 5A and B. Comparisons with this normal distribution also indicate an increased labelling of medium sized parvicellular neurons from ION in the rostral one third of the RN.

Figure 11 near here

Numbers

An average of 1,382+/-333 labelled neurons are counted in red

nucleus following placements of FG in 50% to 100% of the ION in 8 rats. This is less than 20% of the total number of neurons in RN. There are 1,338 neurons labelled with FG following the ION placement of FG in R63 (of figure 10 above), and 2,182 neurons following ION placement in R49. Placement sites are shown in Figure 7B. Further analysis of the number of different types of labelled neurons reveals that on average almost two thirds are parvicellular in appearance. 7% are large, 26% are medium and 35% are small parvicellular neurons, while 6% are large and 20% small magnocellular neurons. The remaining 6% of neurons are unidentifiable. These data are compared to neurons labelled from other targets and to thionin stained neurons in figure 9 above. In general, there are no large differences between percentages of neurons labelled from ION placements and thionin stained controls except for the small parvicellular and magnocellular neurons.

2. Neurons of Origin of the Rubrospinal Tract

Spinal Cord Placement Site

WGA-HRP is placed in the transected dorso-lateral funiculus as shown in figure 12. In earlier studies, DY is used instead of WGA-HRP. Either tracer is taken up by cut fibers providing extensive labelling of RN neurons.

Figure 12 near here

Labelling in Red Nucleus

WGA-HRP reaction product fills the cytoplasm of RN neurons. Care is taken to observe the reaction product during processing and slow its appearance when used in conjunction with other tracers as described in the next paper. An example of WGA-HRP labelled neurons is shown in figure 13. This figure also demonstrates nuclei filled with the fluorescent dye, DY, which in this example is placed in the contralateral cerebellar nuclei discussed in the next section. Many of these neurons, then, are doubly labelled as discussed in the next paper.

Figure 13 near here

Classification

All five types of RN neurons are labelled following tracer placements in the transected dorso-lateral funiculus of the spinal cord. The normalized data are shown by the dark hatched bars in Figure 9 above, along with thionin stained controls. The small parvicellular neurons labelled from the SC are fewer (29%) than controls (48%). Otherwise the values are close to the control values.

Distribution of Neurons

The distribution of neurons labelled from the spinal cord is plotted in the middle row of figure 10 above. The most rostral sections show relatively few labelled neurons compared to those labelled from ION. The same remarks apply to the lack of labelled neurons in the dorsal region as are made above when discussing labelling following ION tracer placements.

Figure 14 near here

The absolute and normalized values of the distributions of the labelled neurons are shown in figure 14A and B. When compared to the control values in figure 4A, the rostral half of RN shows much fewer labelled neurons overall. When examining the normalized values in figure 14B the relative differences are striking. For example, in the rostral area there are fewer small parvicellular neurons than controls, and more of all other types of labelled neurons, especially medium and large parvicellular neurons.

Numbers

Red nucleus neurons from 9 rats are analyzed for reaction product following WGA-HRP placement in the spinal cord, and 3 rats are analyzed for DY label in red nucleus following spinal cord placement. With WGA-HRP, an average of 1,402+/-438 neurons are

labelled (range: 855 to 2044). This is under 20% of the total number of neurons in RN.

When using DY as a tracer, however, only 524 neurons are labelled on average. Since both sets of data are usually obtained in combination with another tracer, a control is performed with a further tracer, FG, alone. This produced 2952 labelled neurons. The percentages of different types are essentially similar, however. Of the average 1402 neurons labelled with WGA-HRP reaction product, 12% are large, 37% are medium and 26% are small parvicellular neurons, with 7% large and 13% small magnocellular neurons. 5% are of uncertain origin. These percentages are remarkably similar to the percentages obtained using DY as the label when 8% are large, 39% medium, and 23% small parvicellular neurons, with 12% large and 12% small magnocellular neurons. A further 6% of neurons are of uncertain origin. Again, the numbers obtained with FG as the label produces similar percentages: 3% are large, 22% medium, and 24% small parvicellular neurons, and 8% large and 11% small magnocellular neurons. A high 32%, however, could not be identified with certainty. For comparison with neurons labelled from other targets and with controls, therefore, the average of these percentages are used as shown by the dark cross hatched bars in figure 9.

3. Neurons of Origin of the Rubrocerebellar Tract.

Dye Placement in the Cerebellum

Plegets of DY-soaked gelfoam are placed above the cerebellar nuclei as described in Methods. An example of such placements is shown in figure 15A where five placements are seen in one section under brightfield illumination. The area of uptake of the dye under fluorescent lighting extends 1 mm beyond the placement sites. This technique usually produces fluorescence of all cerebellar nuclei on one side as illustrated in figure 15B. Since the cerebellar cortex is traversed by the dyes during placement (note the distortion of the cortex in the top section of 15B), it might therefore be a source of uptake of dye by axon terminals of RN neurons. Accordingly, control implants are made by placing plegets of DY-soaked gelfoam in the cortex, no more than 2 mm below the surface of the cerebellum.

Figure 15 near here

Labelling in Red Nucleus

DY labels the nuclei of contralateral RN neurons as shown in figure 13 above where the DY label in the nuclei is shown with HRP reaction product in the cytoplasm. The RN projects to cerebellar nuclei rather than cortex, because when DY is placed only in the cortex, a mere 23 labelled RN neurons are found, in contrast to the many hundreds of neurons labelled by cerebellar nuclear placements

discussed below.

Classification

Applying the classification scheme described in the first part of the Results section, all five types of neurons are labelled following dye placements in cerebellum. These are shown as shaded bars in figure 9. As with the values for neurons labelled by other tracers, the values for the small neurons of both types are different from the control values.

Distribution

The distribution of RN neurons projecting to cerebellum is shown in the bottom row of figure 10. This distribution is unique compared to the distribution of neurons labelled from the other two targets. First, in the caudal pole very few DY labelled neurons are found. Second, in approximately the middle third the neurons tend to lie in the dorsal region compared with neurons labelled from other placement sites. In the rostral pole, the lack of labelled neurons in the dorsal region is similar to the lack of labelled neurons following placement of tracers in other sites.

Figures 16 near here

The absolute and normalized values of the distributions are

shown in figures 16A and B. Compared with the control values of figures 4A and B, the paucity of labelled neurons in the caudal pole is obvious. In addition, where neurons are abundant, there are more large and small magnocellular neurons compared with the numbers of control unlabelled neurons.

Numbers

Red nucleus neurons in 12 rats are analyzed for the presence of dye following Diamidino Yellow dye placement in the cerebellum as described above. An average of 412+/-199 neurons are labelled, ranging from 107 to 813 neurons. Of these, over two-thirds are parvicellular in appearance. Of the parvicellular neurons, 5% are large, 26% are medium and 39% are small. Of the magnocellular neurons, 6% are large and 20% small, with 4% unidentifiable. These data are similar to data on neurons labelled from other targets and to data on unlabelled, thionin stained neurons in figure 9 above.

DISCUSSION

Neuronal Classification

The first part of this paper deals with the cytoarchitecture of rat red nucleus and specifically the classification of its neurons. While staying close to the previously described data for rat (Reid et al., 1975), similarities are noted between the descriptions of monkey RN neuronal morphology described by King et al. (1971) and rat RN neuronal morphology described here. The present data indicate that there are five types of neurons distributed throughout rat RN. These range in diameter from 20 to 55 μm for parvicellular neurons with a trimodal distribution (figure 3A) and 20 to 50 μm for the magnocellular neurons with a bimodal distribution (figure 3B). In monkey RN, neurons are larger: Magnocellular neurons have diameters of 80 to 90 μm (giant), 50 to 70 μm (large) or 30 to 50 μm (medium), the one type of parvicellular neuron has a diameter of 20 to 30 μm, and a small 10 to 15 micron achromatic neuron is described as being present in both divisions (King et al., 1971). The parvicellular RN neurons, therefore, are smaller than the magnocellular neurons in monkey. In rat, however, the parvicellular neurons can overlap the magnocellular neurons in size when using the differentiating criteria discussed next.

There are three major differentiating criteria of RN neurons.

The first is their morphological appearance. Using Nissl stains and Golgi preparations, King et al. (1971) showed that the magnocellular neurons in monkey are multipolar, stellate, ovoid, or narrow and elongated, with many branching dendrites. In contrast, the parvicellular neurons in monkey are triangular or fusiform in shape and have fewer dendrites. These differences are also seen in rat RN when thionin or neutral red stains are used as in the present effort to classify neurons. This classification is independent of neuronal size because some neurons of the same soma diameters exhibit the differentiating criteria of magnocellular neurons and some exhibit the differentiating criteria of the parvicellular neurons. The examples in figure 2 demonstrate this clearly. The present data, however, does not discard information on neuronal size and an analysis based on this criterion is discussed below.

The second and third major criteria for differentiating RN neurons are nuclear size and position. Magnocellular neurons have smaller nuclei giving a larger cytoplasmic/nuclear ratio than the parvicellular neurons which have more prominent nuclei. The small and medium sized parvicellular neurons contain nuclei that lie close to the center of the cell body and appear to push the cytoplasm to one side. The nuclei are almost centrally placed, whereas the magnocellular nuclei are usually eccentric, except for the smallest neurons. Examples are shown in figure 2.

The present results differ from those of Reid et al. (1975). These workers classified neurons according to size. They considered the giant (>40 micron diameter) and large (26-40 micron diameter) neurons as belonging predominantly to the magnocellular category, and the medium (20-25 micron diameter) and small (<20 micron diameter) neurons as belonging to the parvicellular category. These values are close to the demarcation points for the different neuronal sizes described here. The essential difference is that the morphological appearances of the neurons are here used as classifying criteria so that, for example, large neurons could be classified as magnocellular or parvicellular.

Distribution

The distributions reported here differ from other results (Reid et al., 1975) due to the classification system used. Even though large neurons predominate caudally and small neurons predominate rostrally (as shown in figure 4A) in agreement with other workers (Reid et al., 1975), the intermingled distributions cannot be ignored particularily in the caudal and middle sections of the nucleus as seen most clearly in the normalized data (figure 4B). The rostral pole, however, is dominated by small neurons, more frequently parvicellular than magnocellular and this fairly closely resembles the distribution in the monkey (King et al., 1971). The expectation that all parvicellular neurons would lie rostral to the magnocellular neurons as they do in other species

such as monkey (King et al., 1971) has not been fulfilled.

Reid et al. (1975) considered the magnocellular region to be the caudal one-third of the nucleus with an extension into the middle third, and the parvocellular region to lie rostralward. These conclusions may seem to differ from the present results, but perusal of their data indicates that they too found all types of neurons throughout the nucleus, and they draw conclusions based only on the predominant distributions. Similar conclusions could be drawn about the present results, but the numbers of neurons in specific areas cannot be ignored as emphasized in figure 4B where normalized data clearly shows that the caudal pole, for example, contains a significant number of small neurons even though the absolute numbers are small as shown in figure 4A. Visual examination of an area dominated by large neurons, for example, would give the impression that the section is exclusively composed of such neurons especially if neuronal counts are not made. Because each identified neuron was counted in the present effort the numbers of neurons can be systematically analyzed and the distributions plotted. Other analyses of RN neuronal distributions have not quantified the data in this manner.

Numbers

The number of neurons in rat RN is more than expected on a comparative basis. Monkey red nucleus, that occupies approximately

10 times the volume of rat red nucleus, is reported to contain 1,000 magnocellular neurons in its caudal one third, and at least 10,000 parvicellular neurons in its rostral portion (Larsen and Yumiya, 1980). The present findings show that the number of neurons in rat red nucleus equals almost 70% of this number (Table 1). Considering the difference in volume, this suggests that the total number reported for monkey is too conservative. The small percentage of magnocellular neurons in rat (17% of the total), is about twice that reported for monkey (9%), but they are both small proportions of the total.

The different total number of labelled neurons found when different tracers are used is not surprising from the work of Craig and colleagues (1989). They report that tracers are selectively transported when labelling spinothalamic tract neurons with fluoroprobes such as DY or fast blue, or with tracers such as WGA-HRP. The data here suggest that FG is the optimal retrograde tracer from ION to RN. In addition, selective transport is observed after placing various tracers in the transected dorso-lateral funiculus of the spinal cord. When the data is normalized, however, there is no difference between tracers. (DY was the third choice). For comparison with labelling from other targets, therefore, the normalized values are used.

Definition of Rat Red Nucleus

The rostral end of red nucleus has always been difficult to define. When the strict criteria for the five types of neurons is used, the data indicate that there is an intermingling with neurons of the nucleus parafascicularis prerubralis (nPfPr of Carlton et al., 1982). Rather than ending at the fasciculus retroflexus, therefore, the red nucleus extends around and slightly beyond this fasciculus by about 300 µm. It could be argued, however, that structures such as nPfPr should be included as part of the red nucleus since it projects to ION. However, the definition of neuron types excludes nPfPr from being so defined. One can describe the red nucleus in rat, therefore, as an oval structure, up to 2.5 mm long in the adult midbrain, lying between 1 and 2 mm from the midline, about 1 mm below the oculomotor nucleus and central grey. It extends from the vicinity of the fasciculus retroflexus to the caudal pole that narrows to a rounded point. In the caudal half it is crossed obliquely by fibers of the 3rd nerve. Parvicellular neurons predominate rostrally but extend throughout its full extent. Magnocellular neurons lie predominatly in its caudal two-thirds. With this intermingling of parvicellular and magnocellular neurons, distinct histological divisions cannot be defined. An alternative means of defining the nucleus might be to analyze it for the presence of different transmitters or their receptors. Such a chemoarchitectural analysis has been instrumental in defining structures in the basal ganglia as reported by Martin et al. (1990).

Anterograde projections from Red Nucleus

Previous workers have been unable to clearly demonstrate a rubro-olivary projection in the rat (Brown et al., 1977, Carlton et al., 1982, and Rutherford et al,. 1984). Brown et al (1977) reported "only a few small to medium sized positive cells with a relatively light HRP content" after HRP injections into ION. The possibility that this lack of definitive labelling may have been technical in nature is tested by repeating the techniques used by these authors. For example, Fast Blue (FB) or Diamidino Yellow (DY) are placed in the ION using plegets of gelfoam soaked in either dye, with survival times ranging from 2 to 10 days. These placements produce virtually no labelled neurons in RN, in agreement with Rutherford et al.'s (1984) findings with FB. In agreement with Reid et al. (1975), light label is produced by WGA-HRP using modified techniques (Kennedy, 1987b). The connection is also seen using Rhodamine B with survival times of 6, 7 and 9 days. The optimum retrograde tracer reported here is Fluorogold as shown in figure 8. To provide further evidence of the projection from RN to ION, anterograde tracing is reported here using iontophoretic injections of minute amounts of PHA-L. Since tracer placements are largely confined to the nucleus, and since definitive label is found in ION, these findings along with the retrograde transport from ION to RN using FG, WGA-HRP and Rhodamine-B are all strongly suggestive of a projection from RN to ION. The difficulties encountered using previous techniques suggest that the pathway may

be a collateral of another more major pathway, and our companion paper provides evidence for this explanation.

Retrograde Labelling from Three Targets

It is surprising that all three targets receive input from all five types of neurons. The expectation had been that parvicellular neurons should project to ION, magnocellular neurons should project to the spinal cord, and some subset of neurons should project to the cerebellar nuclei. This arrangement of ION and spinal cord projections in the monkey (Miller and Strominger, 1973) and cat (Edwards 1972), is not present in the rat as figure 9 shows. Comparison with the control set of thionin stained neurons shows only small differences in numbers. The distributions, however, are different as discussed in the text for figures 4, 11, 14 and 16 that show the distributions for the control neurons, and those labelled from ION, spinal cord, and cerebellar tracer placements respectively. Similarily, the distributions within each section are different for neurons labelled from different target as shown in figure 10.

Shieh et al. (1983) reported that magnocellular and parvicellular neurons in rat are labelled from spinal cord injections of WGA-HRP. They did not, however, define these neuron types except by location and size. Their "labelled neurons were typical multipolar motor neurons" and "measured 60 to 160 μm" in

diameter, with the magnocellular region considered to be caudal and the parvicellular rostral. The present report emphasizes, however, that location alone does not define RN neurons. When neuronal morphology is considered, the so-called "divisions" intermingle extensively. No report to date has defined RN neurons as we have done here.

The second paper in this series discusses possible explanations of the neuronal diversity. It also discusses the implications for investigators who use this system as a model for recovery of function following lesions.

The data suggest, then, that distinct histological divisions cannot be defined in rat red nucleus on the basis of neuronal classification (parvicellular or magnocellular) since the neurons intermingle so extensively. Nor can a distinction be made on the basis of projections of particular neuronal classes, since both parvicellular and magnocellular neurons of all sizes project to brainstem, spinal cord and cerebellar targets.

LITERATURE CITED

Abercrombie M. (1946) Estimation of nuclear population from microtome sections. Anat. Rec. 94:239-247.

Bebin, J. (1956) The central tegmental bundle: an anatomical and experimental study in the monkey, J. Comp. Neurol. 105:287-332.

Blatt, G.J. and L.M. Eisenman, (1985) Autographic study of the olivocerebellar projection in adult normal aaver mutant mice. Soc. Neurosci. Abstract, 11(1):181.

Brown, J.T. (1974) Rubrospinal projections in the rat. J. Comp.Neurol. 154:169-188.

Brown, J.T., V. Chan-Palay, and S.L. Palay, (1977). A study of afferent input to the inferior olivary complex in the rat by retrograde transport of horseradish peroxidase, J. Comp. Neurol. 176:1-22.

Carlton, S.M., J.R. Leichnetz, and D.J. Mayer, (1982) Projections from the nucleus parafascicularis prerubralis to medullary raphe nuclei and inferior olive in the rat. A horseradish peroxidase and autoradiograpahy study. Neuroscience Letters, 30:191-197.

Conde, F. and H. Conde, (1982) The rubro-olivary tract in the cat, as demonstrated with the method of retrograde transport of horseradish peroxidase. Neuroscience, 7:715-724.

Courville, J., S. Otabe, (1974) The rubro-olivary projection in the macaque: An experimental study with silver impregnation methods. J. Comp. Neurol. 158:479-494.

Craig, A.D., A.J. Linington and K.-D. Kniffki (1989) Significant differences in the retrograde labeling of spinothalamic tract cells by horseradish peroxidase and the fluorescent tracers fast blue and diamidino yellow. Exp. Brain Res. 74:431-436.

Edwards, S.B. (1972) The ascending and descending brainstem projections of the red nucleus in the cat: An experimental study using an autoradiographic method. Brain Res. 48:45-63.

Gerfen. C.R. and P.E. Sawchenko (1984) An anterograde neuroanatomical tracing method that shows the detailed morphology of neurons, their axons and terminals: Immunohistochemical localization of an axonally transported plant lectin, Phaseolus vulgaris leucoagglutinin (PHA-L). Brain Res. 290:219-238.

Huisman, A.M., H.G.J.M. Kuypers, F. Conde, and K. Keizer, (1983) Collaterals of rubrospinal neurons to the cerebellum in rat: a retrograde fluorescent double labeling study. Brain Res. 264:

181-196.

Kennedy, P.R. (1987a) Double labelling of red nucleus neurons from dye injections into the inferior olivary nucleus and dorso-lateral funiculus of the spinal cord in rat. Soc. Neurosci. Abstrs. 13(2):852.

Kennedy, P.R. (1987b) Light labeling of red nucleus neurons following an injection of peroxidase-conjugated wheat germ agglutinin into the inferior olivary nucleus of the rat. Neuroscience Letters, 74:262-268.

Kennedy, P.R., J.C. Houk, A.R. Gibson, (1986) Anatomic and functional contrast between magnocellular and parvicellular divisions of the red nucleus in the monkey. Brain Res. 364:124-136.

Kennedy, P.R. and D.R. Humphrey, (1987) The compensatory role of the parvicellular division of the red nucleus in operantly conditioned rats. Neuroscience Research 5:39-62.

King, J.S., R.C. Schwyn, C.A. Fox, (1971) The red nucleus in the monkey (Macaca mulatta): A golgi and an electron microscope study. J. Comp. Neurol. 142:75-108.

Larsen, K.D., H. Yumija, (1980) The red nucleus in the monkey.

Topographic localisation of somatosensory input and motor output. Exp. Brain Res. 40:393-404.

Martin L.J., J.C. Hedreen, D.L. Price and M.R. DeLong (1990) Chemoarchitectonic delineation of ventral tier nuclei in Macaque Thalamus. Soc. Neurosci. Abstr., 16(1):227.

Massion, J. (1967) The mammalian red nucleus. Physiol. Rev. 47:83-425.

Miller, R.A., N.L. Strominger, (1973) Efferent connections of the red nucleus in the brainstem and spinal cord of the rhesus monkey. J. Comp. Neurol. 152:327-334.

Nathan, P.W. and M.C. Smith, (1982) The rubrospinal tract and central tegmental tracts in man. Brain, 105:223-269.

Paxinos G. and C. Watson (1982) The rat brain in stereotaxic coordinates. Academic Press. 3-4.

Reid, J.M., D.G. Gwyn and B.A. Flumerfelt (1975) A cytoarchitectonic and golgi study of the red nucleus in the rat. J. Comp. Neurol. 162:337-362.

Rutherford J.G., W.A. Anderson and D.G. Gwyn (1984) A reevaluation of Midbrain and Diencephalic Projections to the

Inferior Olive in Rat with Particular Reference to the Rubro-Olivary Pathway. J. Comp. Neurol. 229:285-300.

Shieh J.Y., S.K. Leong and W.C. Wong (1983) Origin of the rubrospinal tract in neonatal, developing and mature rats. J. Comp. Neurol. 214:79-86

Strominger, N.C., T.C. Truscott, R.A. Miller, G.T. Royce, (1979) An autoradiagraphic study of the rubro-olivary tract in the rhesus monkey. J. Comp. Neurol. 183:33-46.

Tucker, C.L. and P.R. Kennedy (1990) Re-defining rat red nucleus: Cytoarchitectural analysis of red nucleus neurons singly and doubly labelled from spinal cord and inferior olivary nucleus. Soc. Neurosci. Abstrs., 16(1):729.

Tucker, C.L., S.A. Lee and P.R. Kennedy (1989) Re-defining rat red nucleus: Cytoarchitecture and connectivity. Soc. Neurosci. Abstrs., 15(1):405.

Waldron, H.A. and D.G. Gwyn, (1969) Descending nerve tracts in the spinal cord of the rat. I. Fibers from the midbrain. J. Comp. Neurol. 137:143-154.

Yu, D.Y., S. Na, J. Wilson and P.R.Kennedy (1991) Redefining rat red nucleus: Multiple labelling of individual neurons from spinal

cord, inferior olivary nucleus and cerebellar nuclei. Soc. Neurosci. Abstr., 17(1):469.

ACKNOWLEDGEMENTS

The authors thank Drs. Johannes Tigges, George F. Martin, Helen H. Molinari and Daniel L. O'Donoghue for their constructive criticisms of an earlier version of this manuscript. The authors also thank Ms. Shakita Dennis for helping with the analysis of the anterograde tracing data. Thanks also to Ms Crystal Tucker for her assistance in the early stages of this project. Supported by NIH grant RO1-NS24602.

FIGURE LEGENDS

Figure 1. A: Fluorogold labelled neuron photographed under fluorescent light.

B: Same neuron with addition of direct light to demonstrate the thionin stain.

C: RN neuron labelled with DY in its nucleus.

D: Doubly-labelled RN neuron, with DY in its nucleus and FG in its cytoplasm.

E: Neurons artifactually labelled with Lipofuchsin granules.

F: FG-labelled neurons as described in the text. Neurons in E and F are photographed, developed and printed under identical conditions. Calibration bars represent 30 µm each, with the upper bar corresponding to A and B, and the lower (shorter) bar corresponding to C, D, E and F.

Figure 2. Photographs of the five different neuronal types. Calibration bar is 30 µm.

Figure 3. A: Trimodal distribution of parvicellular neurons according to soma diameter.

B: Bimodal distribution of magnocellular neurons according to soma diameter.

Figure 4. A: Absolute values of distributions of all five types of neurons. The caudal pole is on the left, the rostral pole is on the right.

B: The same values plotted as normalized data.

Figure 5. A: Example of an iontophoretic injection of WGA-HRP in the caudal pole of RN. This is the widest diameter of the site. The calibration bar is 200 μm.

B: Speckles of reaction product are seen in the ipsilateral principal olivary (PO) nucleus under polarized light. The purple bars are artifact. The calibration bar is 50 μm.

C: The light grey areas are reaction product in the medial accessory and PO nuclei. The large black dots are artifacts due to endogenous reaction product in blood vessels. The calibration bar is 400 μm.

Figure 6. A: Example of PHA-L injection site covering the midsection of RN with surrounding diffusion. The midline aquaduct is at top left surrounded by the central grey. The calibration bar is 500 μm.

B: In a confined area of PO, axons are seen to terminate in probable synaptic boutons. Label is absent from the pyramidal tract below and to the left. The calibration bar is 50 μm.

Figure 7. A: Photograph of a typical placement site in the brainstem, where FG is placed in the pyramid and spreads into the ipsilateral ION. It can produce retrograde filling of neurons in the contralateral ION presumably by uptake from the cut axons of the olivo-cerebellar tract. Calibration bar is 250 μm.

B: Diagram of FG placement site in one ION that spreads into the other ION. The pyramid is usually 1 to 2 mm across.

Figure 8. Examples of bright, white speckles of FG in RN neurons of a young female rat weighing about 100 g. The calibration bar is 50 μm.

Figure 9. Normalized data of different neurons labelled from three different target sites (ION, SC and cerebellum) are compared with each other and with thionin stained controls.

Figure 10. The distribution of neurons labelled from ION, SC and cerebellum are plotted from caudal to rostral with 160 μm between sections. The outlines are obtained by examining thionin-stained neurons after analysis and identification of all labelled neurons. The calibration bar is 1 mm.

Figure 11.A: Absolute values are plotted for the distribution of the different types of neurons labelled from ION. The caudal pole is on the left.

B: The same data are normalized for ease of comparison of the different types.

Figure 12. Plegets of WGA-HRP are placed in the transected dorso-lateral funiculus of the C3 spinal cord diagrammatically shown in cross section. A heavy area and light diffusion area are shown. The calibration bar is 1 mm.

Figure 13. WGA-HRP labels the cytoplasm and DY labels the nuclei of RN neurons photographed under direct and epifluorescent light. The calibration bar is 50 µm.

Figure 14.A: Absolute values are plotted for the distribution of the different types of neurons labelled from the SC. The caudal pole is on the left.

B: The same data are normalized for ease of comparison of the different types.

Figure 15.A: Five plegets of DY-soaked gelfoam (dark masses) are placed in the cerebellum above and adjacent to the nuclei seen under direct light. The calibration

bar is 1 mm.

B: Cross sections of the cerebellum and brainstem showing the labelled areas in black that cover the cerebellar nuclei. The unlabelled nuclei on the opposite side are used for estimating the percentage of nuclei involved. L: Laternal (Dentate) nucleus; I: Intermediate (Interpositus) nucleus; M: Medial (Fastigial) nucleus. The calibration bar is 3.5 mm.

Figure 16.A: Absolute values are plotted for the distribution of the different types of neurons labelled from the cerebellar nuclei. The caudal pole is on the left.

B: The same data are normalized for ease of comparison of the different types.

Table 1. [A brief legend accompanies the table in the text and is placed just under the title.]

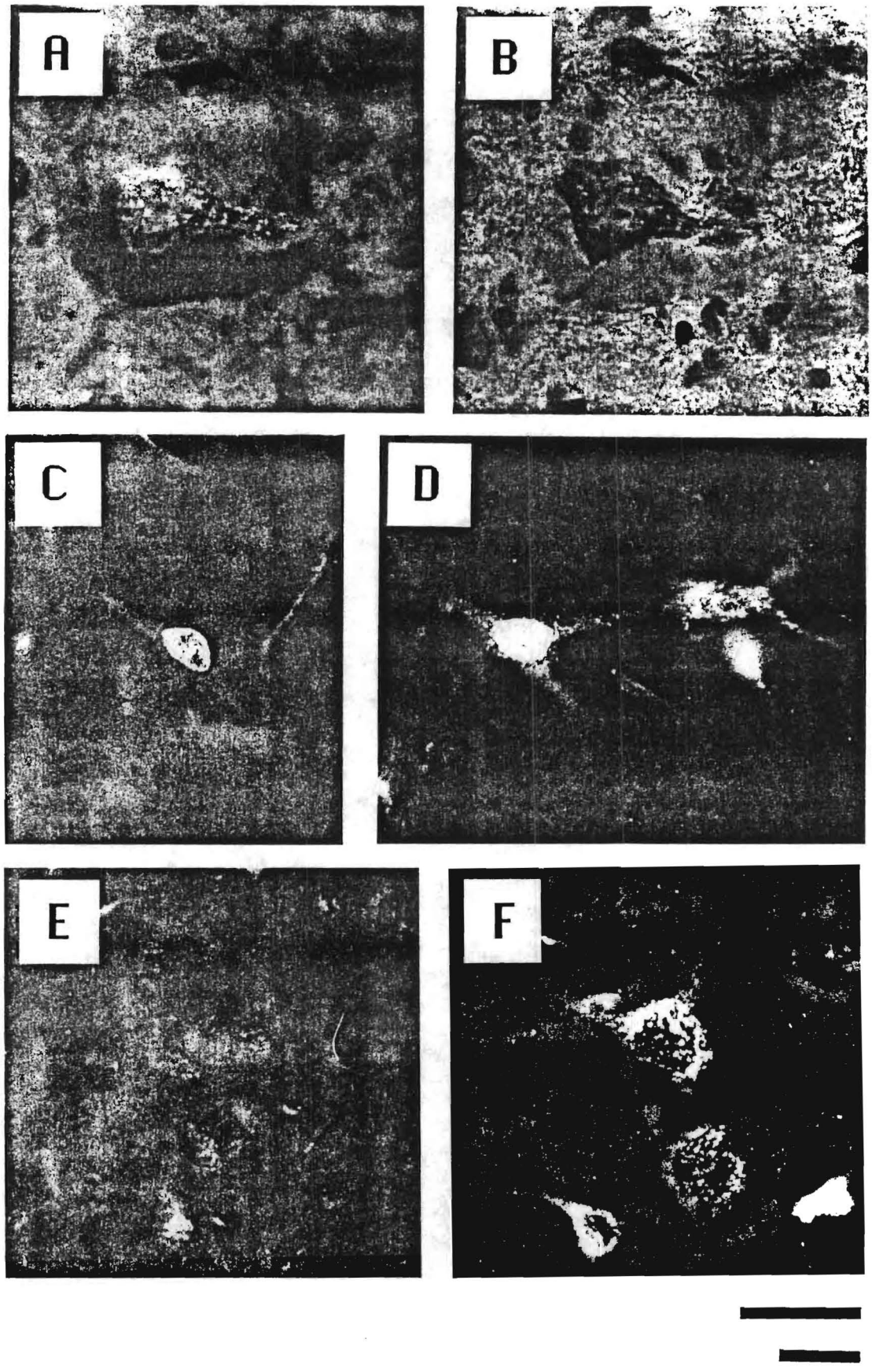
A
B
C
D
E
F

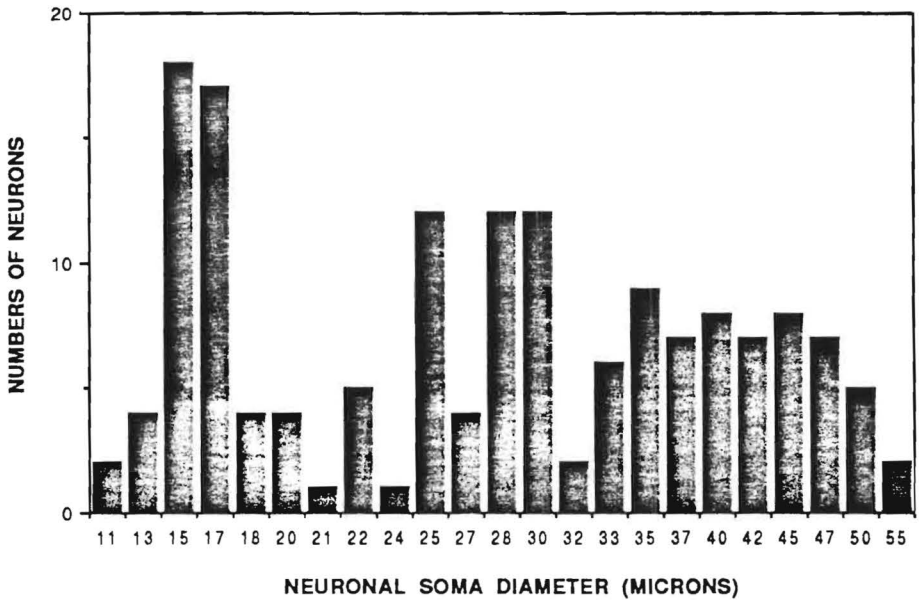
20
10
0
NUMBERS OF NEURONS
11 13 15 17 18 20 21 22 24 25 27 28 30 32 33 35 37 40 42 45 47 50 55
NEURONAL SOMA DIAMETER (MICRONS)

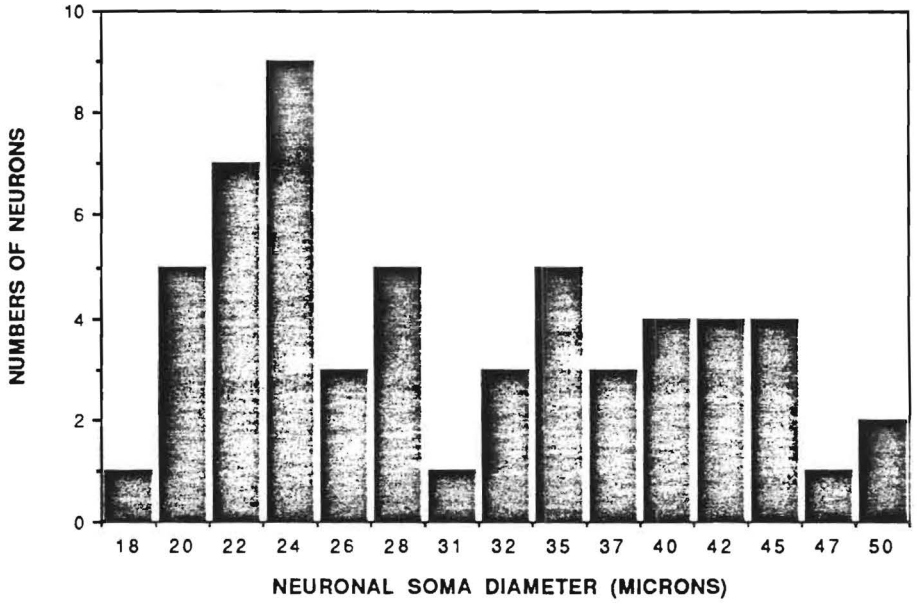
NUMBERS OF NEURONS
0
2
4
6
8
10
18
20
22
24
26
28
31
32
35
37
40
42
45
47
50
NEURONAL SOMA DIAMETER (MICRONS)

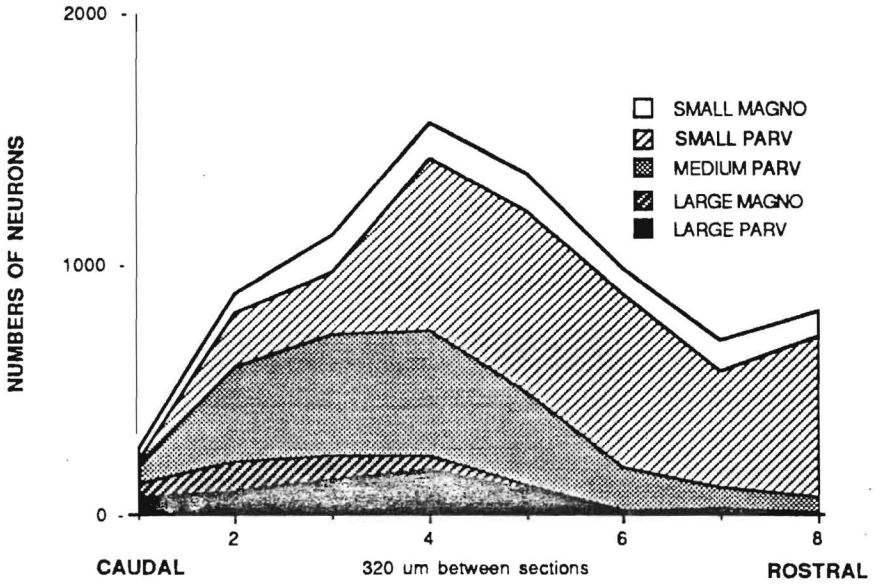
2000
1000
0
NUMBERS OF NEURONS
SMALL MAGNO
SMALL PARV
MEDIUM PARV
LARGE MAGNO
LARGE PARV
2
4
6
8
CAUDAL
320 um between sections
ROSTRAL

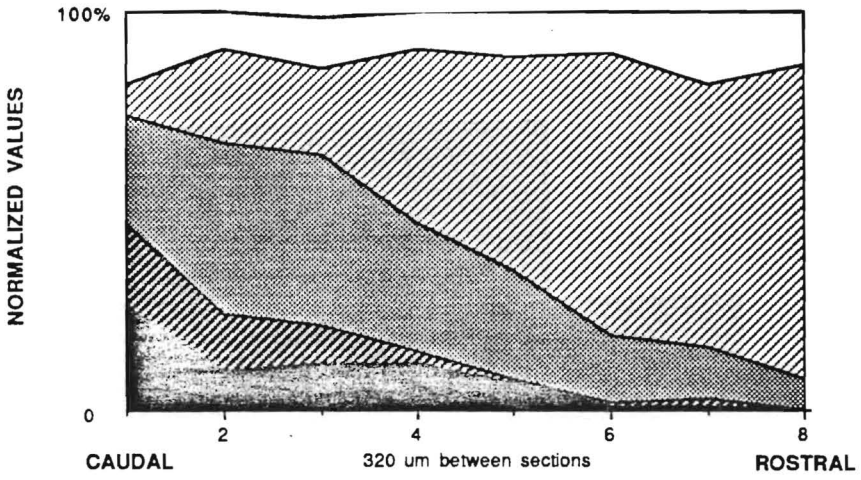
100%
NORMALIZED VALUES
0
2
4
6
8
CAUDAL
320 um between sections
ROSTRAL

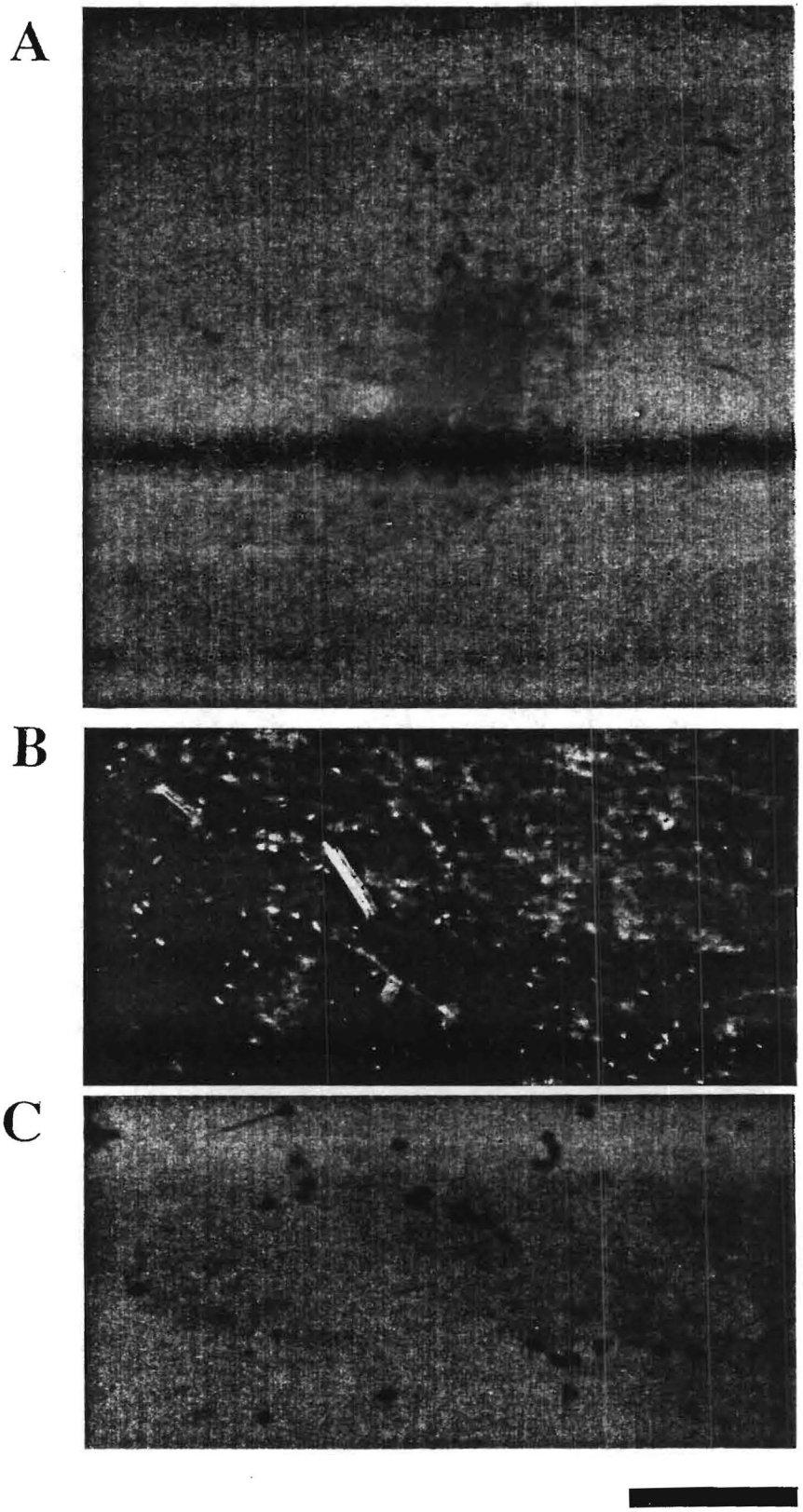
A
B
C

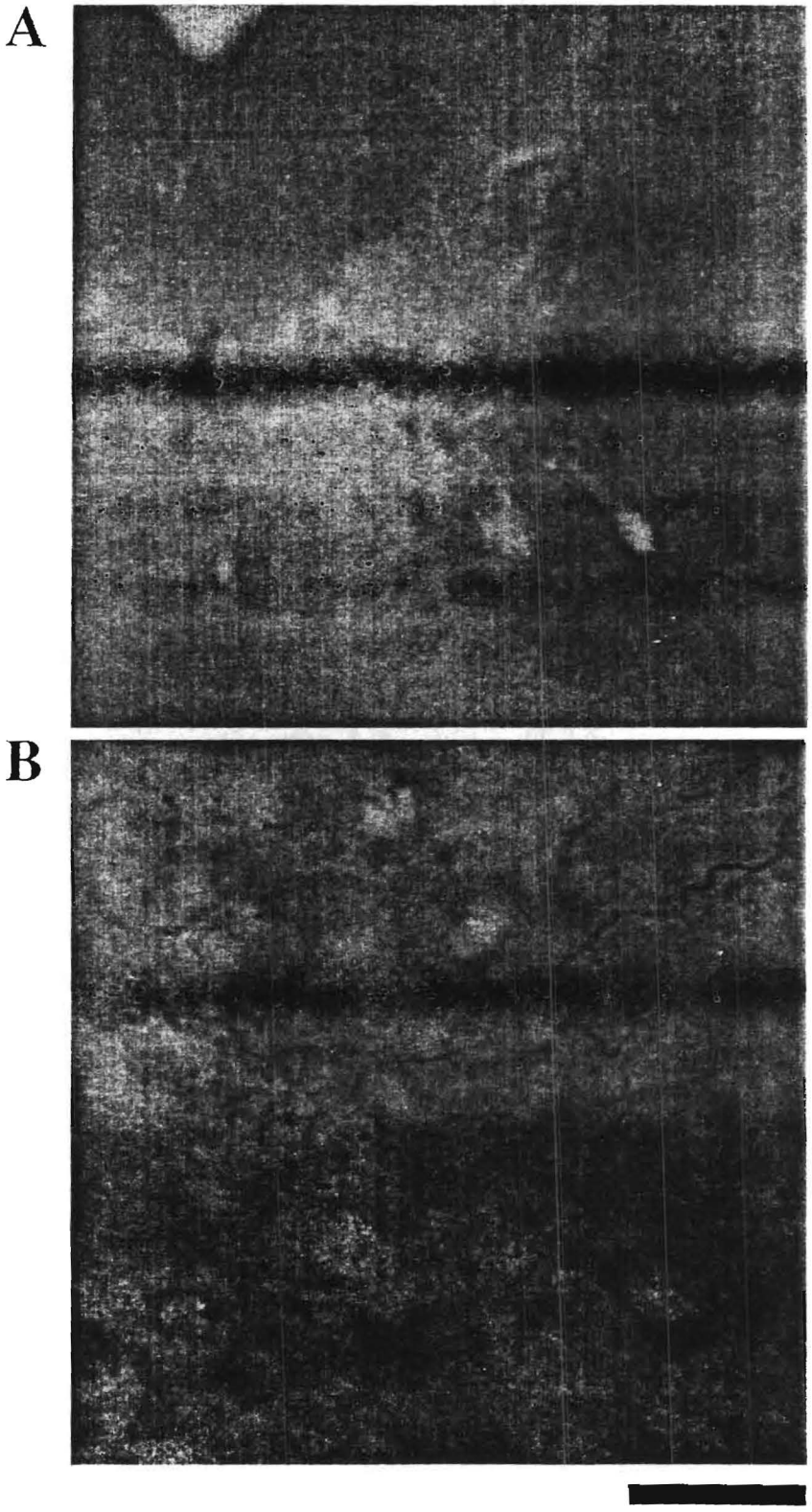
A
B

A

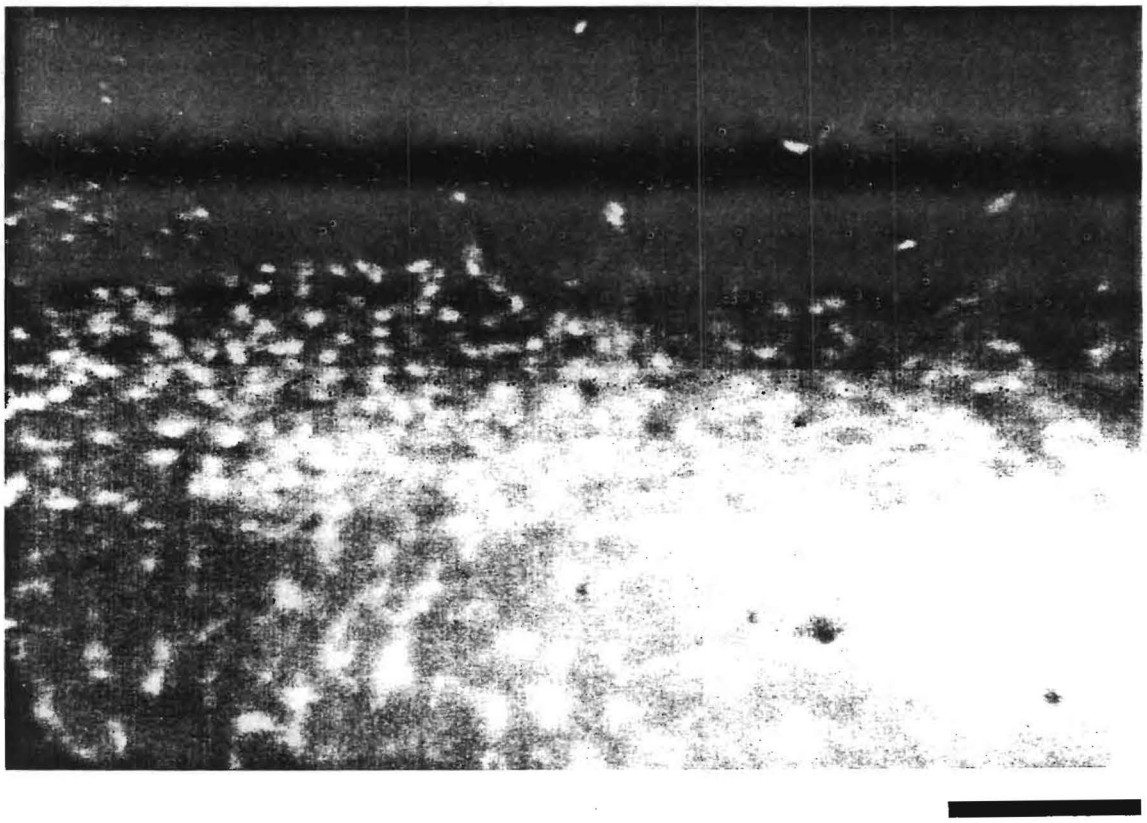

B Coronal sections 400 microns apart

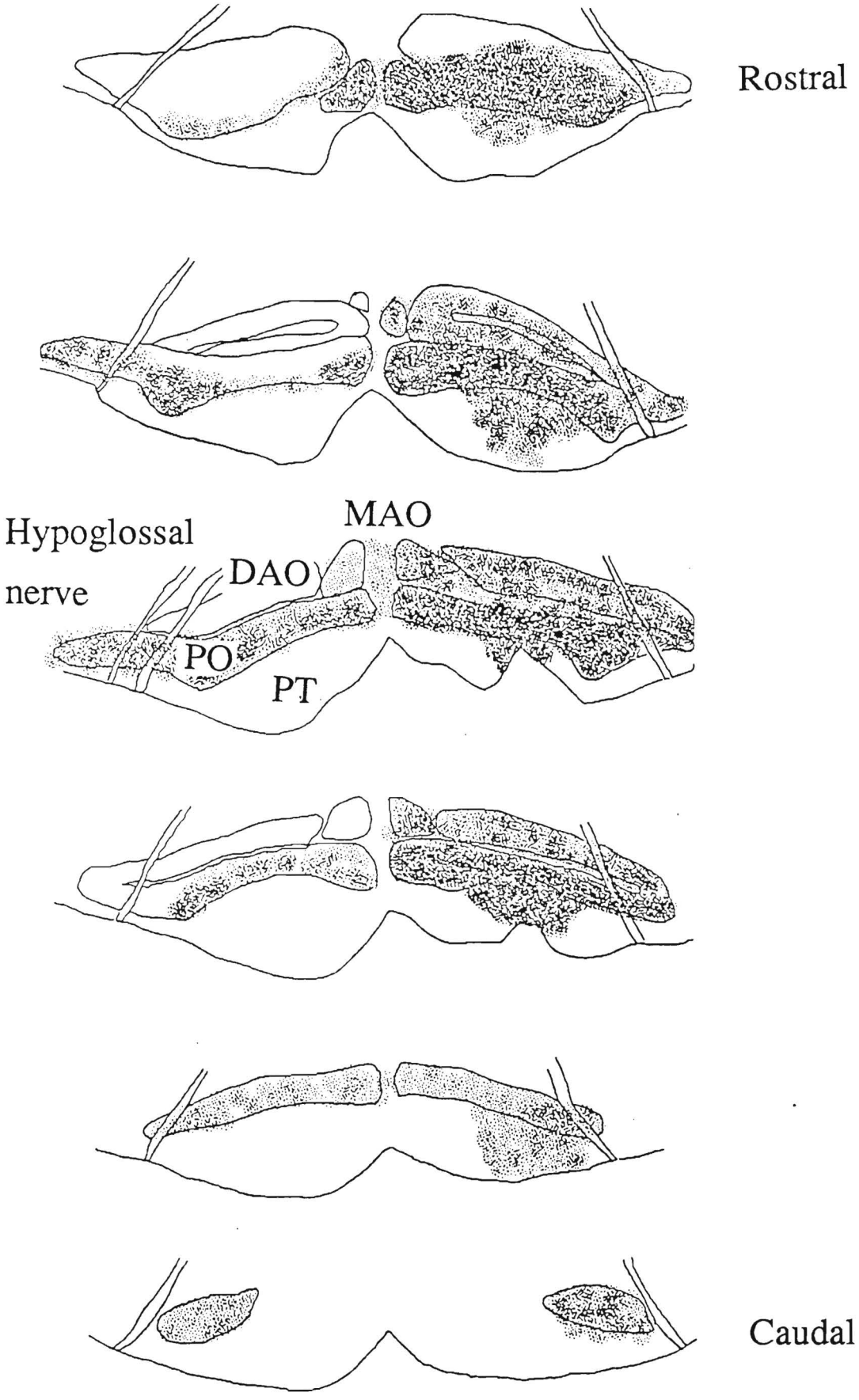

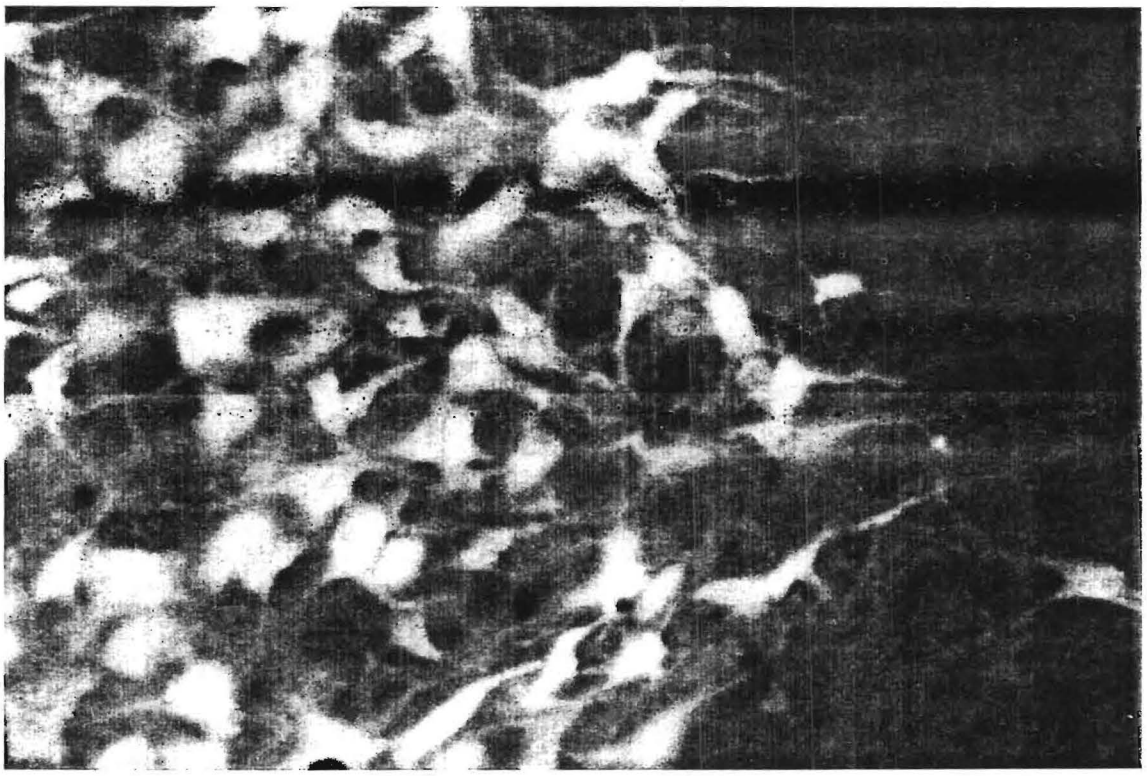

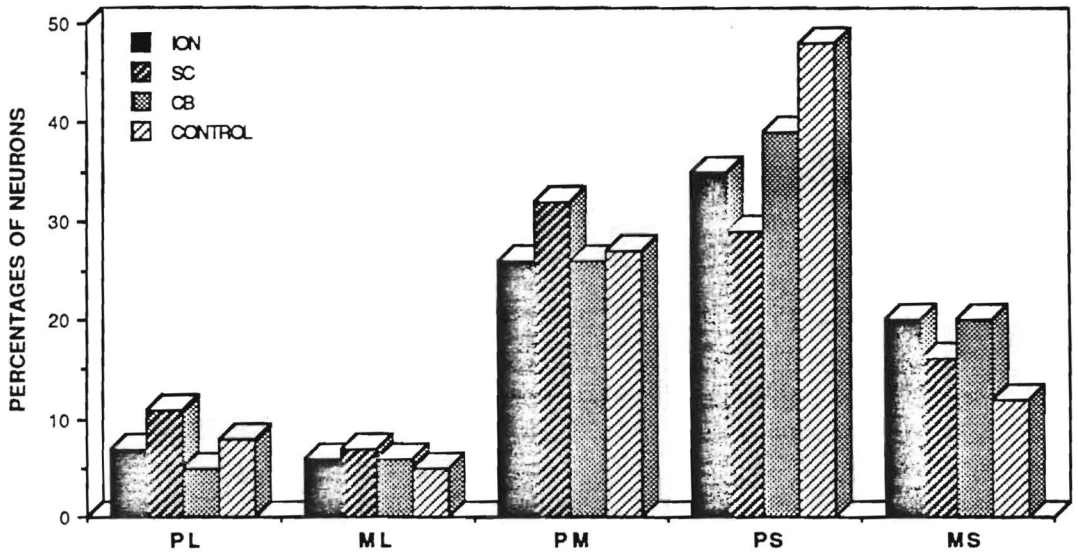
PERCENTAGES OF NEURONS
50
40
30
20
10
0
ION
SC
CB
CONTROL
PL
ML
PM
PS
MS

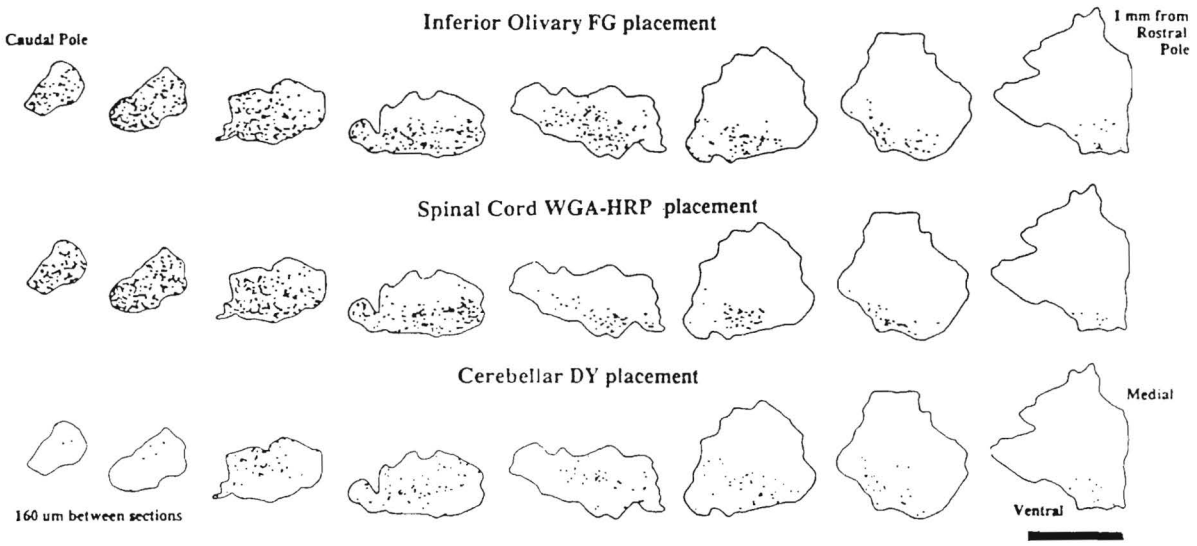
Inferior Olivary FG placement
Caudal Pole
1 mm from Rostral Pole
Spinal Cord WGA-HRP placement
Cerebellar DY placement
Medial
Ventral
160 um between sections

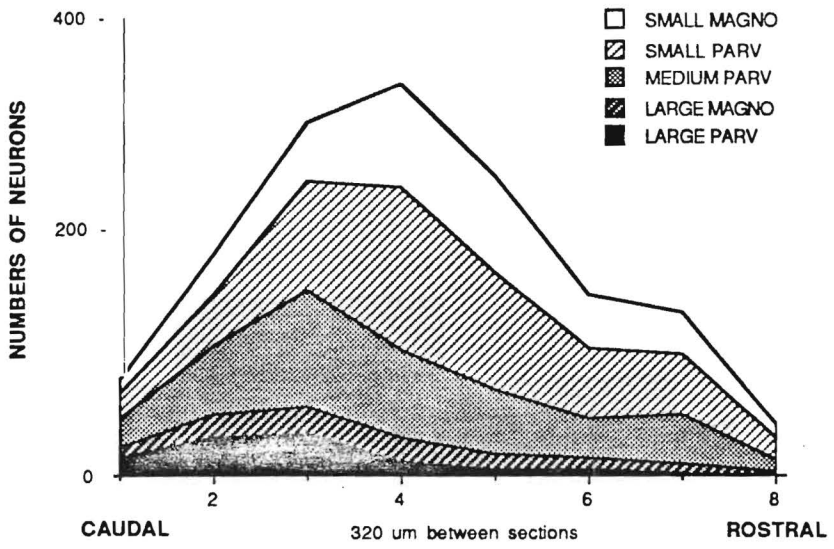
400
200
0
NUMBERS OF NEURONS
SMALL MAGNO
SMALL PARV
MEDIUM PARV
LARGE MAGNO
LARGE PARV
2
4
6
8
CAUDAL
320 um between sections
ROSTRAL

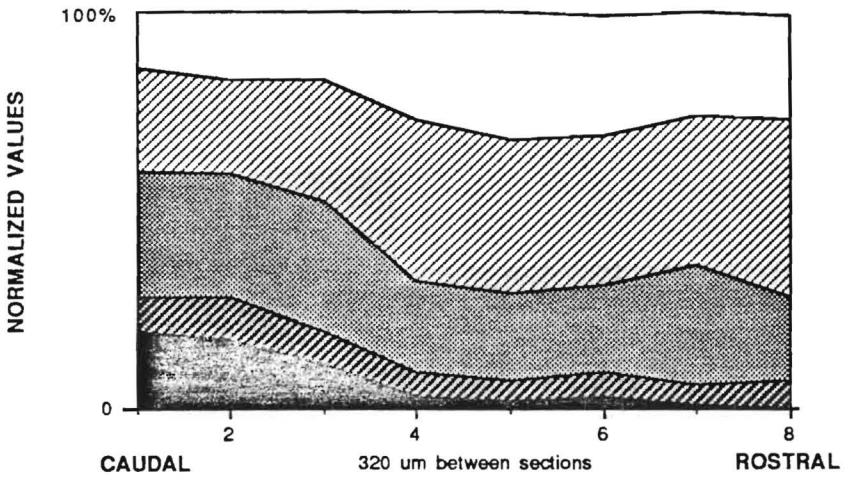
100%
NORMALIZED VALUES
0
2
4
6
8
CAUDAL
320 um between sections
ROSTRAL

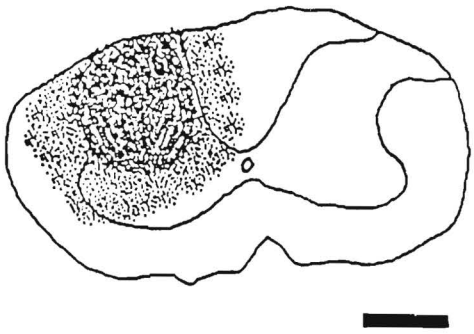

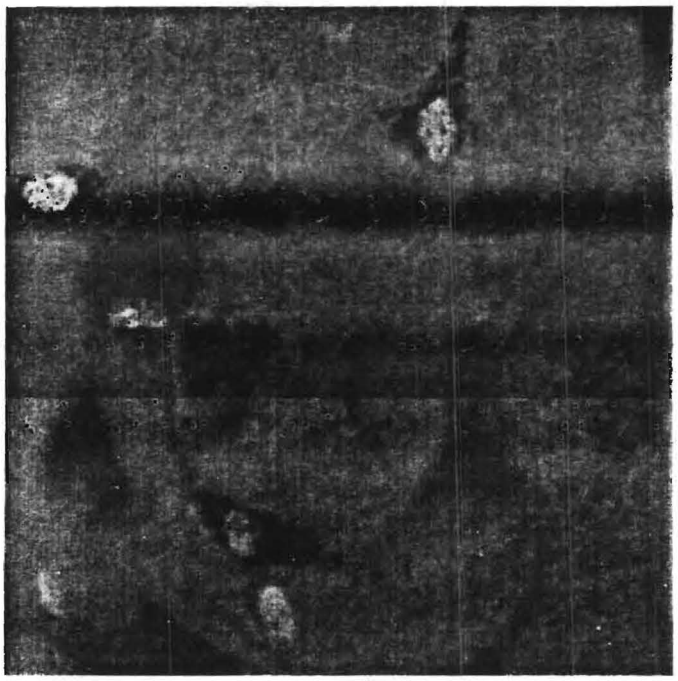

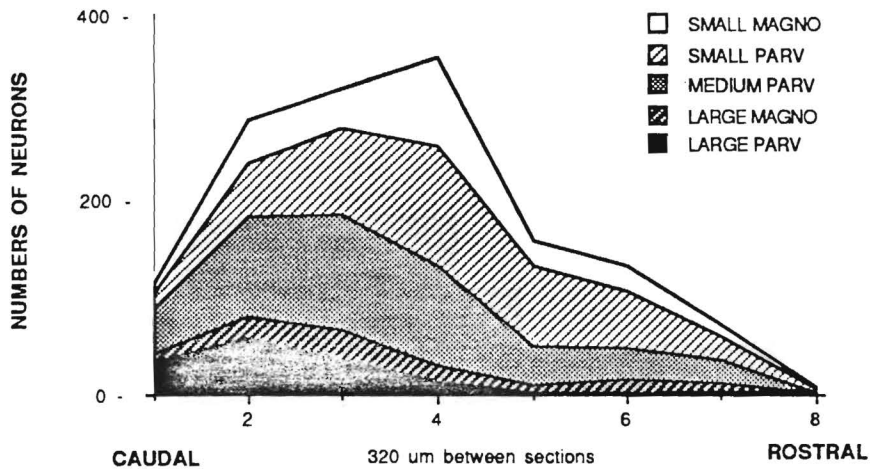
400
200
0
NUMBERS OF NEURONS
SMALL MAGNO
SMALL PARV
MEDIUM PARV
LARGE MAGNO
LARGE PARV
2
4
6
8
CAUDAL
320 um between sections
ROSTRAL

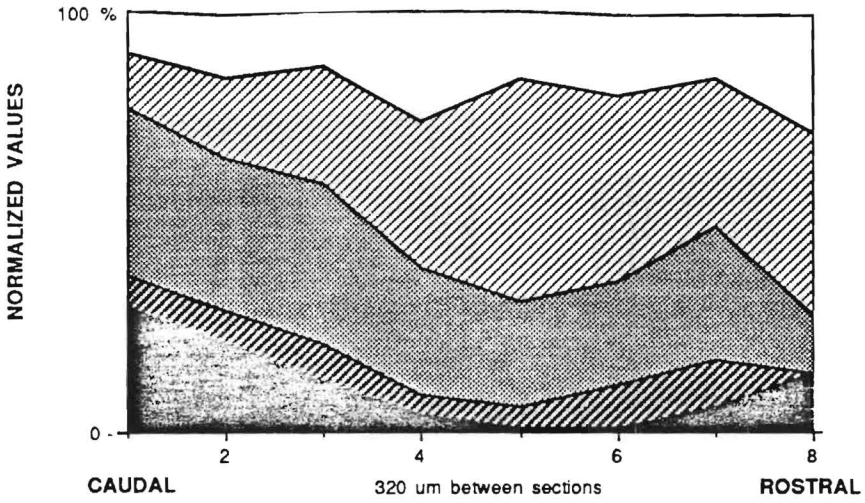
100 %
0
NORMALIZED VALUES
2
4
6
8
CAUDAL
320 um between sections
ROSTRAL

A

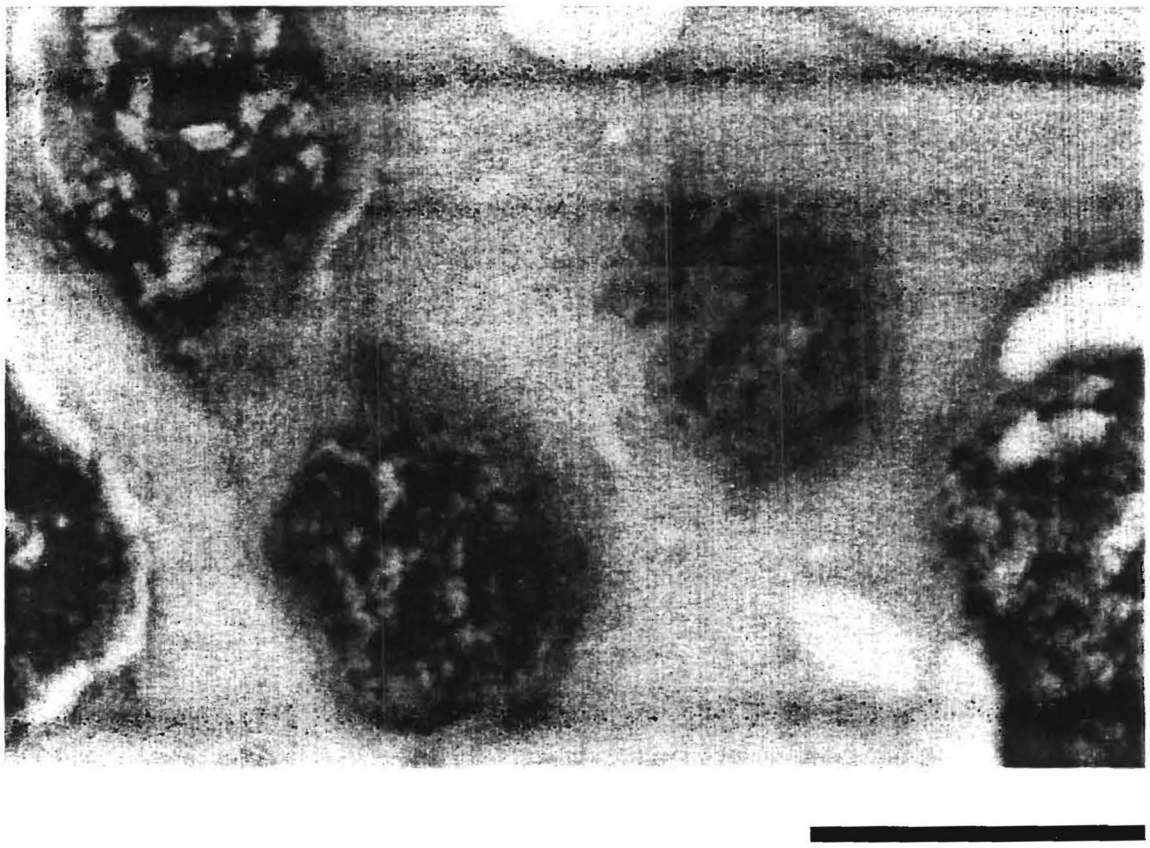

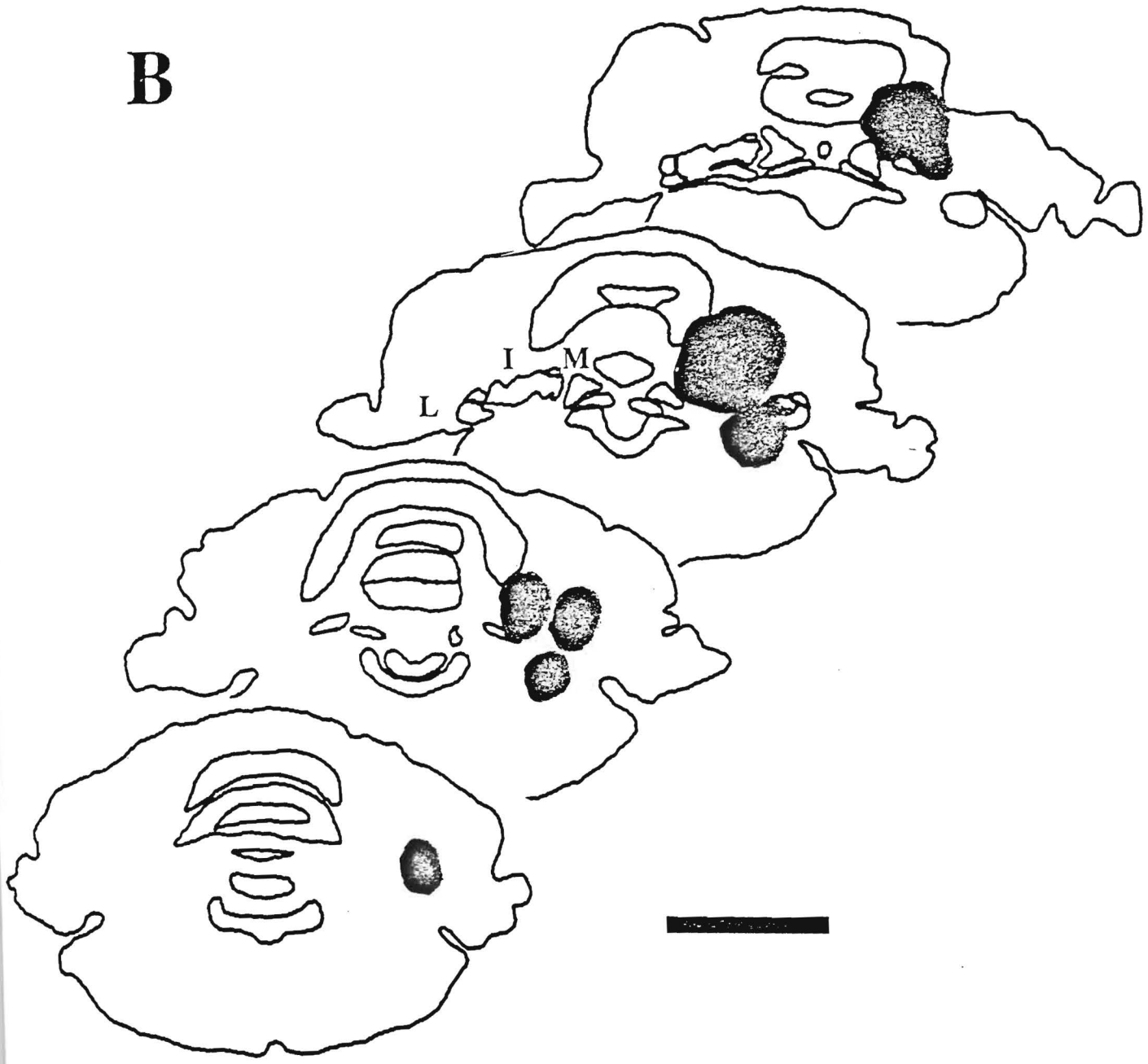
B
I
M
L

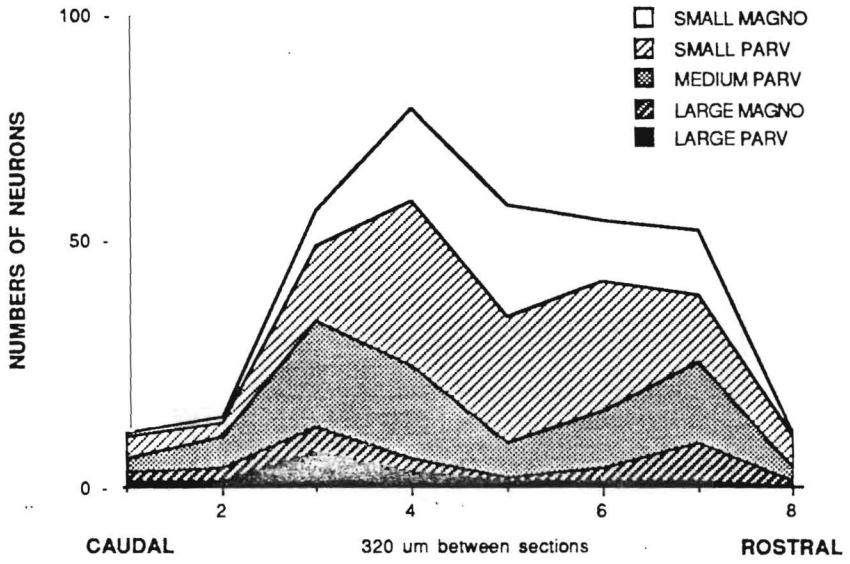
100
50
0
NUMBERS OF NEURONS
SMALL MAGNO
SMALL PARV
MEDIUM PARV
LARGE MAGNO
LARGE PARV
2
4
6
8
CAUDAL
320 um between sections
ROSTRAL

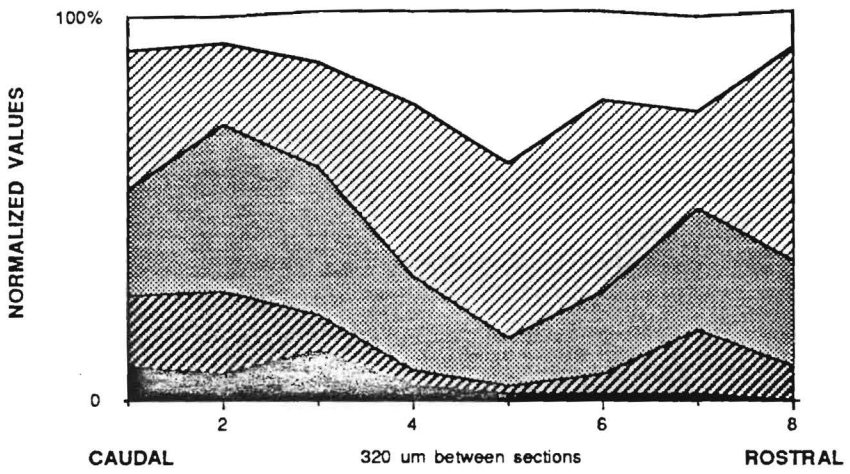
100%
NORMALIZED VALUES
0
2
4
6
8
CAUDAL
320 um between sections
ROSTRAL

SOCIETY FOR NEUROSCIENCE 1989 ABSTRACT FORM

Read all instructions before typing abstract.
See *Call for Abstracts* and reverse of this sheet.
Complete abstract and **all boxes at left and below** before making copy.

____ Check here if this is a REPLACEMENT of abstract submitted earlier. REMIT $25 for each replacement abstract.

First (Presenting) Author

Provide full name (no initials), address, and phone numbers *of first author on abstract. You may present only one abstract.*

Ms. Crystal L. Tucker
Rm. 325 CRB
GEORGIA TECH
400 10th Street
Atlanta, GA 30332
Office: (404) 894-4257 Home: (404) 373-7561

SMALLEST RECOMMENDED TYPE SIZE: 10 POINT

SAMPLE:
1989 Annual Meeting
Phoenix, Arizona
October 29–November 3

DEADLINE FOR POSTMARKING:

MAY 1, 1989

Presentation Preference

Check one: ☒ poster ☐ slide

Themes and Topics

See list of themes and topics. Indicate below a first and second choice appropriate for programming and publishing your paper.

1st theme title: MOTOR SYSTEMS and S-M I theme letter: G

1st topic title CEREBELLUM topic number: 88

2nd theme title: - same - theme letter: G

2nd topic title SPINAL CORD & BRAINSTEM topic number: 92

Special Requests (e.g., projection requirements)

Include nonrefundable ABSTRACT HANDLING FEE of $25 payable to the Society for Neuroscience, **DRAWN ON A U.S. BANK IN U.S. DOLLARS ONLY.**

RE-DEFINING RAT RED NUCLEUS: CYTOARCHITECTURE AND CONNECTIVITY

C.L.Tucker*, S.A.Lee* & P.R.Kennedy, Bioengin. Center, Georgia Tech, Atlanta, GA 30332.

Rat red nucleus (RN) is considered to be limited rostrally by the pre-rubral area. We have studied RN cell types and number, distributions and locations in thionin-stained and fluorescently stained sections. Diamidino Yellow (DY) was placed in the dorsolateral funiculus of the spinal cord that contains the rubrospinal tract (RST); Fluoro-Gold (FG) was placed near the inferior olivary nucleus (ION).

Cells corresponded to parvo and magno cell descriptions (Parvo: large central round nucleus, prominent nucleolus, small cytoplasmic/nuclear ratio, rounded outline; Magno: relatively small oval nucleus, eccentrically placed, large cytoplasmic/nuclear ratio, with rectangular or pyramidal cytoplasmic outline.) Parvos were large (30-45u), medium (15-30u) or small (10-15u). Magnos were larger or smaller than 25u. Counts of nucleus-containing cells revealed 3,008 magnos that were situated mainly caudally, as expected, but also extended into and beyond the pre-rubral area. 19,904 parvos extended from the caudal pole through the pre-rubral area and surrounded the fasciculus retroflexus. The magnos tended to be located ventrally, whereas the parvos were located throughout the nucleus.

Labelling the transected RST at C3 with DY in 6 rats produced labelled magnos and parvos. Surprisingly, only 24% of these labelled cells were magnos and 76% were parvos (combined result from 2 rats analyzed in detail). Even though unlabelled (thionin stained) magnos were seen extending into and beyond the pre-rubral area, DY-labelled magnos were only seen caudal to it. DY-labelled large and small parvos were similarly distributed. DY-labelled medium parvos, however, extended from the caudal pole through the pre-rubral area into the para-fascicular region.

In these two rats accurate injections of FG were made in ION producing extensive labelling of RN. 63% of cells labelled with DY from the spinal cord were also labelled with FG from ION. This confirms a similar report of doubly labelled cells using FG and Fast (or True) Blue (Kennedy PR, Neurosci. Abstr., 13(2):852, 1987). 85% of DY-labelled magnos and 55% of DY-labelled parvos also contained FG.

These results suggest that rat RN is more extensive and complex than previously believed. (Support by grant NIH-RO1NS24602-01A2).

KEY WORDS: (see instructions pg. 4)

1. MAGNOCELLULAR NEURONS
2. PARVOCELLULAR NEURONS
3. DIAMIDINO YELLOW
4. FLUORO-GOLD

Signature of Society for Neuroscience member required below. ***No member may sign more than one abstract.***

The signing member certifies that any work with human or animal subjects related in this abstract complies with the guiding principles for experimental pr

Society for Neuroscience member's signature | PHILIP R. KENNEDY (Printed or typed name) | 404 894-4257 (Telephone number)

SOCIETY FOR NEUROSCIENCE
1990 ABSTRACT FORM

Read all instructions before typing abstract.
See *Call for Abstracts* and reverse of this sheet.
Complete abstract and all boxes
at left and below before making copy.

____ Check here if this is a REPLACEMENT of abstract submitted earlier. REMIT $25 for each replacement abstract. Replacement abstracts must be RECEIVED by MAY 11, 1990.

First (Presenting) Author

Provide full name (no initials), address, and phone numbers *of first author on abstract. You may present only one abstract.*

Ms. Crystal Tucker
Georgia Institute of Technology
CRB - Room 325
400 Tenth Street
Atlanta, GA 30332
Office: (404) 894-4257 Home: (404) 373-7561

SMALLEST RECOMMENDED TYPE SIZE: 10 POINT

SAMPLE:
1990 Annual Meeting
St. Louis, Missouri
October 28–November 2

DEADLINE FOR POSTMARKING:

MAY 1, 1990

Presentation Preference

Check one: ☒ poster ☐ slide

Themes and Topics

See list of themes and topics. Indicate below a first and second choice appropriate for programming and publishing your paper.

1st theme title: Motor Systems & S-M Int. theme letter: G
1st topic title Spinal Cord & Brainstem topic number: 98

2nd theme title: -Same- theme letter: G
2nd topic title Cerebellum topic number: 94

Special Requests (e.g., projection requirements)

Include nonrefundable ABSTRACT HANDLING FEE of $25 payable to the Society for Neuroscience, DRAWN ON A U.S. BANK IN U.S. DOLLARS ONLY.

RE-DEFINING RAT RED NUCLEUS: CYTOARCHITECTURAL ANALYSIS OF RED NUCLEUS NEURONS SINGLY AND DOUBLY LABELLED FROM SPINAL CORD AND INFERIOR OLIVARY NUCLEUS.

C. L. Tucker* and P. R. Kennedy,
Neuroscience Laboratory, Georgia Institute of Technology, Atlanta, GA 30332.

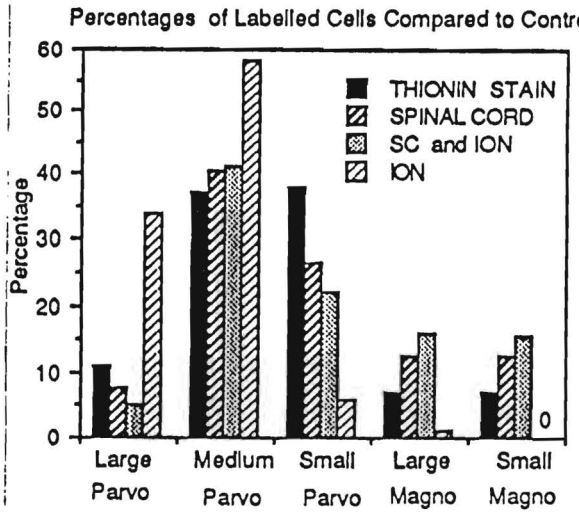

Having reported last year (Soc. Neurosci. Abstrs. 15: (1), 405) that both parvocellular and magnocellular neurons in rat red nucleus project to the spinal cord and inferior olivary nucleus (ION), we determined the types of parvos (large, medium, or small) and magnos (large or small) that project to these targets and their distributions within the nucleus. Thionin stain was used to visualize neurons in direct light (controls), and fluorogold and/or diamidino yellow was used to fluorescently label RN neurons from these targets. The unexpected results (graphed above) show that parvos and magnos are labelled from the spinal cord, whereas parvos almost exclusively are labelled from ION. Double label is found in both cell types. Supported by NIH grant NS24602.

Do not type on or past blue lines (printers' cut lines)

Dimensions of Abstract Form 4 15/16" × 4 13/16"

16 (1): 729

KEY WORDS: (see instructions pg. 4)

1. Red Nucleus
2. Inferior Olive
3. Rubrospinal Tract
4. Rats

Signature of Society for Neuroscience member required below. *No member may sign more than one abstract. The signing member must be an author on the paper.*

The signing member certifies that any work with human or animal subjects related in this abstract complies with the guiding principles for experimental pro

Society for Neuroscience member's signature

Philip R. Kennedy
Printed or typed name

(404) 894-4257
Telephone number

Paper 2 (of 2).

Redefining Rat Red Nucleus: II. Double and Triple Labelling of Red Nucleus Neurons from the Inferior Olivary Nucleus, Spinal Cord and Cerebellum.

Philip R. Kennedy and Dianyi Yu.

Neuroscience Laboratory
Bioengineering Center
Room 325, Centennial Research Building
Georgia Institute of Technology
Atlanta, Georgia 30332.

Short Title: Multiple labeling of Rat Red Nucleus Neurons.

Key Words: Fluorogold; WGA-HRP; Diamidino Yellow; Double labelling; triple labelling.

27 text pages; 13 figures, 1 table

Correspondance: Dr. Kennedy, address as above, phone 404-894-4257, fax 404-894-7025.

Last Update: 9/24/1992.
Filename: ANATPA-2.92

ABSTRACT

The previous paper describes five different types of neurons in rat red nucleus and their projections to inferior olivary nucleus, spinal cord and cerebellum. This paper continues the analysis of connectivity. The data indicate that all types of neurons are doubly and triply labelled from the three targets. Triply labelled neurons are confined to the middle of the nucleus due to restricted distribution of the cerebellar projecting neurons. These data have important implications for investigators who lesion the rubrospinal tract and assess regeneration: It cannot be assumed that morphological changes in the nucleus or regenerating axons in the tract are independent of collaterals. Functionally, the large numbers of neurons that bifurcate and trifurcate to the target nuclei suggest that activity in the descending rubrospinal system is copied to the cerebellum directly and by way of the inferior olivary nucleus.

INTRODUCTION

The previous paper describes the cytoarchitecture and connections of the red nucleus (RN) in the rat. Five categories of neurons are histologically defined in RN, and are found throughout the nucleus in large numbers. Magnocellular neurons are predominant in the caudal two-thirds intermingled with

parvicellular neurons which are present throughout the nucleus and dominate rostrally. Because of the intermingling, distinct histological divisions cannot be defined. In additon, the data suggest that all five types of RN neurons project to all three targets investigated. It was expected, for example, that the spinal cord might receive projections only from magnocellular neurons. It was found, however, that all types of neurons project to this target and that these neurons are widely distributed. Distribution of neurons labelled from ION and cerebellum differ, with ION projecting neurons found ventrally and cerebellar projecting neurons found dorsally and rostrally. Both types of projection neurons intermingle with those projecting to the spinal cord. Other than these differences in distribution, there are few differencs. It cannot be concluded, for example, that neurons of a specific type, size or position within the nucleus, project to a specific target. These data imply, then, that a definition of different divisions cannot be made on the basis of cytoarchitecture or projections of specific neurons to specific targets.

The present paper describes the diversity of connections in greater detail using combinations of tracers from two and three targets. It was expected that doubly or triply labelled neurons might be characteristic of a specific type of neuron or its distribution. It is found, however, that all types of neurons can be doubly or triply labelled from the targets investigated, namely, inferior olivary nucleus (ION), spinal cord (SC) and cerebellum.

In addition, multiply labelled neurons are distributed throughout the extent of the nucleus with a tendency to remain between the ventrally located ION projecting neurons and the dorsally located cerebellar projecting neurons. These multiply labelled neurons do not aid in defining different divisions. Preliminary results have been presented (Kennedy 1987, Tucker et al., 1990, Yu et al., 1991).

METHODS

The methods of dye placement, tissue processing and analysis are essentially unchanged from the descriptions in the preceeding paper. The choice of dyes for multiple labelling is critically important because each dye has to be clearly distinguised from the others. Fluoro-gold (FG) is used routinely in our work to retrogradely label the projection to the ION because it provides optimum labelling compared to other dyes investigated particularly when used in young female rats (see previous paper). FG labels the cytoplasm and is clearly distinguishable from Diamidino Yellow (DY) which is used to label the nuclei of neurons projecting to the cerebellum. Both these dyes are visualized under fluorescent light and are easy to distinguish from WGA-HRP seen under direct light. WGA-HRP, therefore, is used as a retrograde label from the spinal cord. The density of the reaction product has to be carefully controlled, however, to avoid obscuring the fluorescent FG in the same cytoplasm. The density is controlled by slowing the reaction using a low pH collection solution and using 0.01 M acetate buffer instead of 0.1 M phosphate buffer. Most important, raising the pH of the acetate buffer used in the reaction process from 3.3 to 4.5 slows the reaction. This allows light microscopic examination of the tissue to assess the progress of the reaction. As heavy reaction product begins to appear the reaction is discontinued. Later, when counting labelled neurons, light labelling is considered indicative of a neuron retrogradely labelled from the

spinal cord with WGA-HRP reaction product. In this way, the total number of WGA-HRP labelled neurons is not undercounted, and the FG is not obscured. Comparisons of total numbers in triply labelled cases with singly labelled cases confirm the accuracy of the counts.

Examples of singly and doubly labelled neurons are shown in the preceeding paper: [1] Figure 1 shows FG label alone, DY alone and DY combined with FG. [2] Figure 8 shows examples of many FG labelled neurons photographed under low power. [3] Figure 13 shows DY combined with WGA-HRP reaction product. In this paper, figure 1 shows examples of neurons triply labelled with FG, WGA-HRP and DY. The FG is best seen under fluorescent light (A) and the WGA-HRP is best seen under direct light or under combinations of fluorescent and low level direct light (B). In these examples, the luminescent nuclei contain DY (seen in A), indicating that these neurons are triply-labelled.

Figure 1 near here

RESULTS

These results first deal with the classification, distributions and numbers of RN neurons doubly labelled with tracers placed at any two of the three targets, namely, the spinal cord, inferior olivary nucleus and cerebellum. The data on triple labelling from these targets is presented in section D.

A. Double Labeling of Neurons from ION and Spinal Cord.

Classification

All types of parvicellular and magnocellular neurons throughout RN are doubly labelled by placing FG adjacent to the ipsilateral ION (figure 7 of previous paper for placement) and WGA-HRP in the dorso-lateral funiculus of the contralateral spinal cord (Figure 12 of previous paper).

Distribution of Neurons

Distribution of the doubly-labelled neurons is shown in figure 2A,B. All types of neurons are labelled from the caudal pole on the left of figure 2A to the rostral pole on the right. The normalized values are shown in figure 2B for ease of comparison of different types. There is no obvious difference between these

values and [1] those of normally distributed neurons (figure 4 of previous paper) except at the rostral end where labelled neurons are relatively few, or [2] those labelled with FG from the ION or HRP from the spinal cord (figures 11 and 14 respectively in the previous paper).

Figure 2 near here

Numbers

There are an average 674+/-118 RN neurons doubly labelled from the spinal cord and ION (n=4). In two rats, a detailed analysis of neuronal classification reveals an average of 91 large parvicellular and 51 large magnocellular neurons, 230 medium and 199 small parvicellular neurons, along with 90 small magnocellular neurons. The classification of 40 neurons is uncertain. The percentages of all types of neurons singly and doubly labelled from ION and SC are shown in figure 3. There are no major differences within each type. There are differences between the absolute values of different neuron types as expected from the normal distribution shown in figure 4 of the previous paper. For example, large neurons (PL and ML) are less often labelled than medium or small sized neurons.

Figure 3 near here

Collaterals: Doubly-Labelled Neurons as a Percentage of Neurons Labelled from the Spinal Cord and ION

The above data suggest that RN neurons projecting to the spinal cord collateralize to the ION, or vice versa. The percentage of each type of projecting neuron that collateralizes is shown in figure 4. Overall, of those neurons projecting to the spinal cord, between 44 and 58% collateralize to the ION. Of neurons projecting to the ION, a larger percentage (56 to 60%) collateralize to the spinal cord. The data derived from two rats analyzed in detail differ from the overall total for four rats. The most interesting feature of this result is the propensity for parvicellular neurons, particularily the large ones, to branch to both targets. For example, 98% of parvicellular neurons projecting to ION also project to the spinal cord.

Figure 4 near here

B. Double Labeling of Neurons from ION and Cerebellum.

Classification

All types of parvicellular and magnocellular neurons throughout RN are doubly labelled by placing FG adjacent to the ipsilateral ION (figure 7B of previous paper) and DY adjacent to

the contralateral cerebellar nuclei (Figure 15 of previous paper).

Distribution of Neurons

The distributions of the doubly-labelled neurons are shown in figure 5A,B. All types of neurons are labelled from close to the caudal pole on the left of figure 5A to the rostral pole on the right. There is an obvious lack of doubly labelled neurons near the caudal pole due to the sparsity of neurons labelled from the cerebellum as discussed and illustrated in figures 10 and 16 of the previous paper. The normalized values are shown in figure 5B for ease of comparison of different types. There are no great differences between these values and those of normally distributed neurons (figure 4 of previous paper), or those labelled with FG from the ION or DY from the cerebellum (figures 11 and 16 respectively in the previous paper).

Figure 5 near here

Numbers

There are an average 226+/-49 RN neurons doubly labelled from the ION and cerebellum (n=5). In three rats, a detailed analysis of neuronal classification reveals an average of 12 large parvicellular and 16 large magnocellular neurons, 76 medium and 90 small parvicellular neurons, along with 60 small magnocellular

neurons. The classification of 15 neurons is uncertain. Figure 6 shows the percentages of all types of neurons singly and doubly labelled from ION and Cerebellum. There are no major differences within each type. There are differences, as expected, between the absolute values of different neuron types. For example, large neurons (PL and ML) are less often labelled than medium or small sized neurons.

Figure 6 near here

Collaterals: Doubly-Labelled Neurons as a Percentage of Neurons Labelled from the ION and Cerebellum

The above data suggest that RN neurons projecting to the ION collateralize to the Cerebellum, or vice versa. The percentage of each type of spinally projecting neurons that collateralizes is shown in figure 7. Between 58% and 78% of all cerebellar projecting neurons collateralize to the ION, while only 16% of neurons projecting to ION collateralize to the cerebellum. The data for the different types of neurons are derived from the three rats analyzed in detail and differ somewhat from the overall total for 6 rats. The most interesting feature of this result is the small percentage of ION projecting neurons that collateralize to the cerebellar nuclei.

Figure 7 near here

C. Double Labeling of Neurons from the Spinal Cord and Cerebellum.

Classification

All types of parvicellular and magnocellular neurons throughout RN are doubly labelled by placing WGA-HRP in the dorsolateral funiculus of the contralateral spinal cord (Figure 12 of previous paper), and DY adjacent to the contralateral cerebellar nuclei (Figure 15 of previous paper).

Distribution of Neurons

The distributions of the doubly-labelled neurons are shown in figure 8A,B. All types of neurons are labelled from the caudal pole on the left of figure 8A to the rostral pole on the right. There is an obvious lack of doubly labelled neurons near the caudal pole due to the sparsity of neurons labelled from the cerebellum as discussed and illustrated in figures 10 and 16 of the previous paper. The normalized values are shown in figure 8B for ease of comparison of different types. Differences between these values and those of normally distributed neurons (figure 4 of previous paper), are confined to the rostral pole where there are more doubly-labelled small magnocellular and medium parvocellular neurons. Similar differences with the normal distribution are seen

for those labelled with FG from the ION and DY from the cerebellum (figures 11 and 16 respectively in the previous paper).

Figure 8 near here

Numbers

There are an average 335+/-120 RN neurons doubly labelled from the spinal cord and cerebellum (n=5). In two rats, a detailed analysis of neuronal classification reveals an average 8 large parvicellular and 11 large magnocellular neurons, 54 medium and 45 small parvicellular neurons, along with 22 small magnocellular neurons. The classification of 11 neurons is uncertain. Figure 9 shows the percentages of all types of neurons singly and doubly labelled from the spinal cord and Cerebellum. There are no major differences within each type, except for the increased percentage of large parvicellular neurons labelled from the spinal cord (11% compared to 5%). There are differences, as expected, between the absolute values of different neuronal types.

Figure 9 near here

Collaterals: Doubly-Labelled Neurons as a Percentage of Neurons Labelled from the Spinal Cord and Cerebellum

The above data suggest that RN neurons projecting to the

spinal cord collateralize to the Cerebellum, or vice versa. The percentage of each type of spinally projecting neuron that collateralizes is shown in figure 10. Between 50% and 52% of all cerebellar projecting neurons collateralize to the spinal cord, while only 16% to 23% of neurons projecting to the spinal cord collateralize to the cerebellum. The data are derived from the two rats analyzed in detail and differ somewhat from the overall total for 6 rats. The most interesting feature of this result is the small percentage of spinal cord-projecting neurons that collateralize to the cerebellar nuclei. The exception is the 39% of small magnocellular neurons that collateralize to the cerebellum.

Figure 10 near here

D. Triple Labeling of Neurons from the ION, Spinal Cord and Cerebellum.

Classification

All types of parvicellular and magnocellular neurons throughout RN are triply labelled by placing tracers in the three RN targets described above.

Distribution of Neurons

The distributions of the triply-labelled neurons are shown in figure 11A,B. All types of neurons are labelled, but not as extensively as doubly-labelled neurons. For example, there is a sparsity of triply-labelled large parvicellular and magnocellular neurons from the midsection to the rostral pole. In addition, there is an obvious lack of triply-labelled neurons near the caudal pole due to the sparsity of neurons labelled from the cerebellum as discussed above and illustrated in figures 10 and 16 of the previous paper. The normalized values are shown in figure 11B for ease of comparison of different types. This figure highlights the disproportionally large distribution of small magnocellular neurons in the rostral pole compared with the normal distribution (figure 4 of previous paper).

Figure 11 near here

Numbers

There are an average 110+/-26 RN neurons triply labelled from the three targets (n=4). In two rats, a detailed analysis of neuronal classification reveals an average 6 large parvicellular and 10 large magnocellular neurons, 43 medium and 37 small parvicellular neurons, along with 17 small magnocellular neurons. The classification of 10 neurons is uncertain. The percentages of triply-labelled neurons is compared with singly-labelled neurons in

figure 12A. As expected, some variability is seen within each type, and larger neurons are less often labelled than medium and small neurons as expected from the normal distribution (figure 4 of previous paper). Doubly-labelled neurons are compared with triply-labelled neurons in figure 12B. These data demonstrate less variability within groups in comparison to figure 12A. There are, however, more large parvicellular neurons doubly-labelled from ION and spinal cord than from other targets (13% versus 5%). Similarily, small magnocellular neurons are more often doubly-labelled from ION and cerebellum than from any other target combinations. There is some variability in the percentages of these neurons in the other groups as well. Unclassifiable neurons make up the difference between 100% and the total percentage in each class. In all cases this difference is less than 10%.

Figure 12 near here

Collaterals: Triply-Labelled Neurons as a Percentage of Neurons Labelled from the three targets

The above data indicate that individual RN neurons collateralize to three targets, namely, ION, spinal cord and cerebellum. The percentage of collateralization of each type of projecting neuron is shown in figure 13. 41% of all cerebellar projecting neurons collateralize to both the ION and spinal cord. In contrast, only 10% of neurons projecting to the ION

collateralize to both the spinal cord and cerebellum, and only 9% of neurons projecting to the spinal cord collateralize to ION and cerebellum. The data are derived from two rats analyzed in detail and differ very little from the overall total for 4 rats. Two other features are worth mentioning: (1) Of the small magnocellular neurons projecting to the spinal cord, 30% also project to both the ION and cerebellum. This contrasts with the collateralization percentage of 10% or less of the other four types of triply-labelled neurons that project to the spinal cord. Similarily, of all the large magnocellular neurons projecting to the cerebellum, 62% are triply-labelled. This contrasts with the 28% to 48% of other types of triply-labelled neurons that project to the cerebellum.

Figure 13 near here

DISCUSSION

The double and triple labelling studies reported in this paper continue the analysis of RN neuronal projections reported in the first paper for singly labelled neurons. The most remarkable feature of the analysis is the lack of any clear organizational principles. Some organizational features are present, however, and are discussed below.

Distribution

The distribution patterns of doubly and triply labelled neurons (figures 2, 5, 8 and 11) tend to follow the patterns for singly labelled neurons (figures 11, 14 and 16 of paper 1). They are similar also to the pattern for control neurons (figure 4 of paper 1) except that neurons projecting to the cerebellar nuclei are very scant in the caudal pole. Furthermore, these triply labelled neurons tend to aggregrate in the middle of the nucleus and avoid the ventral part (figure 10 of paper 1) where neurons projecting to the other two targets are dense. This distribution pattern necessarily confines the distribution of doubly labelled neurons that involve the cerebellar projection neurons. As a further consequence, triply-labelled neurons are also confined to the mid-section of the nucleus and avoid the dorsal and ventral regions as can be deduced from figure 10 of paper 1.

Neurons <u>un</u>labelled from any of the three targets are seen in the dorsal and rostral region of RN. These neurons probably project to other targets such as lateral reticular nucleus, trigeminal nucleus and facial nucleus and so are not labelled from the present targets. The trigeminal and facial nuclear projections ought to be extensive because they may be related to control of whisker function which is important in the rat. The lack of label in dorso-rostral RN is probably not due to lack of tracer placement at the three investigated targets. The retrograde tracer placement

technique has been used in 117 rats over six years. The technique involves placing large amounts of tracer-soaked gelfoam that covers the target areas thoroughly as shown in figures 7, 12 and 15 in paper 1.

Numbers

The numbers of labelled neurons are inversely related to the number of labels. This is illustrated in table 1. An average of 1,382+/-333 neurons are singly labelled with FG from ION, an average of 1402+/-438 neurons are singly labelled with WGA-HRP from the spinal cord and an average of 412+/-199 neurons are singly labelled from cerebellum. These numbers contrast with an average of only 110+/-26 triply labelled neurons and low numbers of doubly-labelled neurons shown in table 1. The lower average numbers of multiply labelled neurons are not due to inadequate tracer placements and consequent lower numbers of labelled neurons because preparations producing histological counts of less than 840 neurons labelled from ION, 855 neurons labelled from the spinal cord and 222 neurons labelled from the cerebellum were rejected from the analysis. The obvious reason for low numbers of triply labelled neurons is the limitation imposed by the lowest number of singly labelled neurons from a specific target, namely, cerebellum. Another reason is neuronal distribution. For example, triply-labelled neurons lie in the mid-section of the nucleus and avoid the dorsal and ventral regions which are dense with neurons

projecting to the other targets as discussed above. For example, cerebellar projecting neurons avoid the ventral region and are more commonly found dorsally where the others are absent. A similar pattern of distribution explains the limited number of doubly-labelled neurons.

Table 1.
Numbers of Labelled Neurons

ION	SC	CB	ION/SC	ION/CB	SC/CB	TRIPLES
1,382 +/-333	1,402 +/-438	412 +/-199	674 +/-118	335 +/-120	226 +/-49	110 +/-26

Classification

All types of neurons are singly, doubly and triply labelled from all three targets. One expectation had been that specific categories of neurons might be selectively labelled. This expectation has not been borne out as the data in figures 3, 6, 9, 12A and 12B demonstrate. When collaterals projection are examined, however, some interesting differences are seen between categories of neurons.

Collateral Projections

Obvious differences in percentages of collaterals between RN neurons labelled from the three targets are seen for the triply-

labelled neurons (figure 13). Over 40% of RN neurons projecting to the cerebellar nuclei collateralize to both ION and spinal cord. Over 50% of neurons are doubly-labelled from cerebellar nuclei and the other targets, indicating that some doubly-labelled neurons are not triply-labelled. When the distribution within RN of cerebellar-projecting neurons is examined (see discussion above and figure 10 of paper 1), the singly-labelled cerebellar-projecting neurons are found in the dorsal region. They could possibly be labelled if other neurons projecting to such targets as facial, trigeminal or other brainstem nuclei were labelled from those targets. In other words, all neurons projecting to cerebellum might have been triply-labelled if more targets could have been injected at the same time. Nevertheless, the 40% of triply-labelled cerebellar-projecting neurons provides a far higher percentage of collaterals than those projecting to the other two targets. Only about 10% of neurons projecting to spinal cord are triply-labelled, and a similar percentage of ION-projecting neurons are triply-labelled. Further examination of the doubly-labelled data indicates that these low percentages are due to the low percentages of doubly-labelled neurons that involve the cerebellar projection. Only 16% of neurons projecting to ION (and between 16 and 23% to spinal cord) collateralize to cerebellar nuclei (figures 7 and 10). Conversely, more than half the neurons projecting to cerebellar nuclei collateralize to the other two targets as mentioned above. In conclusion, it appears as if relatively low percentages of neurons projecting to ION and spinal cord

collateralize to the cerebellar nuclei.

The triply-labelled neurons are of all types as shown in figure 13. However, only a small percentage of the large parvicellular neurons projecting to ION (6%) and to spinal cord (4%) are triply-labelled. Interestingly, 30% of small magnocellular neurons projecting to spinal cord are triply-labelled which is about 3 times higher than the average.

Double labelling between ION and spinal cord is more robust. Approximately one half of neurons projecting to ION and spinal cord cross collateralize (figure 4). All types of neurons provide collaterals. Interestingly, however, in both cases the highest percentages of doubly-labelled neurons are the large parvicellular neurons followed by the medium and small parvicellular neurons, and then the magnocellular neurons. There is a wide range in these differences, 25% to 98% (ION) and 26% to 61% (spinal cord). The observations in monkeys that parvicellular neuyrons project to the ION from rostral RN and magnocellular neurons project to the spinal cord from caudal RN is contradicted in the rat. In monkey, the possibility that some neurons in the parvicellular region adjacent to the magnocellular region might project to the spinal cord was first suggested by Courville and Otabe in 1974. The possibility that such neurons might collateralize to ION and spinal cord has not been tested by double labelling studies. In the rat, clearly, parvicellular neurons project not just to ION (figure 4 and 13) but

collateralize to the spinal cord (figure 4) and cerebellar nuclei (figure 7). Similarily, magnocellular neurons in the rat project not only to the spinal cord, but collateralize also to the ION (figure 4) and cerebellar nuclei (figure 10).

Previous investigators (Huisman et al., 1983) studied double labelling from the spinal cord and cerebellar interpositus nucleus. In agreement with the present findings, they find that cerebellar-projecting neurons largely avoid the caudal pole. Their figure 6 is in agreement with figures 10 and 16 of paper 1, and figures 5 and 8 of this paper. In apparent disagreement, they find higher percentages of neurons doubly-labelled from the spinal cord and cerebellum. They inject primarily the interpositus nucleus with true blue dye and report that about 90% of labelled neurons are also labelled with Diamidino (or Nuclear) Yellow from the spinal cord. Conversely, 37% of neurons labelled from the spinal cord are also labelled from the cerebellum. These figures compare with 52% and 16-23% respectively for the present work which involves dye placements on all cerebellar nuclei, not just the interpositus nucleus. In the present work, the highest percentages of doubly-labelled neurons (75% and 61%) occur when the interpositus nucleus is 100% and 60% involved. The probable reason the percentage labelling is not still higher in the present work is because dye is placed in other nuclei (assuming that other nuclei are not involved in receving projections from RN). The differences in the results, then, are due to the more selective injections in the interpositus

nuclei in Huisman et al.'s experiments.

Morphological Neuronal Diversity

The data presented here begs the question of why are there so many different types of neurons and connections? What underlying principle of organization lies behind this profligacy? There is no straight forward answer yet. Several possibilities suggest themselves, however.

1. Somatotopy: The largest neurons have the longest myelinated axons and project the furthest, such as to the lumbo-sacral spinal cord. Studies of somatotopy demonstrate that neurons labelled by tracers placed in the lumbosacral spinal cord are located ventrolaterally (Shieh et al., 1983; Waldron and Gwyn, 1969). Similar pilot studies in this laboratory using Fluorogold demonstrate a dense projection of lumbo-sacral neurons in the caudal pole that extends rostro-ventrally. The data above show that large neurons, whether magnocellular or parvicellular, are not confined to a ventrolateral location, however. They are found in dorsal regions that project to cervical spinal cord. This suggests that large neurons are not somatotopically organized for the lower limbs only.

2. Chemoarchitecture: The different neurons might be organized

according to different transmitters or receptors. Specific receptors might be found on specific types of neurons. This kind of organizing principle is seen for the chemoarchitecture of monkey thalamus (Martin et al., 1990) and might be operative here also.

3. Highly Specific ION Connections: Perhaps specific sub-nuclei of ION receive input from specific types of neurons in specific sub-regions of RN. There is a hint of this in the results of the anterograde studies. For example, figure 5B of paper 1 shows that a specific subdivision of ION receives tracer from a relatively confined region of RN shown in figure 5A of that paper. One possibility is that specific neurons in that confined region project to specific sub-nuclei of ION.

4. Activity Dependence: A more remote possibility is that the cytoarchitecture, including distribution and morphology, might be dependent on motor activity and daily use of the body part. The rats used in the reported experiments were confined to standard cages and received no specific training in motor tasks. One possible explanation for the diversity of neuronal morphology is that it is dependent on activity. In other words, acquisition of motor skills might have a reorganizing effect on the cytoarchitecture. In highly skilled rats, a more organized cytoarchitecture might be seen. This suggestion is not without precedence. An example is the neural correlates of song production in canaries (Nottenbohm, 1991). In late summer when canaries

acquire new songs, small neurons in the HVC (high vocal center) that project to RA (robust nucleus of the archistriatum) are replaced. A more modest re-organization might occur in rat RN as motor skills are acquired and expressed. The rats in these experiments are not skilled. A corollary of this proposal is that there may be only one kind of RN neuron that assumes different forms as a function of activity. This use-dependency may determine the morphological appearance of neurons and the cytoarchitecture of the nucleus.

Functional Implications

The patterns of collateralization suggest that whenever signals are tranmsitted to the spinal cord via RN projecting neurons, a major proportion of the same signals are transmitted via collaterals to the ION and hence to cerebellum. A minor proportion are transmitted to cerebellar nuclei via the direct and collateral pathways described above. This implies that the function of RN neurons is intimately associated with both cerebellar function and motor output. In the monkey there is now a large body of evidence implicating the neurons of origin of the rubrospinal tract (RST) in motor control (Kohlerman et al., 1983, Gibson et al., 1985, Kennedy et al., 1986, Kennedy 1987). In the rat, motor function is considered to act in parallel with other descending motor pathways such as corticospinal. Lesions of RST produce transient motor deficits, suggesting a rapid compensation (Kennedy and Humphrey,

1987, Kennedy 1990). Lesions of RN, however, produce long-lasting deficits, suggesting a much slower compensation. It is suggested that this slow compensation is due to the destruction of neurons that rpoject to ION and cerebellum as well as to the spinal cord. These pathways remain intact during the rapid compensation after RST lesions. The present data provide a firm anatomical basis for these conclusions. In sum, the present data indicate that the large numbers of neurons that bifurcate and trifurcate to the target nuclei provide activity in the descending rubrospinal system that is copied to the cerebellum directly and by way of the inferior olivary nucleus.

Implications for Other Studies

The above data have important implications for functional studies of the red nucleus. Almost any lesion of the nucleus will involve all five neuronal types projecting to the ION, spinal cord and cerebellum. Because of this one cannot hope to lesion the caudal end, for example, and interrupt only the magnocellular projection to the spinal cord without interrupting the projection to ION. This appears possible in monkey, but not in rat. When recording from individual neurons similar problems in identification will arise requiring antidromic activation from spinal cord, ION, cerebellar nuclei and other projection nuclei. There are projections to other brainstem nuclei such as facial, trigeminal and lateral reticular nuclei (see Introduction) which

further confound the problem of identification. It will be difficult to use antidromic activation for long-term recording studies because it will hardly be possible to place a sufficiently large number of stimulating electrodes in all target sites. Studies of axonal regeneration and morphological changes in RN following rubrosinal tract transections are difficult to interpret because the viability of neurons can be maintained by collaterals such as those to brainstem and cerebellar targets. Despite awareness of this problem and careful identification of involved neurons, correct interpretation of the results of such experiments may be very difficult.

LITERATURE CITED

Courville, J., S. Otabe, (1974) The rubro-olivary projection in the macaque: An experimental study with silver impregnation methods. J. Comp. Neurol. 158:479-494.

Gibson, A.R., J.C. Houk, and N.J. Kohlerman, (1985) Magnocellular red nucleus activity during different types of limb movements in the macaque monkey. J. Physiol. 358:527-549.

Gibson, A.R., J.C. Houk, and N.J. Kohlerman, (1985) Relation between red nucleus discharge and movement parameters in trained macaque monkeys. J. Physiol. 358:551-570.

Huisman, A.M., H.G.J.M. Kuypers, F. Conde, and K. Keizer, (1983) Collaterals of rubrospinal neurons to the cerebellum in rat: a retrograde fluorescent double labeling study. Brain Res. 264: 181-196.

Kennedy, P.R. (1987) Double labelling of red nucleus neurons from dye injections into the inferior olivary nucleus and dorso-lateral funiculus of the spinal cord in rat. Soc. Neurosci. Abstrs. 13(2):852.

Kennedy, P.R., J.C. Houk, and A.R. Gibson, (1986) Anatomic and functional contrast between magnocellular and parvicellular

divisions of the red nucleus in the monkey. Brain Res. 364:124-136.

Kennedy, P.R. and D.R. Humphrey, (1987) The compensatory role of the parvicellular division of the red nucleus in operantly conditioned rats. Neuroscience Research 5:39-62.

Kennedy, P.R. (1990) Corticospinal, rubrospinal and rubro-olivary projections: a unifying hypothesis. Trends in Neurosciences, 13(2):474-479.

Martin L.J., J.C. Hedreen, D.L. Price and M.R. DeLong (1990) Chemoarchitectonic delineation of ventral tier nuclei in Macaque Thalamus. Soc. Neurosci. Abstr., 16(1):227.

Nottenbohm F. (1991) Reassessing the mechanisms and origins of vocal learning in birds. Trends in Neurosciences, 14(5):206-211.

Shieh J.Y., S.K. Leong and W.C. Wong (1983) Origin of the rubrospinal tract in neonatal, developing and mature rats. J. Comp. Neurol. 214:79-86

Tucker, C.L. and P.R. Kennedy (1990) Re-defining rat red nucleus: Cytoarchitectural analysis of red nucleus neurons singly and doubly labelled from spinal cord and inferior olivary nucleus. Soc. Neurosci. Abstrs., 16(1):729.

Waldron, H.A. and D.G. Gwyn, (1969) Descending nerve tracts in the spinal cord of the rat. I. Fibers from the midbrain. J. Comp. Neurol. 137:143-154.

Yu, D.Y., S. Na, J. Wilson and P.R.Kennedy (1991) Redefining rat red nucleus: Multiple labelling of individual neurons from spinal cord, inferior olivary nucleus and cerebellar nuclei. Soc. Neurosci. Abstr., 17(1):469.

Acknowledgements

The authors thank Dr. Johannes Tigges for his constructive criticisms of an earlier version of this manuscript. The authors also thank Ms. Shakita Dennis for helping with the analysis of the anterograde tracing data. Thanks also to Ms Crystal Tucker for her assistance in the early stages of this project. Supported by NIH grant RO1-NS24602.

FIGURE LEGENDS

Figure 1. A: The center neuron contains DY in its nucleus and FG in its cytoplasm. The other out-of-focus neurons contain only FG.

B: The same neurons are photographed under low level direct light. This illuminates the WGA-HRP reaction product in the cytoplasm. Thus this neuron is triply labelled with all three tracers. The calibration bar is 50 μm.

Figure 2. A: Absolute values of the distributions of all five types of neurons doubly labelled from ION and the spinal cord. The caudal pole is on the left.

B: The same values plotted as normalized data.

Figure 3. Normalized values of the different neurons singly labelled from ION and spinal cord (SC), and doubly labelled from both ION and spinal cord.

Figure 4. Summary diagram of the percentages of the different types of RN neurons that are doubly labelled with reference to the individual targets. For example, 60% of RN neurons labelled from ION with FG are also labelled with WGA-HRP from the spinal cord.

Figure 5. A: Absolute values of the distributions of all five types of neurons doubly labelled from ION and cerebellum. The caudal pole is on the left.

B: The same values plotted as normalized data.

Figure 6. Normalized values of the different neurons singly labelled from ION and cerebellum, and doubly labelled from both ION and cerebellum.

Figure 7. Summary diagram of the percentages of the different types of RN neurons that are doubly labelled with reference to the individual targets. For example, 16% of RN neurons labelled from ION with FG are also labelled with DY from the cerebellum.

Figure 8. A: Absolute values of the distributions of all five types of neurons doubly labelled from the spinal cord and cerebellum. The caudal pole is on the left.

B: The same values plotted as normalized data.

Figure 9. Normalized values of the different neurons singly labelled from the spinal cord and cerebellum, and doubly labelled from both the spinal cord and cerebellum.

Figure 10. Summary diagram of the percentages of the different types of RN neurons that are doubly labelled with reference to the individual targets. For example, 52% of RN neurons labelled from cerebellum with DY are also labelled with WGA-HRP from the spinal cord.

Figure 11.A: Absolute values of the distributions of all five types of neurons triply labelled from the ION, spinal cord and cerebellum. The caudal pole is on the left.

B: The same values plotted as normalized data.

Figure 12.A: Normalized values of the different neurons singly labelled from the ION, spinal cord and cerebellum, and triply labelled from all three targets.

B: Normalized values of all neurons doubly labelled from the ION, spinal cord and cerebellum, and triply labelled from all three targets.

Figure 13. Summary diagram of the percentages of the different types of RN neurons that are triply labelled with reference to the individual targets. For example, 10% of RN neurons labelled from the ION with FG are also labelled with WGA-HRP from the spinal cord and

DY from the cerebellum.

Table 1. [A brief legend accompanies the table in the text and is placed just under the title.]

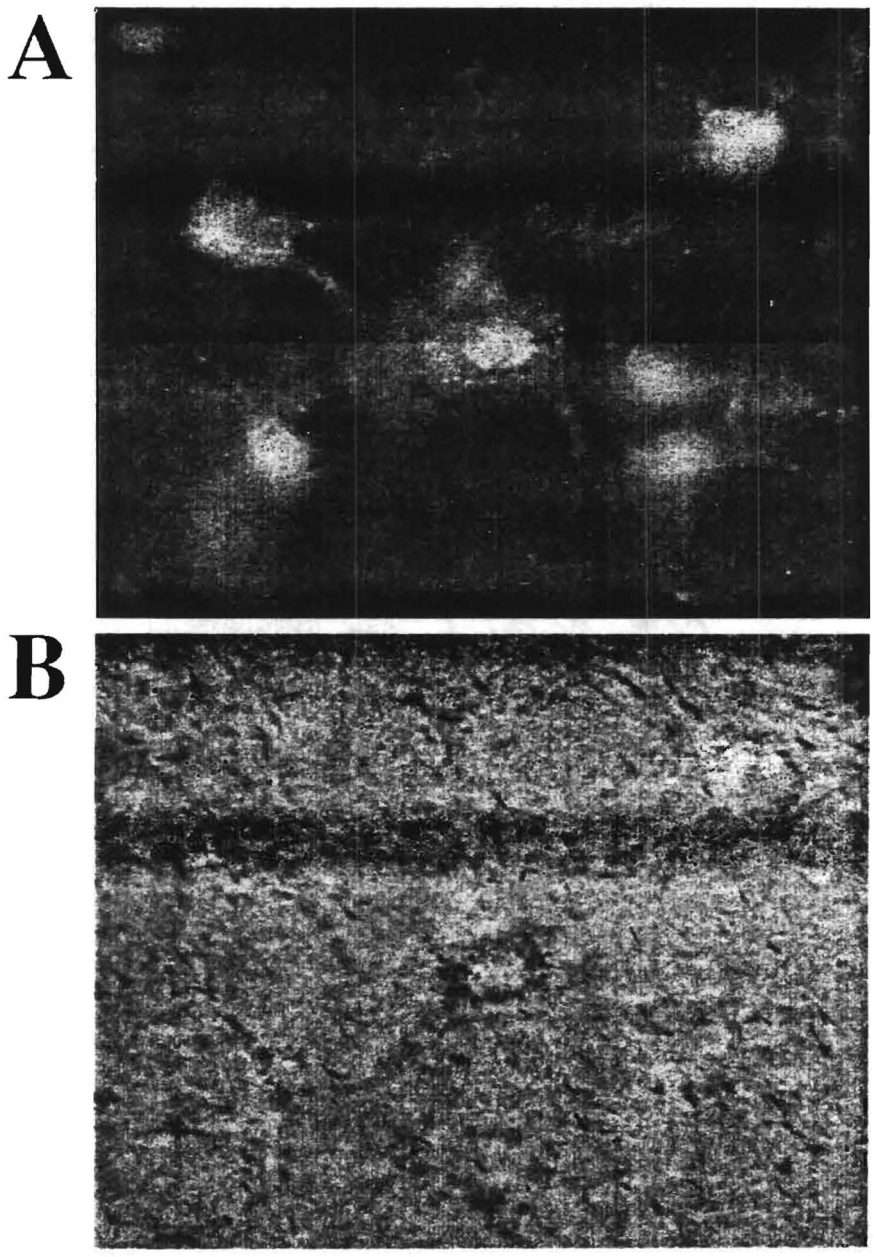
A
B

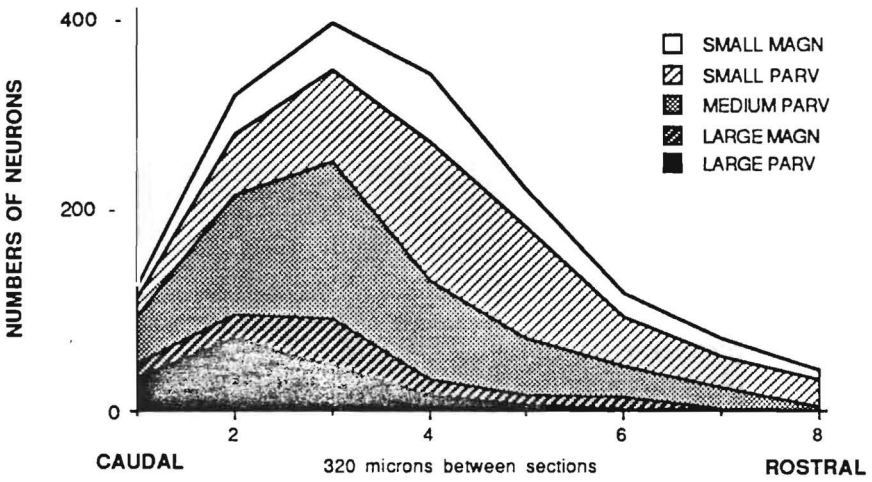
400
200
0
NUMBERS OF NEURONS
SMALL MAGN
SMALL PARV
MEDIUM PARV
LARGE MAGN
LARGE PARV
2
4
6
8
CAUDAL
320 microns between sections
ROSTRAL

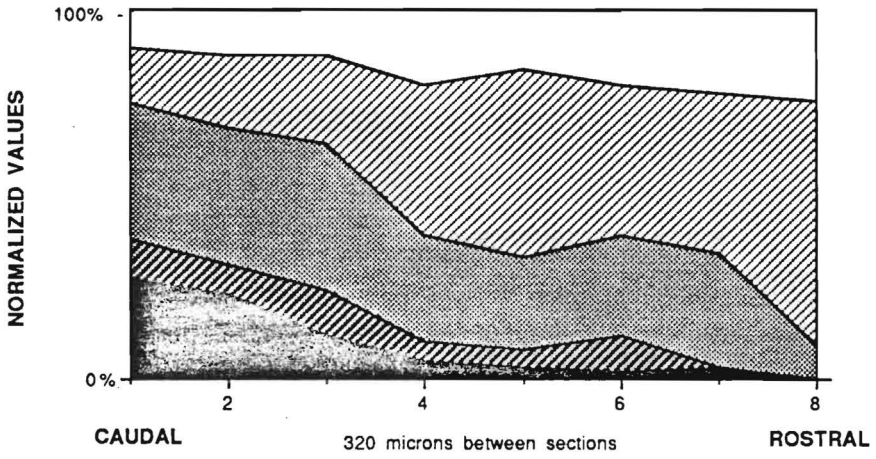
100%
0%
NORMALIZED VALUES
2
4
6
8
CAUDAL
320 microns between sections
ROSTRAL

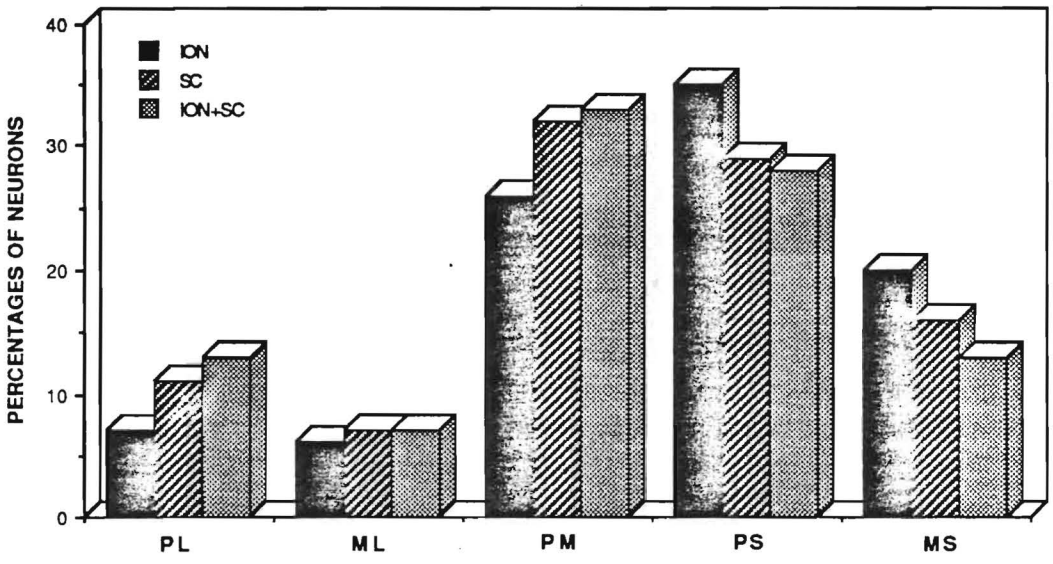
PERCENTAGES OF NEURONS
40
30
20
10
0
ION
SC
ION+SC
PL
ML
PM
PS
MS

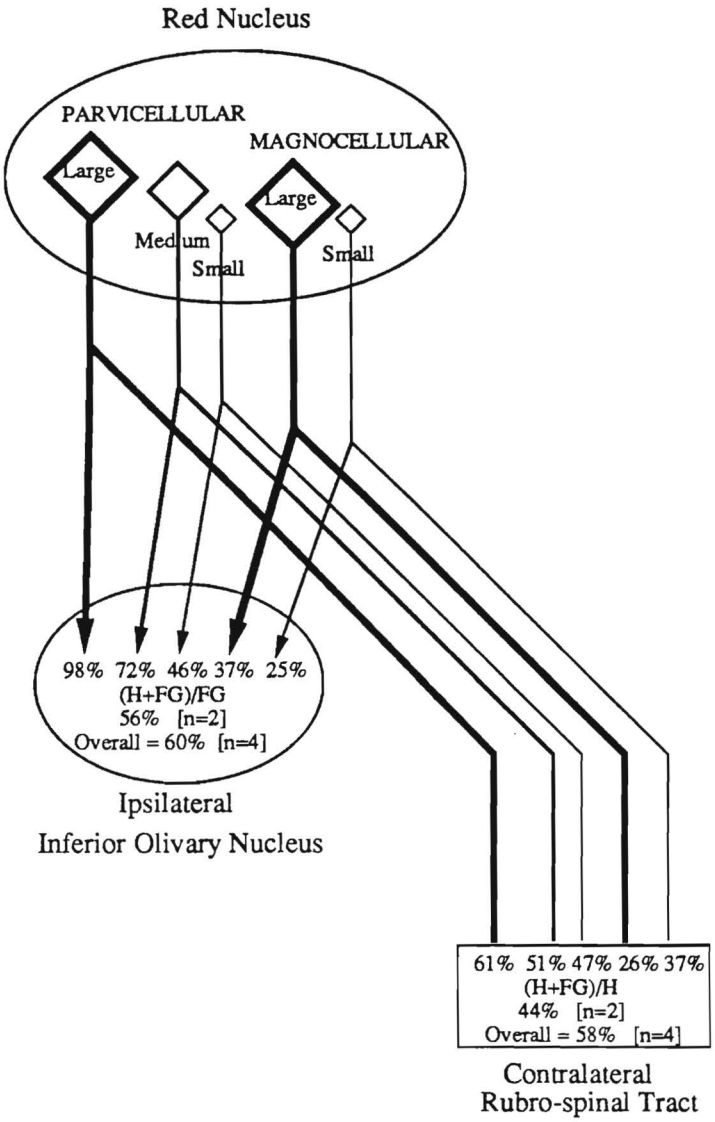
Red Nucleus
PARVICELLULAR
MAGNOCELLULAR
Large
Medium
Small
Large
Small
98% 72% 46% 37% 25%
(H+FG)/FG
56% [n=2]
Overall = 60% [n=4]
Ipsilateral
Inferior Olivary Nucleus
61% 51% 47% 26% 37%
(H+FG)/H
44% [n=2]
Overall = 58% [n=4]
Contralateral
Rubro-spinal Tract

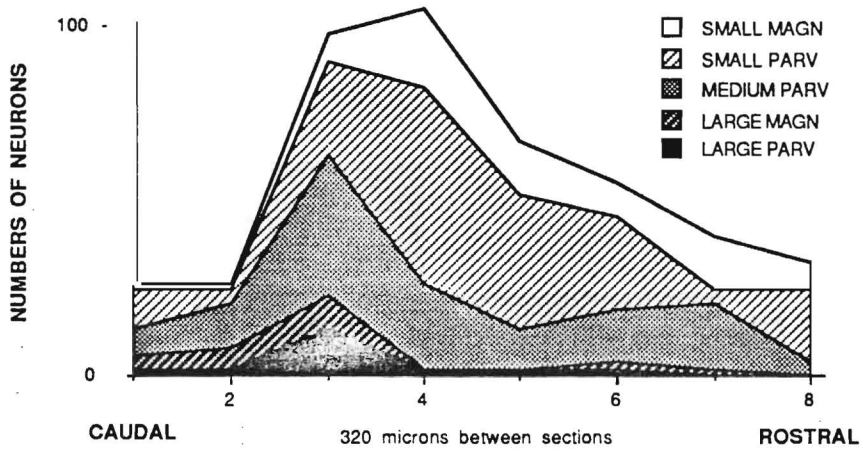
100
0
NUMBERS OF NEURONS
SMALL MAGN
SMALL PARV
MEDIUM PARV
LARGE MAGN
LARGE PARV
2
4
6
8
CAUDAL
320 microns between sections
ROSTRAL

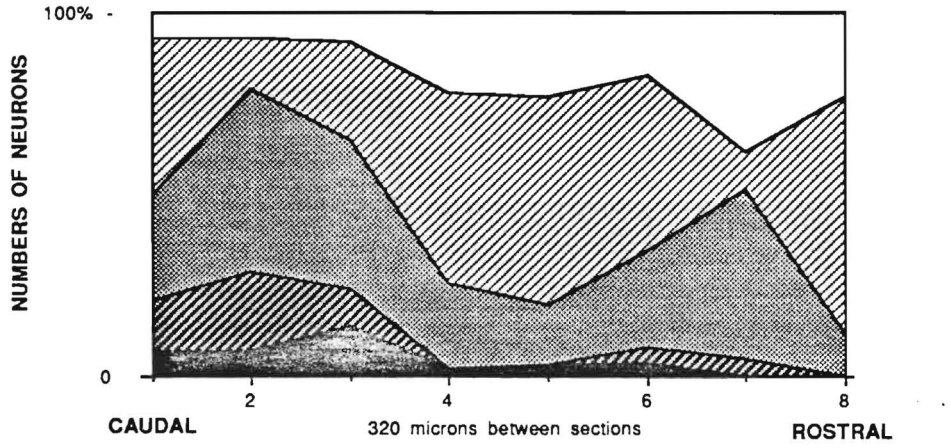
100%
NUMBERS OF NEURONS
0
2
4
6
8
CAUDAL
320 microns between sections
ROSTRAL

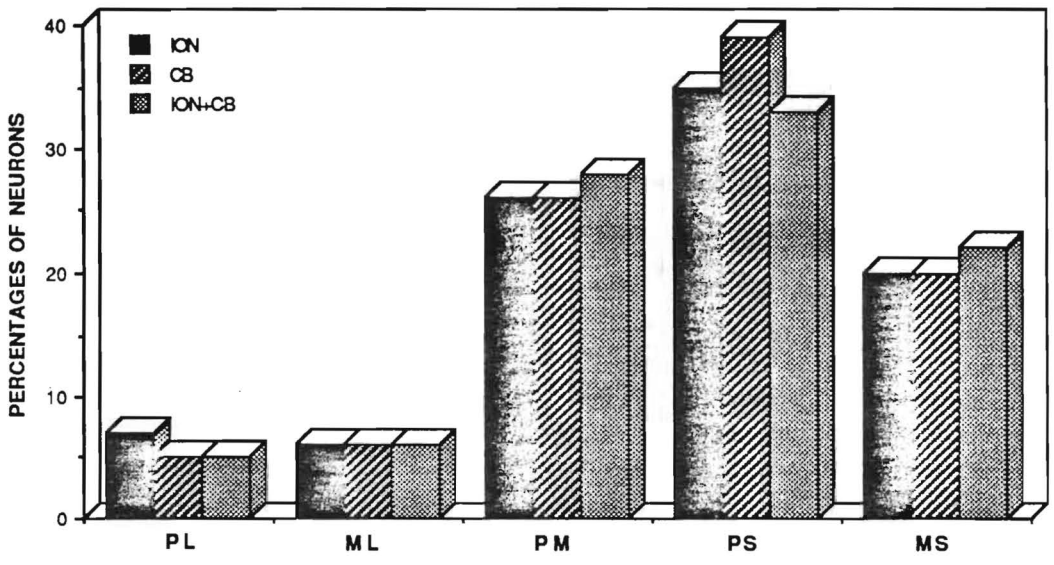
40
30
20
10
0
PERCENTAGES OF NEURONS
ION
CB
ION+CB
PL
ML
PM
PS
MS

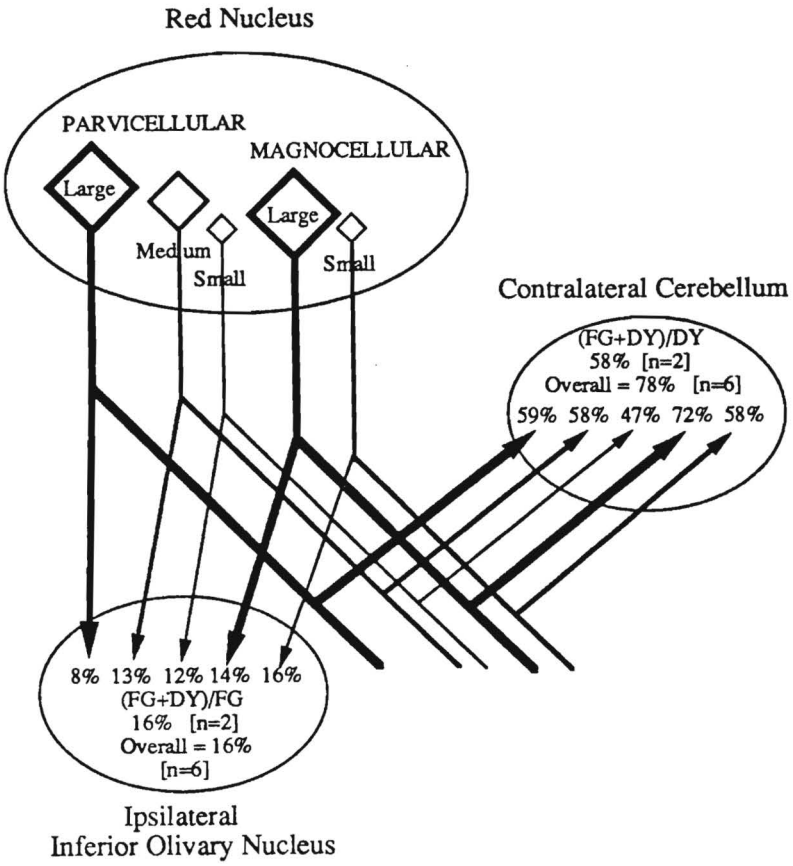
Red Nucleus
PARVICELLULAR
MAGNOCELLULAR
Large
Medium
Small
Large
Small
Contralateral Cerebellum
(FG+DY)/DY
58% [n=2]
Overall = 78% [n=6]
59% 58% 47% 72% 58%
8% 13% 12% 14% 16%
(FG+DY)/FG
16% [n=2]
Overall = 16%
[n=6]
Ipsilateral
Inferior Olivary Nucleus

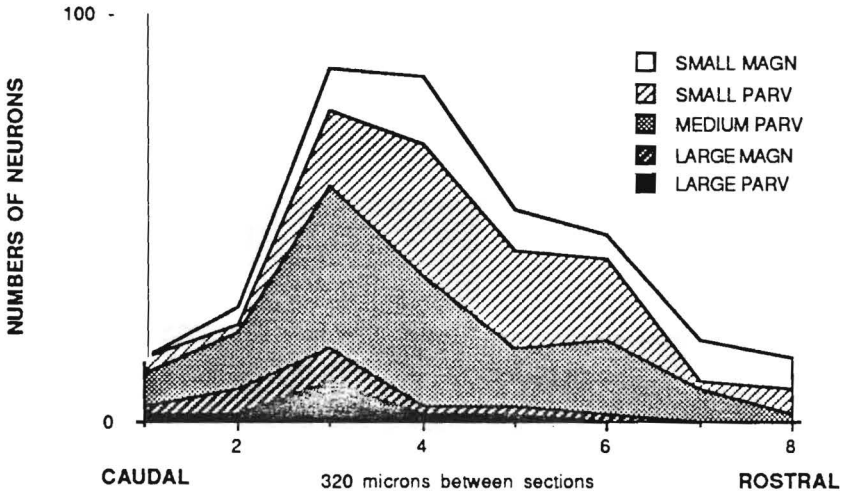
100
0
NUMBERS OF NEURONS
SMALL MAGN
SMALL PARV
MEDIUM PARV
LARGE MAGN
LARGE PARV
2
4
6
8
CAUDAL
320 microns between sections
ROSTRAL

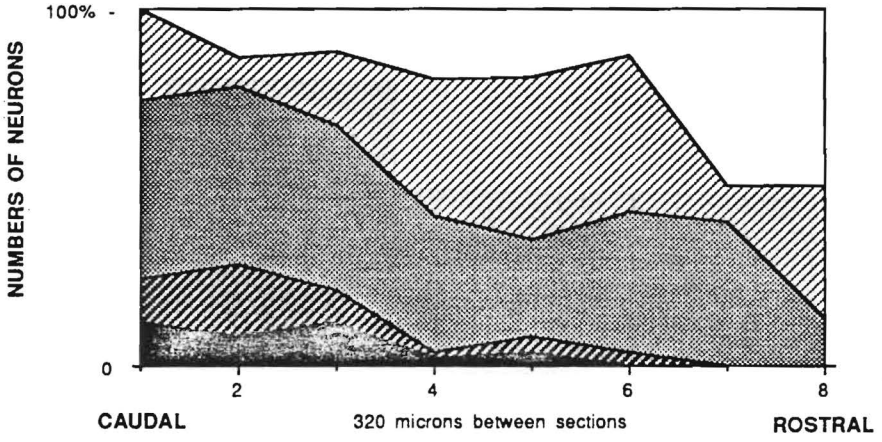
100% -
NUMBERS OF NEURONS
0
2
4
6
8
CAUDAL
320 microns between sections
ROSTRAL

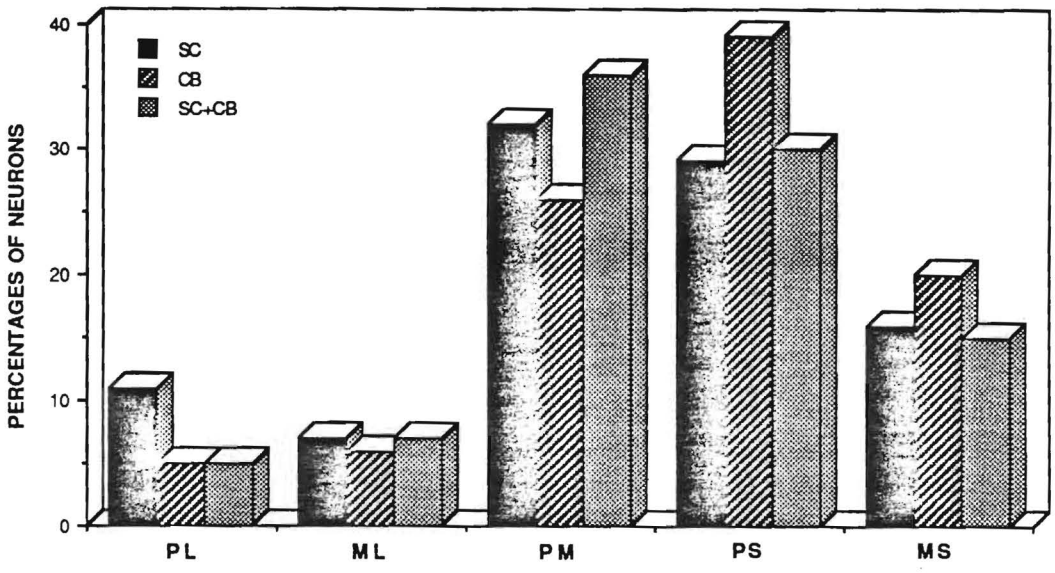
PERCENTAGES OF NEURONS
40
30
20
10
0
SC
CB
SC+CB
PL
ML
PM
PS
MS

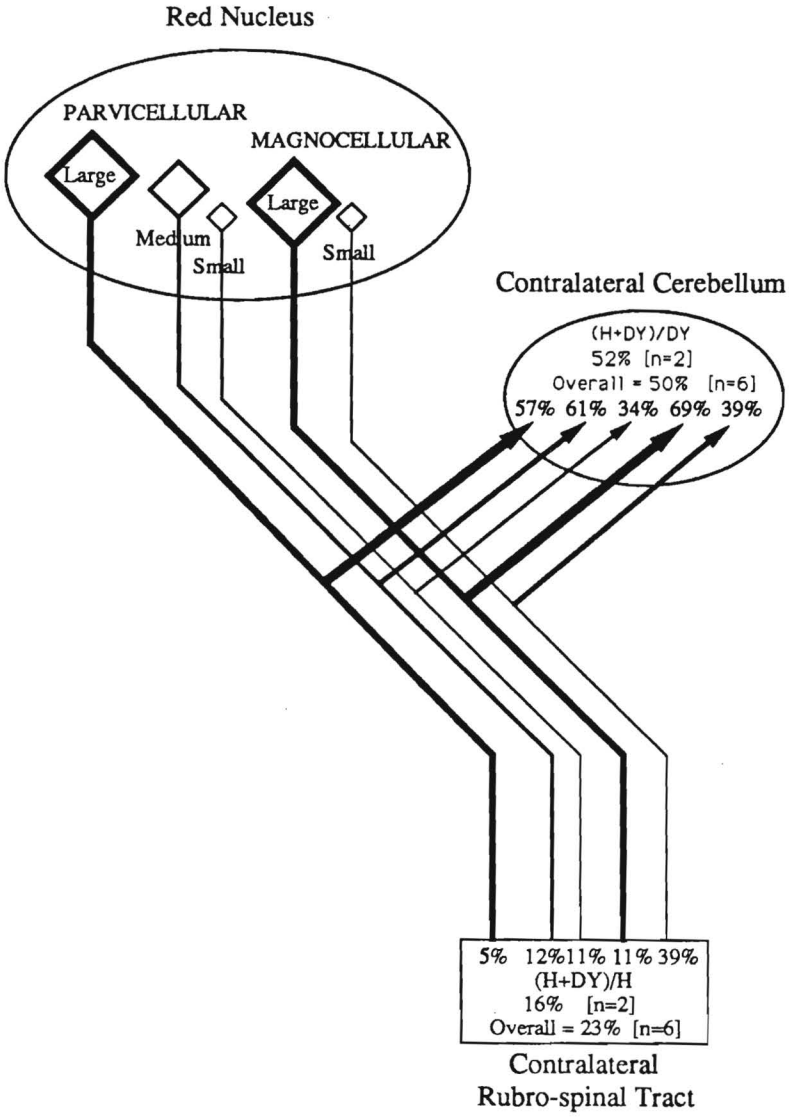
Red Nucleus
PARVICELLULAR
MAGNOCELLULAR
Large
Medium
Small
Large
Small
Contralateral Cerebellum
(H+DY)/DY
52% [n=2]
Overall = 50% [n=6]
57% 61% 34% 69% 39%
5% 12% 11% 11% 39%
(H+DY)/H
16% [n=2]
Overall = 23% [n=6]
Contralateral
Rubro-spinal Tract

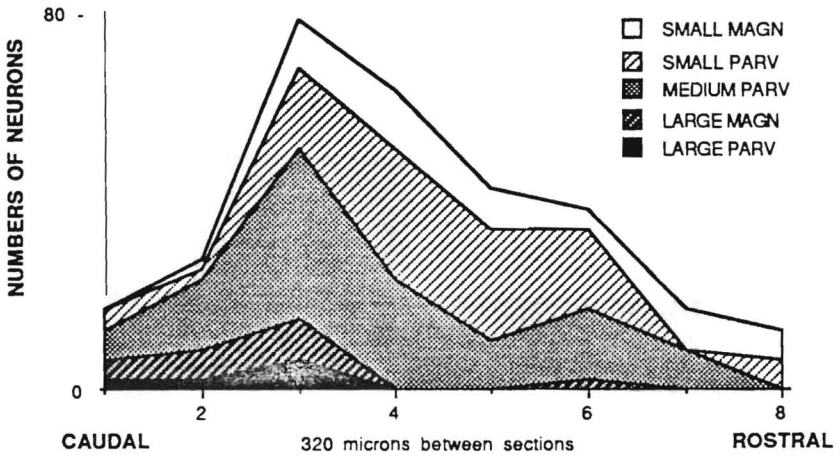
80 -
0
NUMBERS OF NEURONS
SMALL MAGN
SMALL PARV
MEDIUM PARV
LARGE MAGN
LARGE PARV
2
4
6
8
CAUDAL
320 microns between sections
ROSTRAL

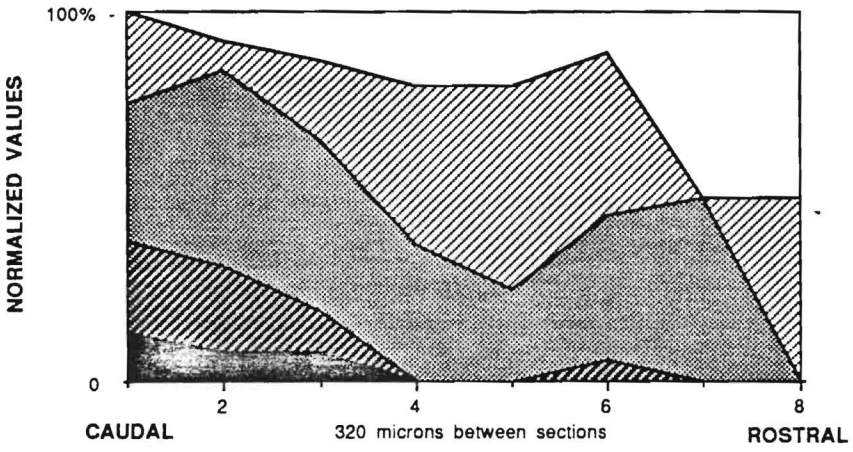
100%
0
NORMALIZED VALUES
2
4
6
8
CAUDAL
320 microns between sections
ROSTRAL

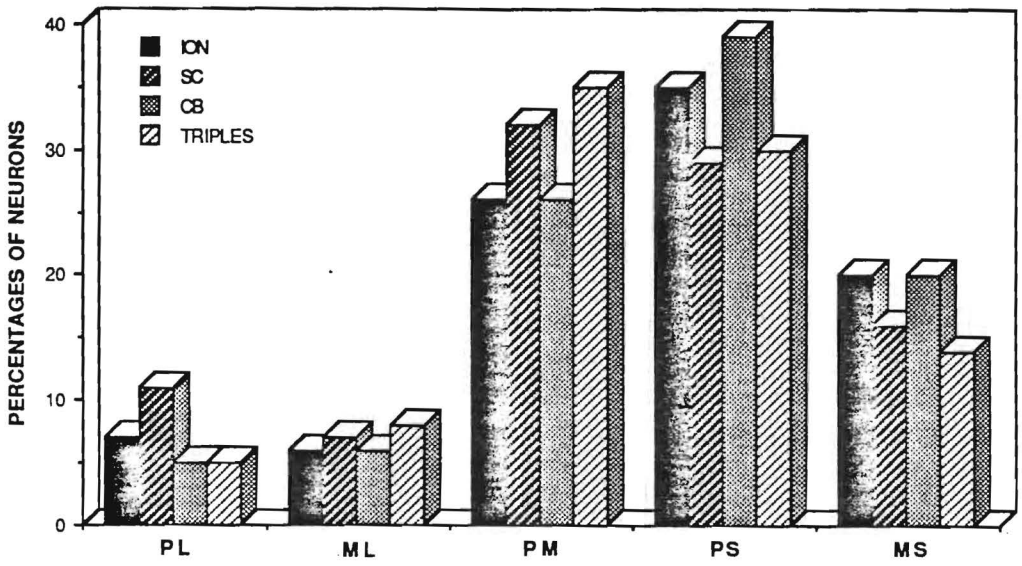
40
30
20
10
0
PERCENTAGES OF NEURONS
ION
SC
CB
TRIPLES
PL
ML
PM
PS
MS

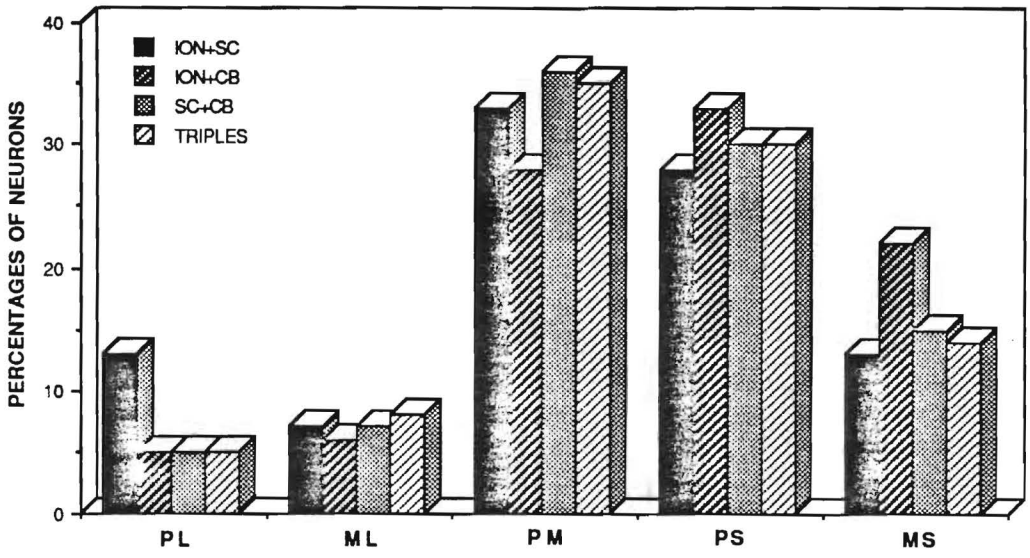
ION+SC
ION+CB
SC+CB
TRIPLES
PERCENTAGES OF NEURONS
40
30
20
10
0
PL
ML
PM
PS
MS

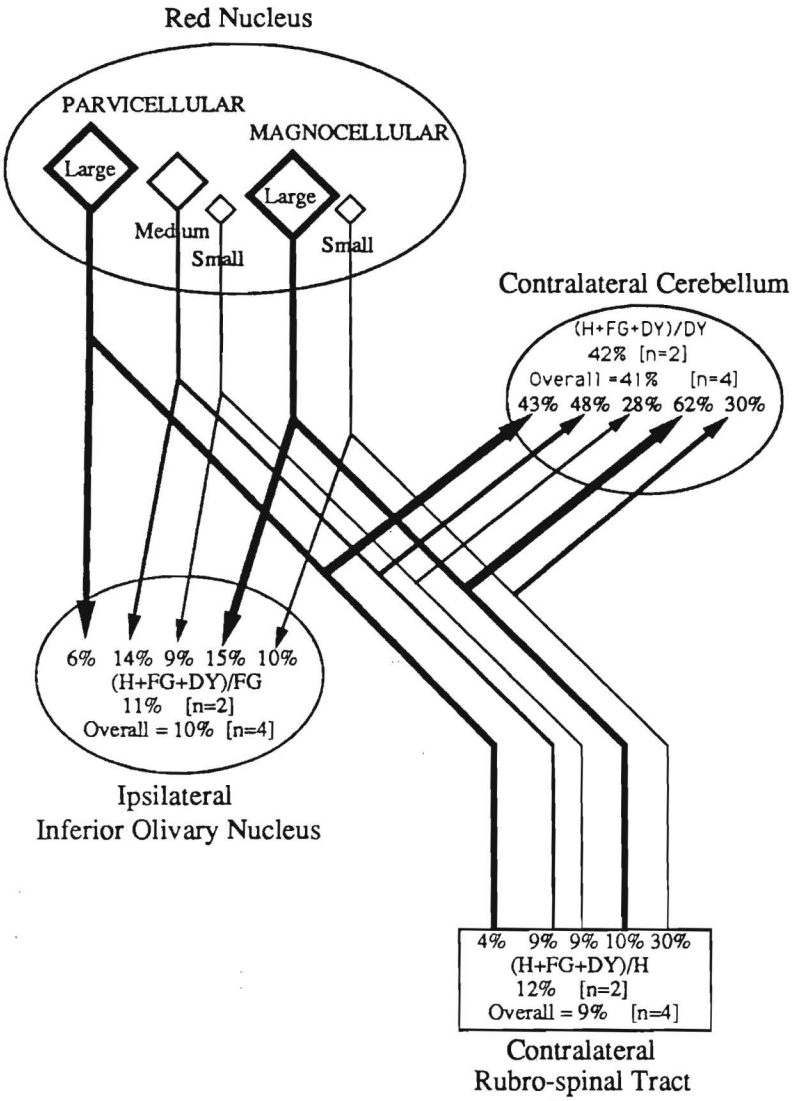
Red Nucleus
PARVICELLULAR
MAGNOCELLULAR
Large
Medium
Small
Large
Small
Contralateral Cerebellum
(H+FG+DY)/DY
42% [n=2]
Overall =41% [n=4]
43% 48% 28% 62% 30%
6% 14% 9% 15% 10%
(H+FG+DY)/FG
11% [n=2]
Overall = 10% [n=4]
Ipsilateral
Inferior Olivary Nucleus
4% 9% 9% 10% 30%
(H+FG+DY)/H
12% [n=2]
Overall = 9% [n=4]
Contralateral
Rubro-spinal Tract